

Mineralogical, radiographic and uranium leaching studies on the uranium ore from Kvanefjeld, Ilimaussaq complex, South Greenland

Makovicky, M.; Makovicky, E.; Leth Nielsen, B.; Karup-Møller, S.; Sørensen, Emil

Publication date:
1980

Document Version
Publisher's PDF, also known as Version of record

[Link back to DTU Orbit](#)

Citation (APA):
Makovicky, M., Makovicky, E., Leth Nielsen, B., Karup-Møller, S., & Sørensen, E. (1980). Mineralogical, radiographic and uranium leaching studies on the uranium ore from Kvanefjeld, Ilimaussaq complex, South Greenland. (Denmark. Forskningscenter Risoe. Risoe-R; No. 416).

DTU Library Technical Information Center of Denmark

General rights

Copyright and moral rights for the publications made accessible in the public portal are retained by the authors and/or other copyright owners and it is a condition of accessing publications that users recognise and abide by the legal requirements associated with these rights.

- Users may download and print one copy of any publication from the public portal for the purpose of private study or research.
- You may not further distribute the material or use it for any profit-making activity or commercial gain
- You may freely distribute the URL identifying the publication in the public portal

If you believe that this document breaches copyright please contact us providing details, and we will remove access to the work immediately and investigate your claim.

DK 8100115

Risø-R-416

Risø-R-416

RISØ

Mineralogical, Radiographic and Uranium Leaching Studies on the Uranium Ore from Kvanefjeld, Ilímaussaq Complex, South Greenland

**Milota Makovicky, Emil Makovicky,
Bjarne Leth Nielsen, Svend Karup-Møller, and
Emil Sørensen**

**Risø National Laboratory, DK-4000 Roskilde, Denmark
June 1980**

MINERALOGICAL, RADIOGRAPHIC AND URANIUM LEACHING STUDIES
ON THE URANIUM ORE FROM KVANEFJELD, ILIMAUSSAQ COMPLEX,
SOUTH GREENLAND

Milota Makovicky¹, Emil Makovicky², Bjarne Leth Nielsen¹,
Sven Karup-Møller³ and Emil Sørensen⁴

Abstract. 102 samples of low-grade uranium ore from 70 drill holes at Kvanefjeld, Ilimaussaq alkaline intrusion, South Greenland were studied by means of autoradiography, fission-track investigations, microscopy, microprobe analyses and uranium-leaching experiments. The principal U-Th bearing mineral, steenstrupine, and several less common uranium minerals are disseminated in lujavrite (nepheline syenite) and altered volcanic rocks. Steenstrupine has average composition $\text{Na}_{6.7}\text{H}_x\text{Ca}_{1.0}(\text{REE}+\text{Y})_{5.8}(\text{Th},\text{U})_{0.5}(\text{Mn}_{1.6}\text{Fe}_{1.8}\text{Zr}_{0.3}\text{Ti}_{0.1}\text{Al}_{0.2})\text{Si}_{12}\text{O}_{36}(\text{P}_{4.3}\text{Si}_{1.7})\text{O}_{24}(\text{F},\text{OH}) \cdot n\text{H}_2\text{O}$; n and x are variable. It either is of magmatic origin (type A) or connected with metasomatic processes (type B), or occurs in late veins (Type C). Preponderance of grains are metamict (usually 2000-5000 ppm U_3O_8) or altered (usually above 5000 ppm U_3O_8), sometimes zoned with both

(continue on next page)

June 1980

Pisø National Laboratory, DK-4000 Roskilde, Denmark

components present. Occasionally they are extremely altered with U content falling to 500-5000 ppm U₃O₈ and local accumulations of high-U minerals formed. Replacement by crystalline monazite (± metamict uranothorite and other components) is locally important. Uranium recovery by carbonate leaching (NaHCO₃+Na₂CO₃+O₂) depends both on alteration of steenstrupine and on hydration of parent rocks. Yield is between 98 and 50%, the average U concentration in the examined rock around 350 ppm U.

INIS descriptors: AUTORADIOGRAPHY, ELECTRON MICROPROBE ANALYSIS, GREENLAND, FISSION TRACKS, HYDRATION, IGNEOUS ROCKS, LEACHING, LUJAVRITES, MEDIUM PRESSURE, MICROSTRUCTURE, MINERALOGY, ORE PROCESSING, PETROLOGY, SODIUM CARBONATES, STEENSTRUPINE, URANIUM MINERALS, URANIUM ORES.

UDC 669.822.3

1) Geological Survey of Greenland, Copenhagen, 2) University of Copenhagen, 3) Technical University of Denmark, Lyngby, 4) Risø National Laboratory, Roskilde.

ISBN 87-550-0681-7

ISSN 0106-2840

Risø Repro 1981

CONTENTS

	Page
1. INTRODUCTION	5
1.1. General problems, project aims	5
1.2. Selection of material and sample preparation	7
2. AUTORADIOGRAPHIC WORK	8
2.1. Techniques, scope of work	8
2.2. Results	9
2.3. Classification of lujavrites	12
3. MICROSCOPY	14
3.1. Scope of work	14
3.2. General mineralogical description of lujavrites ..	14
3.3. Description and classification of steenstrupine ..	20
4. FISSION TRACK INVESTIGATIONS	37
4.1. Techniques, scope of work	37
4.2. Associations of U-bearing minerals	38
4.3. Description of individual associations and the uranium contents in the minerals	41
5. CHEMICAL AND MINERALOGICAL STUDIES OF STEENSTRUPINE ...	60
5.1. Microprobe analysis	60
5.2. Scanning electron microscopy	65
5.3. Mineralogical studies on the crystalline steen- strupine No. 199104 from Tunugdliarfik, the Ilímaussaq Complex	81
5.4. Discussion	85
6. RECOVERY OF URANIUM	109
6.1. General	109
6.2. Carbonate pressure leaching	110
6.3. Relationship between the U yield and the petro- logical and mineralogical characteristics	113
6.4. Regional variations of U yield	117

	Page
7. SUMMARY AND CONCLUSIONS	122
7.1. Geology, petrology	122
7.2. Mineralogy and fission-track data	125
7.3. Chemistry of steenstrupine	129
7.4. Uranium recovery	132
7.5. General conclusions and proposals	133
 ACKNOWLEDGEMENTS	 136
 REFERENCES	 137
 TABLES	 139

1. INTRODUCTION

Since 1976 the Ministry for Commerce has financed a number of research and development projects on energy. One of the projects concerned the extraction of uranium from lujavrite from the Kvanefjeld area, the Ilimaussaq complex, South Greenland (Fig. 36). The name of the project is "Uranudvinding"; it commenced in 1978 and is conducted by Risø National Laboratory, Roskilde. The present investigation, which deals with the distribution and extraction of uranium and the mineralogy of the ore, is a part of the project, and has been carried out by the Geological Survey of Greenland (GGU) in cooperation with the Risø National Laboratory, since January 1st 1978.

1.1. General problems, project aims

Extraction of uranium from lujavrite has been carried out at the Department of Chemistry at Risø National Laboratory for a number of years. The research work has resulted in two different techniques by which the refractory ore can be treated. The first one is based on roasting the ore in a SO_2 -atmosphere and the second one on extraction with a carbonate solvent in a pressurized tube reactor. The uranium yield from both processes has varied tremendously and being a heterogeneous ore with respect to the fixation of the uranium it became clear that a better understanding of the microstructure, the mineralogy and the small scale distribution of the uranium was important in order to understand, and to improve the efficiency of the extraction process. The distribution of uranium has been studied by a number of techniques: autoradiography, fission track investigation, general microscopy, microprobe and scanning electron microscopy. Classification of the lujavrite ore on the basis of these investigations is then compared with the results of a series of laboratory extraction tests on identical lujavrite material.

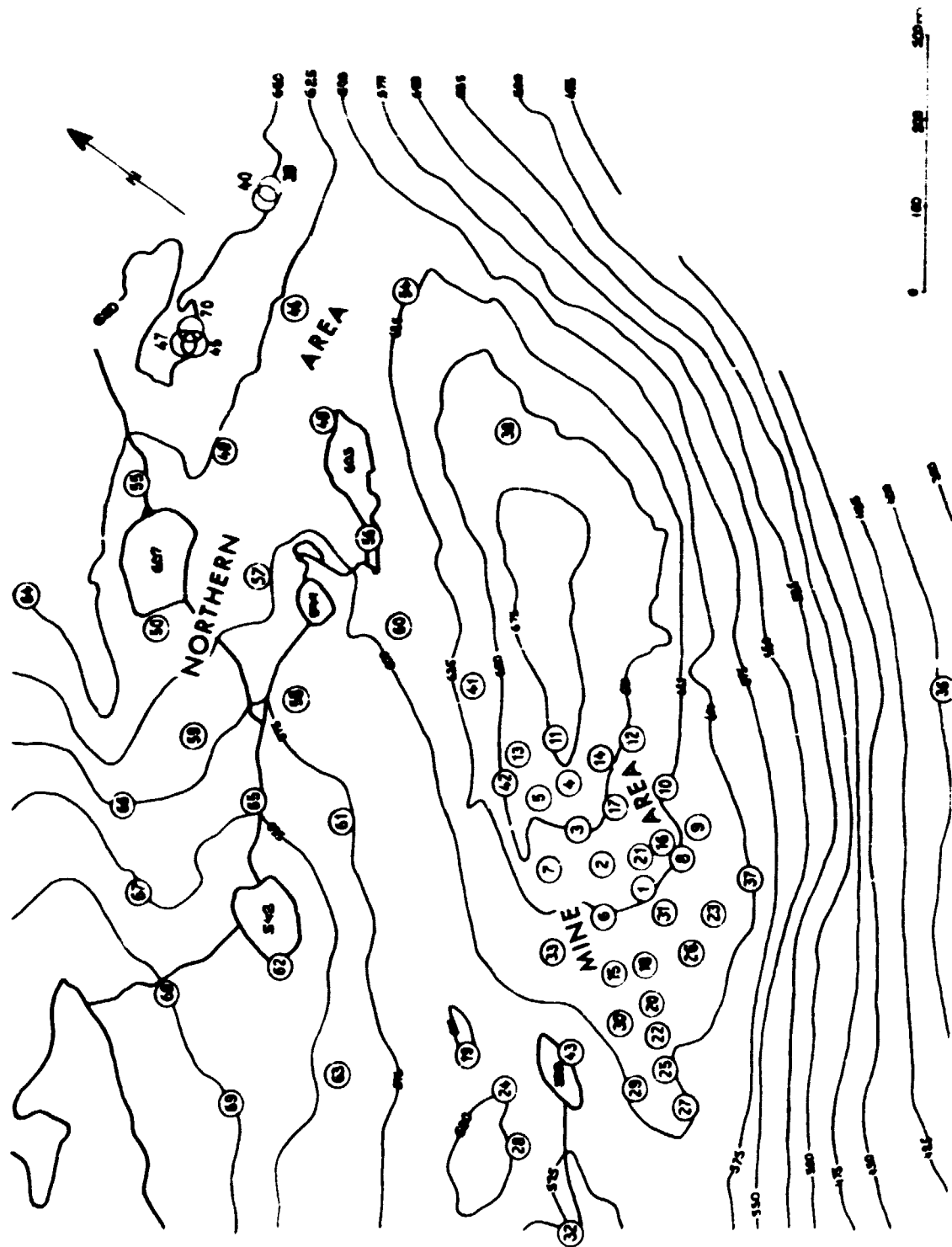


Fig. 1. Schematic map of the Kvanefjeld area with the location of drill holes.

1.2. Selection of material and sample preparation

Core material from various drilling projects at Kvanefjeld was available in the form of continuous drill cores 32 mm in diameter. The total number of drill holes is 70 which corresponds to approximately 9000 metres of core. From this material 102 samples were chosen to represent the following criteria: large variation in uranium extraction yield, and large variation in lithology and representative spatial distribution. Fig. 1 shows the distribution of drill holes at Kvanefjeld and Table 1 lists the positions of the rock samples selected for analysis.

Each drill core is fully documented petrographically in unpublished reports. The contents of U and Th are determined for the entire length of the drill core using gamma-ray spectrometry (Løvborg et al. 1972, Sørensen et al. 1974, Nyegaard et al. 1977).

The selection of representative samples on the basis of the combination of the petrological data and uranium content resulted in the documentation of all of the five principal rock types which represent the potential U ore, each with a large range in radioactivity. These are: medium to coarse grained (MCG) lujavrite, arfvedsonite lujavrite, aegirine lujavrite, deformed lava and naujakasite lujavrite. Naujaite and undeformed lava do not display sufficiently high uranium concentrations to warrant study. In addition, some steenstrupine-analcime veins and mineralized rock contacts were sampled. For each drill hole usually two (rarely one or three) of the most abundant types were selected (Table 1). The samples were taken from the parts of the drill core which displayed a reasonably constant uranium content over considerable core lengths.

High U contents in lujavrite comprising only negligible core lengths were not considered. However, the highest anomalies from the entire material connected with the above mentioned veins and contacts, were also included, mainly for their mineralogical interest.

The length of each sample was about 15 cm of drill core. It was split lengthwise into 3 portions using a rockcutting saw. The central slab, about 4 mm thick was used for autoradiography, microprobe and fission-track observations. One semicylindrical portion was saved whereas the other was used for the extraction experiments at Risø.

2. AUTORADIOGRAPHIC WORK

Autoradiographic study of the samples was undertaken with the aim of recognizing the distribution of radioactive minerals in the rock prior to their detailed study by more elaborate methods. The choice of material for thin section and polished thin sections was based on the autoradiographs.

In the course of the study it was confirmed that the autoradiographs of rock slabs represented an excellent record of the radioactive fabric of the rock types.

2.1. Techniques, scope of work

Autoradiographs were prepared in the photographic laboratory of GGU. The central rock slabs were placed with the cut surfaces directly on the emulsion side of the Fuji Lith. HO 100 film (13x18 cm). Exposure time of 14 days was chosen as it gave the optimal image.

The outline of the slabs was recorded together with their serial number in order to facilitate the comparison of photographic characteristics with radioactive fabric. The quality of radiograms was mostly very satisfying except for some cases of rough surfaces.

2.2. Results

Five categories of radioactive fabric were described in the studied material.

1) Homogeneous (or relatively homogeneous) fine to medium grained type of distribution of radioactive grains in the rock. This type is very abundant. Concentration of radioactive grains varies from high to low (Table 2, Fig. 2).

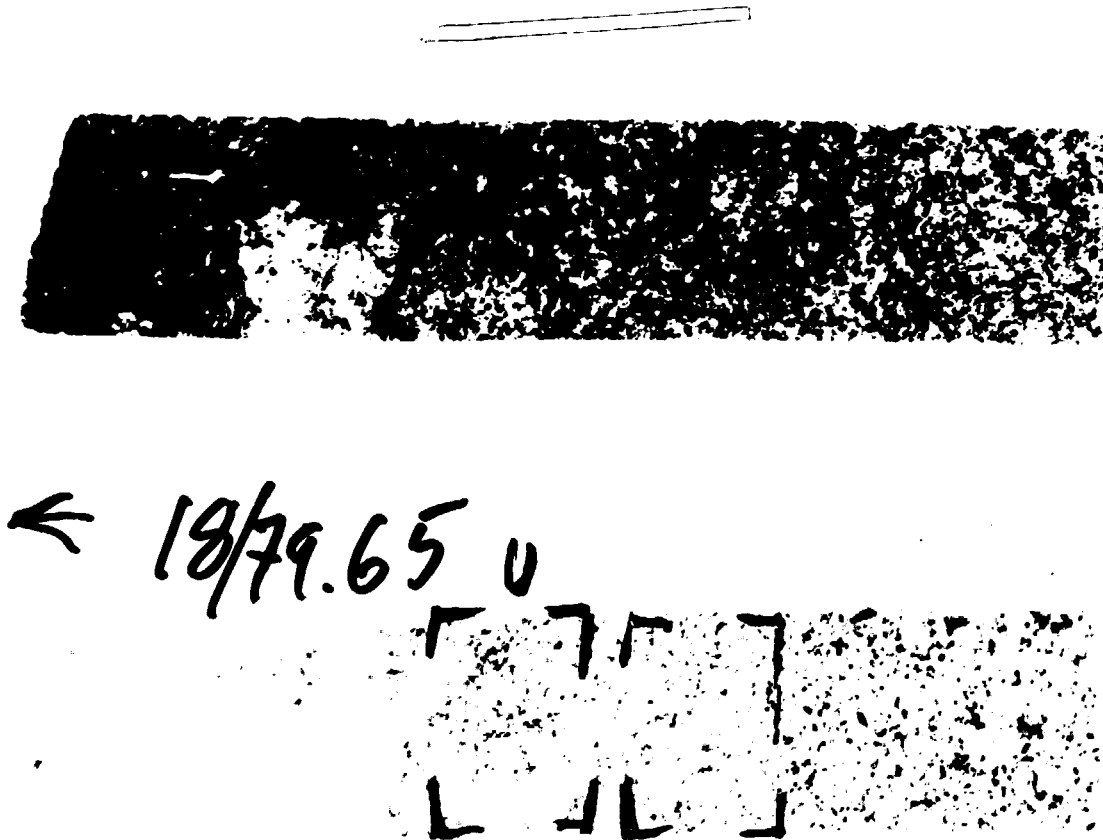


Fig. 2. Autoradiographs and the corresponding rock samples representing homogeneous distribution of fine to medium grained radioactive minerals.

2) Veins or layers with medium to fine grained radioactive minerals. The thickness of layers or veins is of the order of 0.5 to 1.0 cm. They are interlayered with more or less sterile layers of usually greater thicknesses. Distribution of ore-bearing layers is usually irregular (Table 3, Fig. 3).

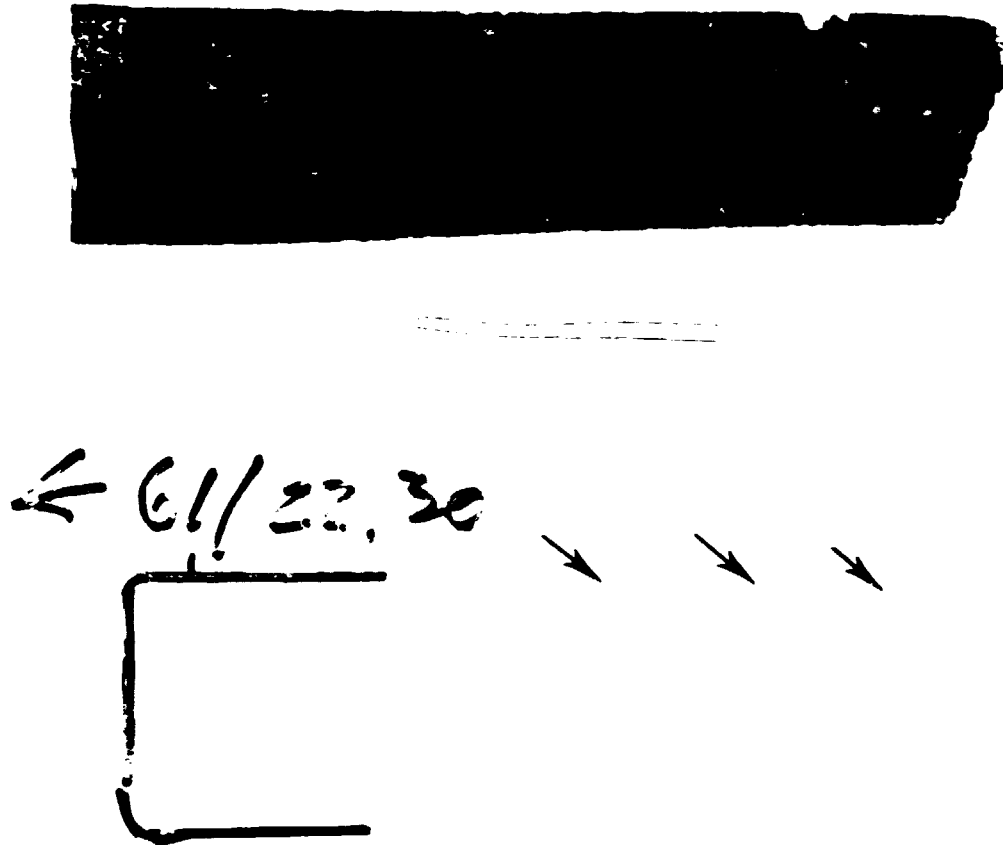


Fig. 3. Autoradiographs and the corresponding rock samples with veins or layers of medium to fine grained radioactive minerals.

3) Patches or nests of medium to coarse grained (0.5-1.5 mm in diameter) radioactive minerals (Table 4, Fig. 4). The distribution is always irregular and at lower concentrations they represent transition to the next fabric type.



← 17/11/10

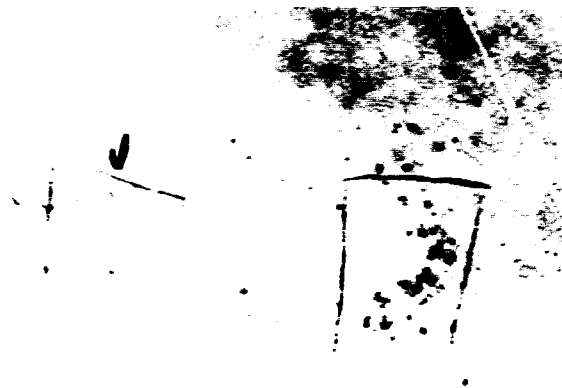


Fig. 4. Autoradiographs and the corresponding rock samples with patches or nests of medium to coarse grained radio-active minerals.

4) Individual scattered large radioactive grains. Typical diameter is about 2 to 3 mm. Medium to high concentrations prevail (Table 5, Fig. 5).

5) Rock samples which, inspite of being selected for their U content, left no discernible marks on their autoradiographs. Although containing a certain amount of uranium this type is termed "barren rock" (Table 6).

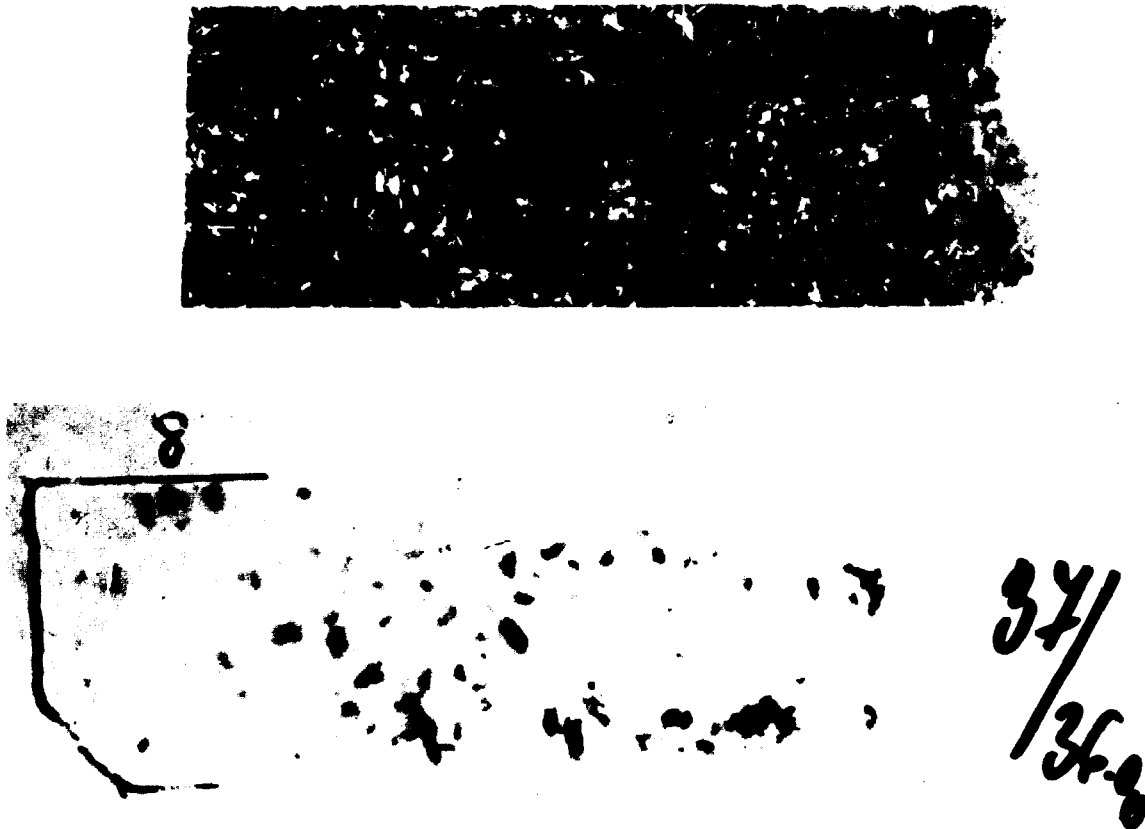


Fig. 5. Autoradiographs and the corresponding rock samples with individual large scattered grains of radioactive minerals.

2.3. Classification of lujavrites

Frequency diagrams of different types of radioactive fabric for the principal rock types disclosed interesting correlations (Fig. 6).

As expected, the radioactive minerals in the medium to coarse grained lujavrite primarily occur as large scattered grains and in appreciable concentrations. All the other fabrics occur in this rock type with much lower frequency.

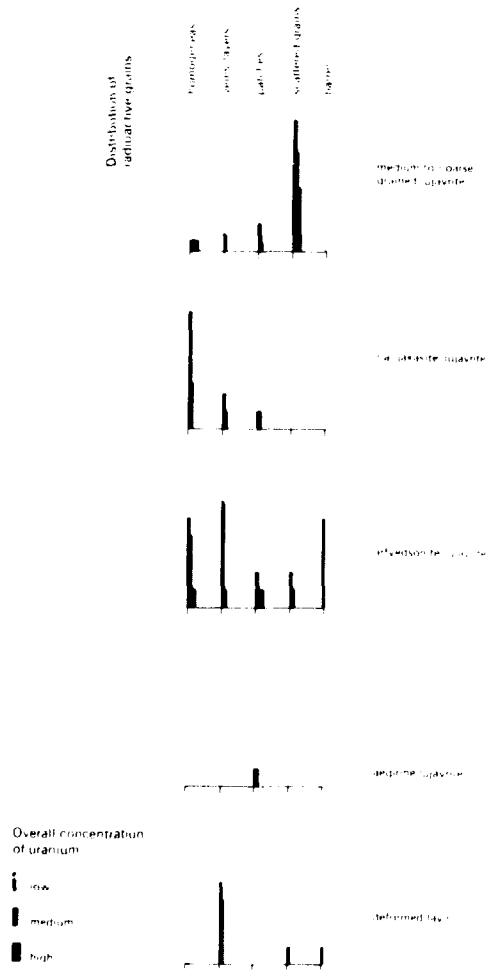


Fig. 6. Frequency distribution of different types of radioactive fabrics of principal rock types.

Naujakasite lujavrite displays predominantly the "homogeneous fine to medium grained fabrics" and medium to low uranium concentrations. Only in rare instances does the distribution of radioactive minerals occur in layers (patches).

Arfvedsonite lujavrite represents the most abundant rock type in the examined area. It shows a complete spectrum of radioactive fabric types and has uranium concentrations varying from high to low. The homogeneous, layered and "barren" types are the most abundant.

Only one specimen of aegirine lujavrite was examined (with a patchy distribution). This rock type is not abundant in the area and only this single sample was taken.

The principal fabric type of deformed lava is the layer type. The content of radioactive grains is usually medium to low.

3. MICROSCOPY

3.1. Scope of work

Petrographic characteristics of the studied rock specimens were described, and the optical study of steenstrupine in them was performed on thin sections and polished thin sections. The sections were selected from the drill cores by means of the autoradiographic study. The cuts selected for the thin and polished sections (about 3 x 4.5 cm in size) were taken from the portions which:

- 1) displayed radioactive grains of a character typical for the rock sample.
- 2) had concentrations of radioactive grains sufficiently high to warrant their representative cross-section in the finished sections.

The polished thin sections were also used for microprobe analyses and fission track investigations of uranium minerals. Altogether 97 sections were completely described. The microscope used in the study is ZEISS Universal.

3.2. General mineralogical description of lujavrites

For each of the studied specimens principal felsic, mafic and accessory minerals were determined and tabulated (Table 7a-e).

During the study we found that the degree of alteration of primary felsic minerals represented a general phenomenon independent of the boundaries between the various rock types in the area. A working hypothesis was made that the degree of alteration (called "hydration" below) might also partly control the alteration of steenstrupine. Furthermore, it could have influence on some stages of ore dressing. In the description, the rock specimens are therefore divided into 4 groups on the basis of the degree and sometimes also the type of hydration. The 4 groups are the following:

- 1) weakly hydrated rocks
- 2) medium hydrated rocks
- 3) very intensely to completely hydrated rocks
- 4) hydrated rocks with ussingite

In the distribution maps from Fig. 7 to Fig. 10 the black coloured sector of a circle may be 120° , 240° or 360° indicating that one, two or three samples belong to a single drill hole.

In the weakly hydrated rocks the bulk of the original felsic minerals are preserved. Among them nepheline, sodalite, microcline, albite and in some cases naujakasite are most abundant. Hydration processes primarily attack nepheline which is replaced from the margins by analcime. Sodalite is similarly attacked whereas naujakasite and albite are usually fresh in this group. As a rule natrolite occurs as an accessory mineral.

Weakly hydrated rocks are abundant in the studied area where they represent almost one third of the studied specimens (Fig. 7, Table 7a). This category contains a fair number of specimens from each of the principal rock types (arfvedsonite and naujakasite lujavrites, deformed lava and aegirine lujavrite). The only exception is MCG lujavrite - from which only one weakly hydrated specimen was found.

In the group of medium hydrated rocks the alteration of original felsic minerals is pronounced and the hydration products become substantial components of the rock. Nepheline

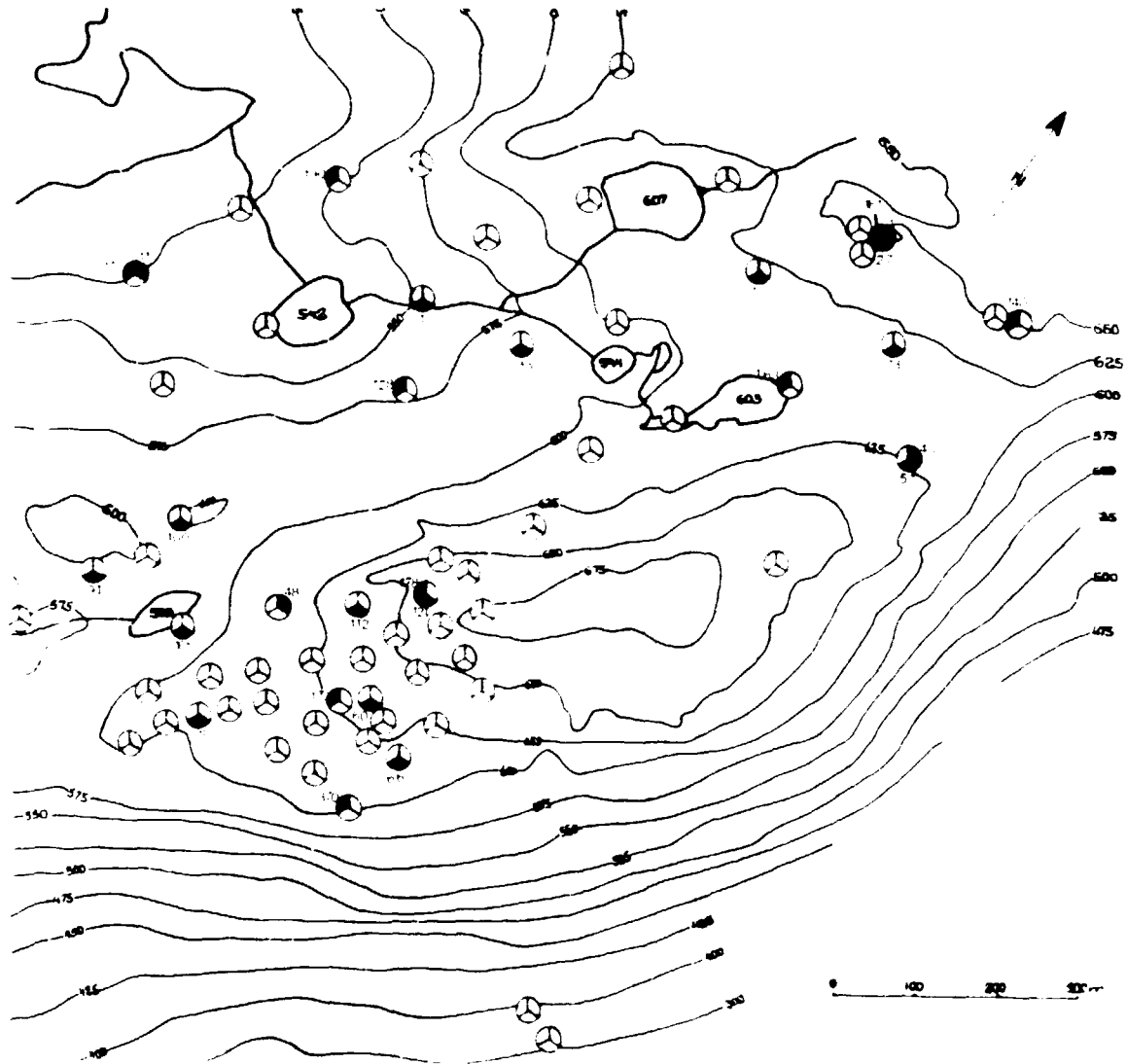


Fig. 7. Weakly hydrated rocks. Numbers denote depth (in meters) under surface.

is substantially replaced by slightly anisotropic analcime. It is still present in abundant, small to medium sized relics embedded in the analcime matrix. Microcline is also considerably attacked whereas albite seems to be still fresh. Besides abundant analcime, also natrolite represents a substantial component of the rock. This category is somewhat less common than the previous one and it mainly contains arfvedsonite lujavrite and naujakasite lujavrite (Table 7b). The spatial distribution can be seen from Fig. 8.

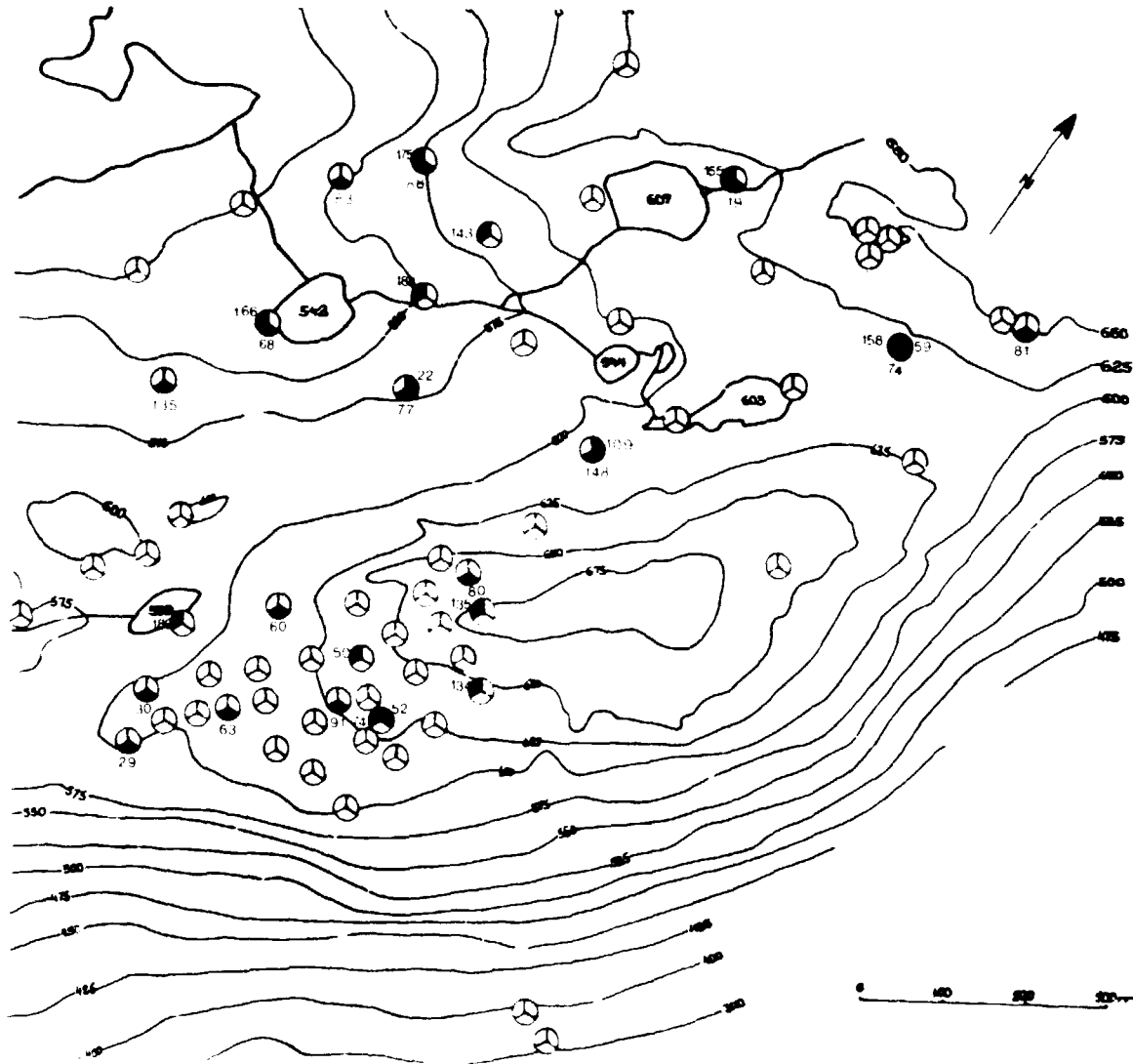


Fig. 8. Medium hydrated rocks.

In the group of very intensely to completely hydrated rocks analcime and natrolite represent the basic felsic minerals. Only small relics of the primary felsic minerals, nepheline, microcline, albite and sodalite, are occasionally found in the analcime matrix. Natrolite is present in much larger amounts than in the previous group; sometimes it is even more abundant than analcime. Besides the more common fibrous natrolite also fine to medium grained mosaic-like aggregates are present. This group again contains nearly all the rock types. Except for 2 samples it is confined to a relatively small area of Kvanefjeld - the so called "mine area" (Fig. 1, Fig. 9, Table 7c).

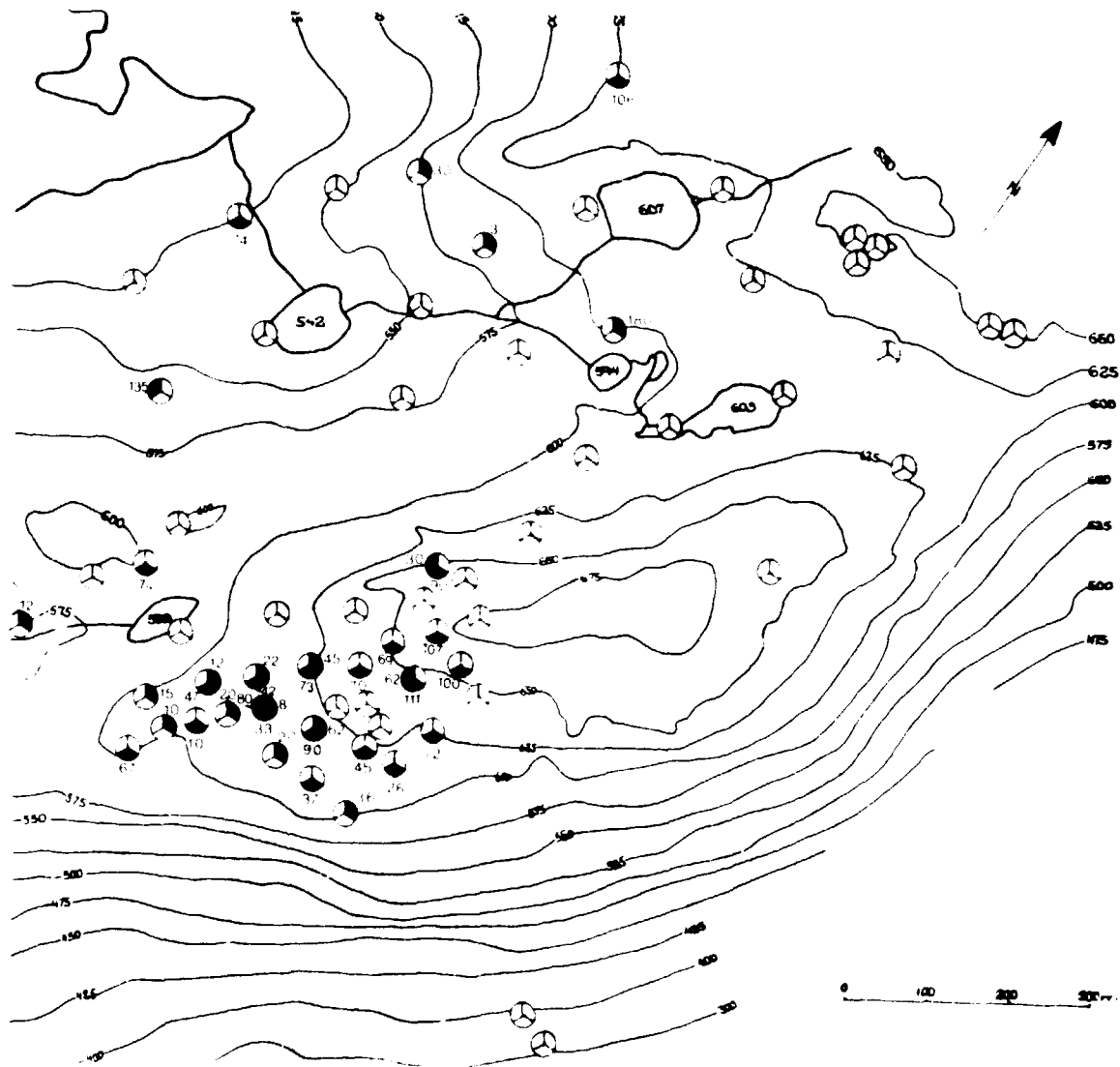


Fig. 9. Completely hydrated rocks.

A special type of strongly hydrated rocks are those which besides analcime and natrolite contain large amounts of large tabular crystals of primary microcline. In this rock type natrolite occurs in smaller amounts than analcime, albite is less abundant and nepheline was not found at all.

This group is almost entirely confined to one rock type - the MCG lujavrite and it represents the bulk of its samples. Again it is confined to the "mine area" (Fig. 9, Table 7d).

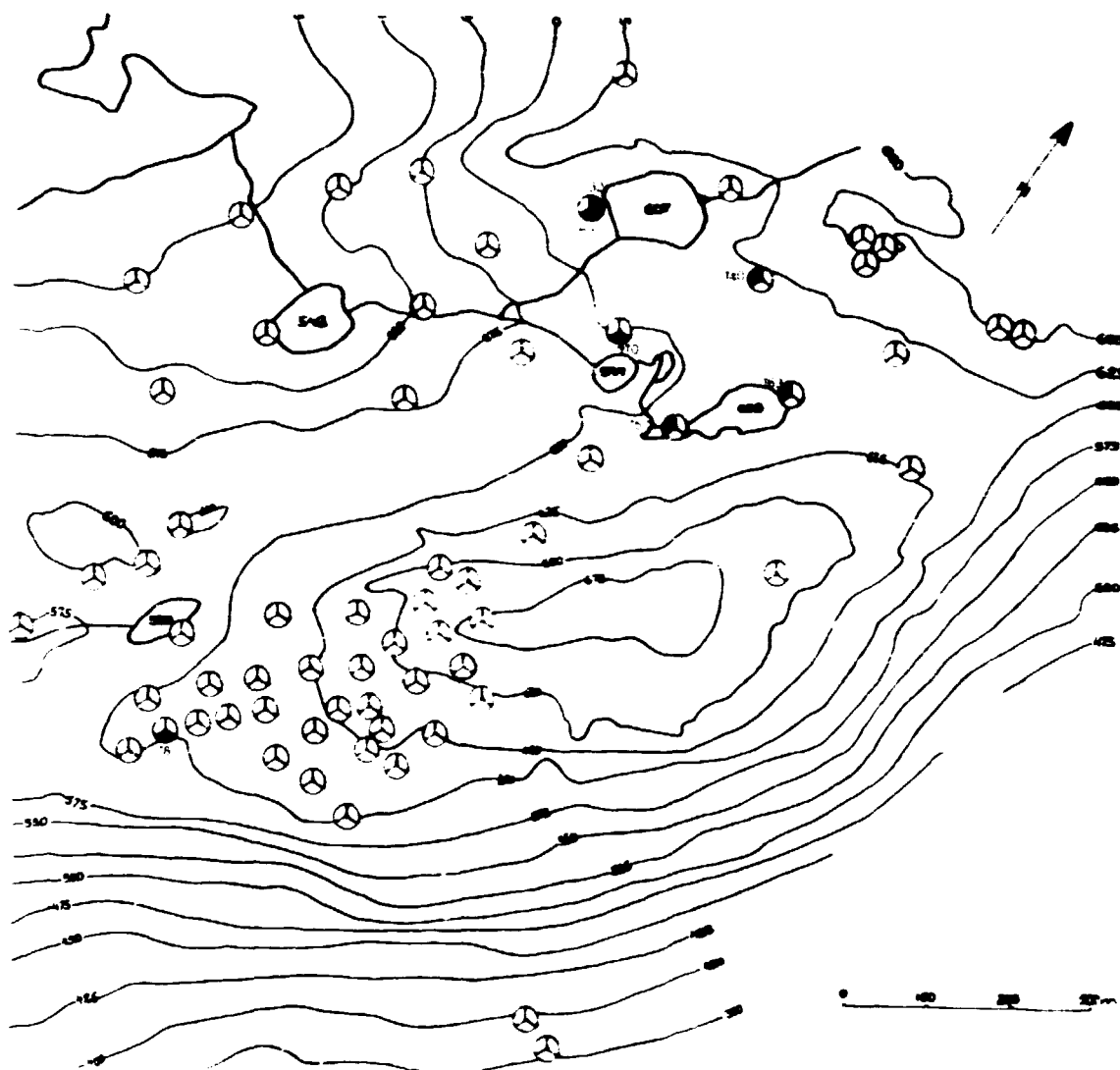


Fig. 10. Hydrated rocks with ussingite.

Another special type of alteration present in a small number of weakly, medium to strongly hydrated rocks is the development of ussingite + analcime. Ussingite seems to replace the original albite in the rock. Typical for this type is a very irregular development of hydration, with both hydrated and unaltered portions present in the same section. This type of hydration was found in arfvedsonite and naujakasite lujavrite, primarily confined to one area in the NW part of Kvanefjeld. (Drill holes 48, 49, 50, 57 and 25). (Fig. 10, Table 7e).

The various alteration processes show a distinct regional pattern. With rare exception the occurrence of strongly hydrated rocks is confined to the mine area drilled in 1958, 1962 and 1969. Nearly all samples of MCG lujavrite, taken from relatively shallow to medium depths of the complex MCG lujavrite intrusion, which is situated in fine grained lujavrite (Sørensen et al. 1974), are completely hydrated (with primary microcline). The specimens of arfvedsonite and naujakasite lujavrite taken from below MCG lujavrite are usually only medium hydrated. Strong hydration continues, primarily in arfvedsonite lujavrite and deformed lava, to NE of the MCG lujavrite intrusion, below the sheets of roof rocks.

The NW and N areas, drilled in 1977 yield about equal amounts of weakly hydrated and medium hydrated rock specimens (primarily arfvedsonite lujavrite). Sporadically strongly altered rocks occur. No distinct distribution pattern of hydration can be recognized except for the accumulation of ussingite-bearing rocks in one area close to the northern end. The latter rocks usually occur as the portions of arfvedsonite lujavrite overlain by a thicker volcanic complex (Nyegaard et al. 1977).

3.3. Description and classification of steenstrupine

Steenstrupine, the principal uranium-bearing mineral of the studied rocks was first described by Lorenzen (1881) from the material collected by J.K.V. Steenstrup. The mineral displayed trigonal symmetry and its formula was variably given as $\text{Na}_2\text{Ce}(\text{Mn}, \text{Ta}, \text{Fe} \dots) \text{H}_2 ((\text{Si}, \text{P}) \text{O}_4)_3$ (Strunz, 1944) or $(\text{Na}, \text{Ca})_3 \text{CaCe Nb} (\text{OH}, \text{F}) ((\text{Si}, \text{P})\text{O}_4)_3$ (Bøggild, 1953). The early authors only studied steenstrupine from veins and pegmatites. Buchwald and Sørensen (1961) and Sørensen (1962) were the first who also studied in detail the steenstrupine-bearing lujavrites, and this work plays an important part in the later large-scale exploration at Kvanefjeld (Wollenberg 1971; Sørensen et al. 1974).

The present microscopic study of thin sections from the drill cores of the Kvanefjeld area has shown that steenstrupine in the studied rock types occurs in two distinct forms which will be called A and B. They substantially differ in size, shape and origin.

The A type represents euhedral, small to medium (0.10-0.15 x 0.10-0.30 mm), fairly regular grains with hexagonal cross-sections, sometimes with rounded corners. In many cases it contains a small amount of inclusions, mainly arfvedsonite needles. The steenstrupine occurs as small crystals among the arfvedsonite and the felsic components indicating its primary origin.

The B type of steenstrupine is far less abundant. Its shape and size show considerable variation. The generally subhedral crystals are bounded by large crystal faces but they also partly enclose the surrounding minerals which have their own crystal outlines. The steenstrupine crystals of this type are in general heavily loaded with inclusions. Most abundant is arfvedsonite, followed by microcline, albite and nepheline. Sometimes analcime replaces primary lath-shaped felsic components enclosed in steenstrupine. Some of these large crystals are intimately connected with arfvedsonite felt. They are heavily loaded with this type of arfvedsonite so that sometimes they imperceptibly grade out into a felt-like arfvedsonite mass.

The steenstrupine of the type B was almost exclusively found in MCG lujavrite. Its formation may be connected with general metasomatism and recrystallization processes, producing the medium to coarse grained variety of lujavrite in the late stages of rock formation. The steenstrupine of the examined analcime - steenstrupine veins (described as the type C) is morphologically is fairly close to this category. Our observations and resulting classification are in general agreement with division of steenstrupine in the Ilfmaussaq lujavrites into two types by Sørensen et al. (1974) or into the type i and (ii & iii) by Sørensen (1962). In some samples of altered lavas the affinities of steenstrupine remain uncertain.

Steenstrupine of the Kvanefjeld area in most cases underwent alteration of varying intensity.

Practically all "unaltered" steenstrupine in all rock types of the Kvanefjeld area is already transformed into a metamict, optically isotropic state.

Combination of the two genetic types with the intensity and the structure of alteration yields 7 principle types of steenstrupine for the studied rocks:

type A: (primary, basically small to medium euhedral grains):

- a) metamict (unaltered)
- b) altered unzoned
- c) altered zoned
- d) extremely altered

type B: (late, metasomatic, basically large, subeuhedral grains):

- a) fresh anisotropic
- b) metamict (unaltered)
- c) altered

In the examined rocks fresh anisotropic steenstrupine of the type A only occurs as rims of the metamict or altered grains. It will be described further together with these categories.

The metamict steenstrupine of type A has a high refractive index and light creamy colour (Fig. 11). In some cases slight alteration on margins and cracks is observed.

The concentration of the mineral in the rock varies greatly from abundant, ca. 5-10% (sample 39/140), to scarce (sample 63/135.30). Samples of this type are evenly spread all over the examined area and occur at all possible depths depending on local geological conditions (Fig. 12).



Fig. 11. Metamict type of steenstrupine, Aa. Magnification 120x.

The unzoned altered type of steenstrupine, Ab, represents a broad group from occurrences in which only parts of the grains are altered to occurrences in which entire grains underwent alteration. Consequently, this type is the most abundant in the Kvanefjeld area (Fig. 14). It is characteristic for all rock types (except MCG lujavrite), and it is distributed all over the examined area except at places where one of the more special types of steenstrupine (described below) becomes typical. In many instances it occurs combined with other types of euhedral, A, steenstrupine, primarily with the metamict type.

In thin sections its colour varies between light yellow, brownish yellow and rusty brown for the more altered parts. Refractive index is lower than in the previous case.

Unaltered, fresh portions of the grains are isotropic whereas the altered parts represent fine-grained products which often display anisotropy in the form of aggregate polarization. The euhedral shape of steenstrupine crystals usually remains preserved. Only in some cases it becomes obliterated (e.g. 65/51).

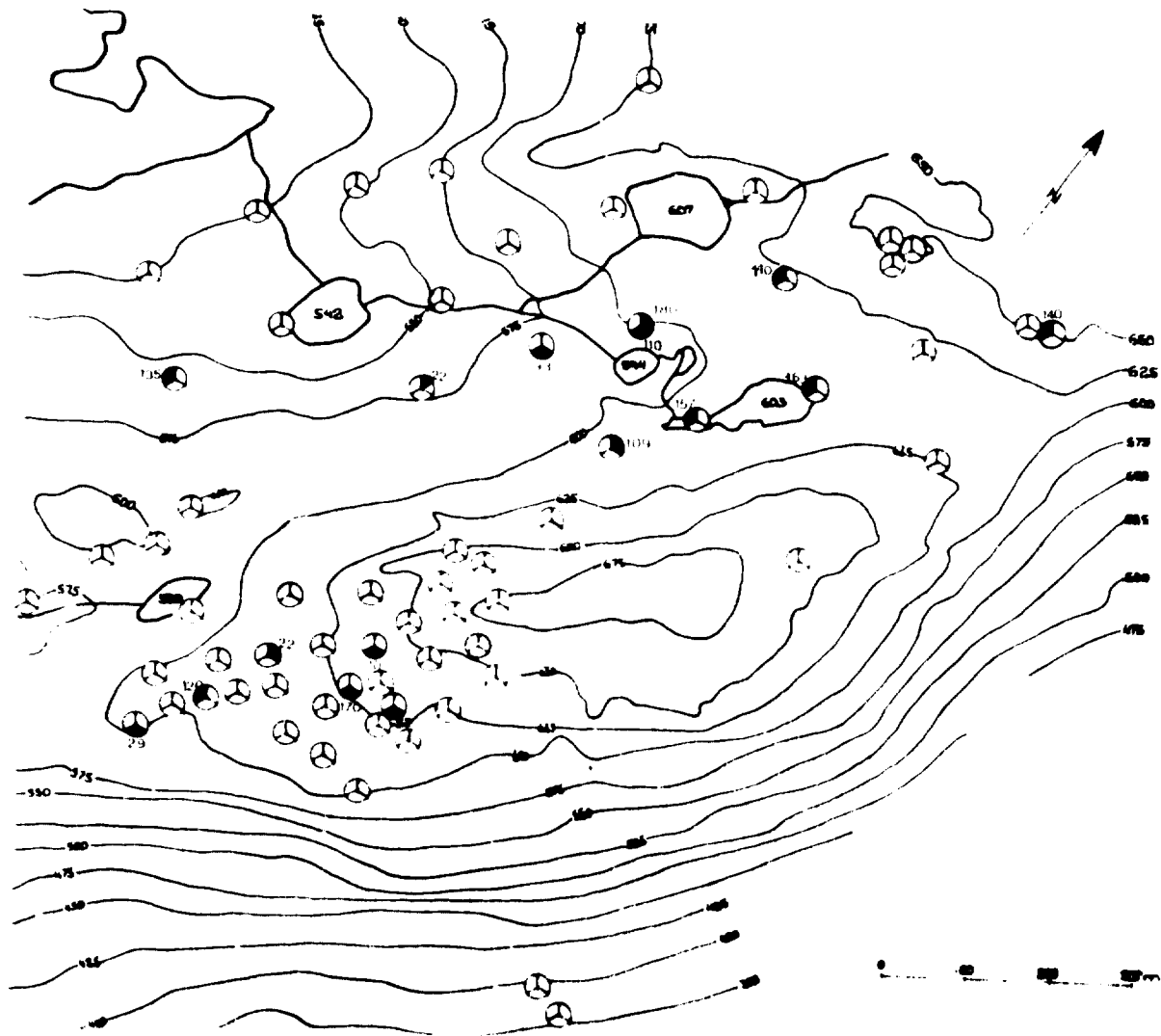


Fig. 12. Distribution of metamict steenstrupine, type Aa.

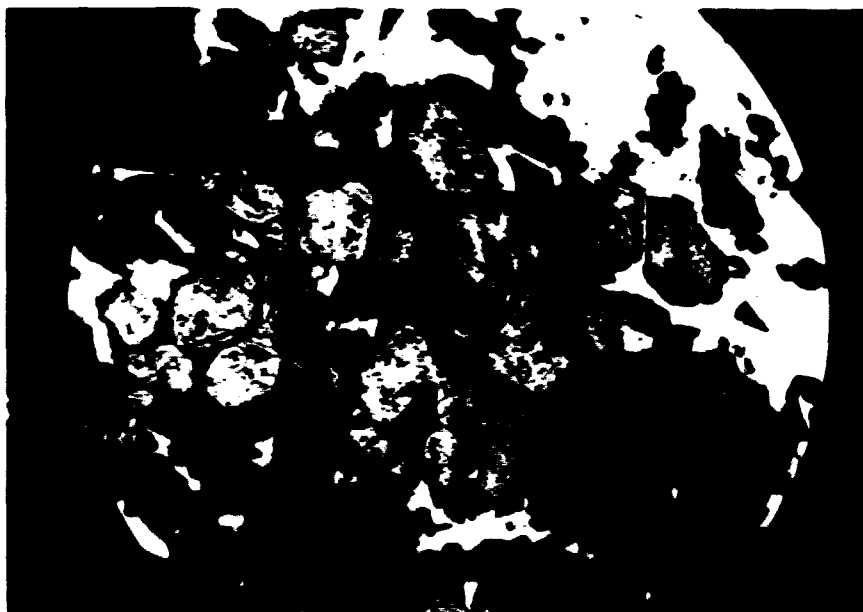


Fig. 13. Unzoned altered type of steenstrupine, Ab.
Magnification 90x.

This type of steenstrupine shows greater variability in size, than the previous one (Aa). The majority of the grains are bigger than in the Aa type (Fig. 13).

A very characteristic variety of the type A steenstrupine, occurring primarily in arfvedsonite and naujakasite luja-rite of the mine area is the altered zoned variety. The zonation manifests itself in the partly to fully altered grains. It is not observed in metamict grains and extremely altered grains. Thus we presume that the primary compositional zonation appears only in the process of alteration which will develop in the compositionally suitable grain portions. Types of zonation and the intensity of alteration vary within broad limits. In the most abundant case steenstrupine displays dark altered core and light rims which are in most cases anisotropic with single-crystal extinction (Fig. 15). Opposite cases are known: in 28/90 steenstrupine has light isotropic cores and altered dark rims (Fig. 16). In a number of samples also grains with two or more altered and unaltered zones are present. It should be stressed that the zonation types and alteration stage is uniform

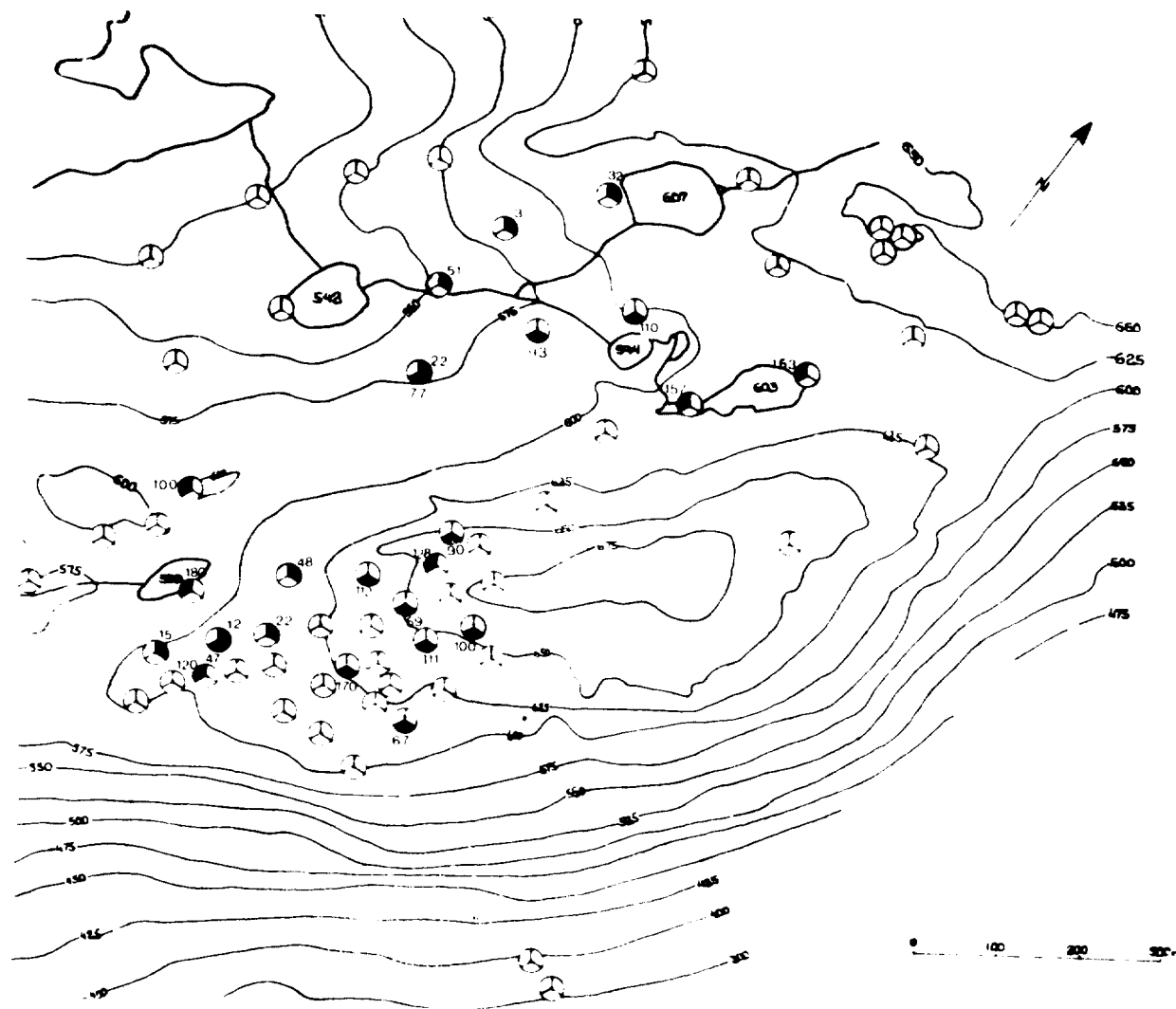


Fig. 14. Distribution of unzoned altered type of steenstrupine, Ab.



Fig. 15. Altered zoned variety of steenstrupine, Ac.
Magnification 120x.



Fig. 16. Altered zoned variety of steenstrupine, Ac. in
naujakasite lujavrite. Magnification 90x.

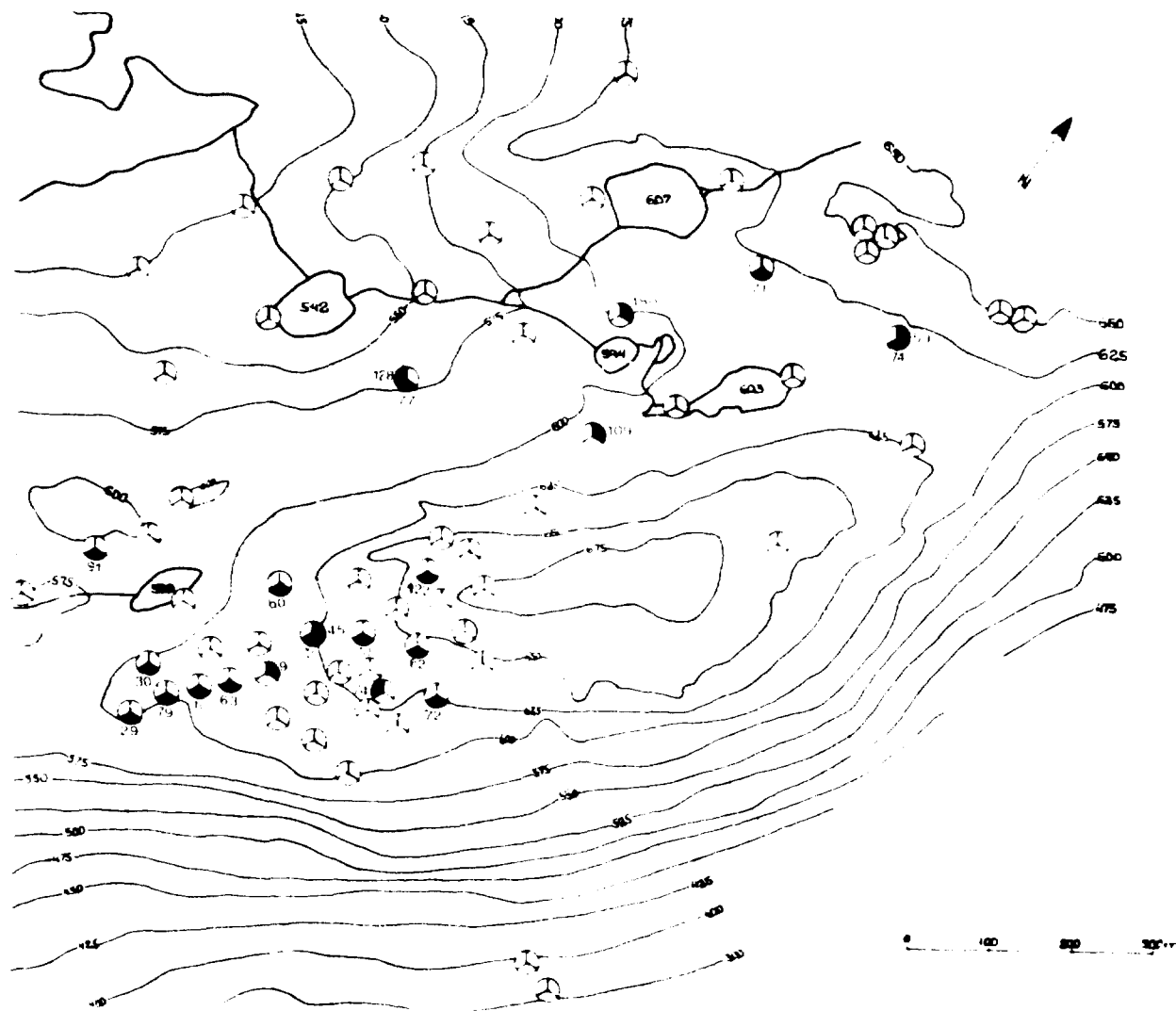


Fig. 17. Distribution of altered zoned variety of steenstrupine, Ac.

and typical for each sample. In this group there are almost no samples which contain different types of steenstrupine in thin section. The map (Fig. 17) of the distribution of various steenstrupine types suggests that the zoned steenstrupine is primarily situated in the upper layers of fine grained lujavrite in the mine area, below the layers of MCG lujavrite and altered lava.

In the case of extreme alteration of steenstrupine of type A the shape of (completely altered) grains becomes gradually obliterated. They become nebulous in thin section and disintegrate (Fig. 18). Sometimes they may be replaced by other phases, primarily neptunite.

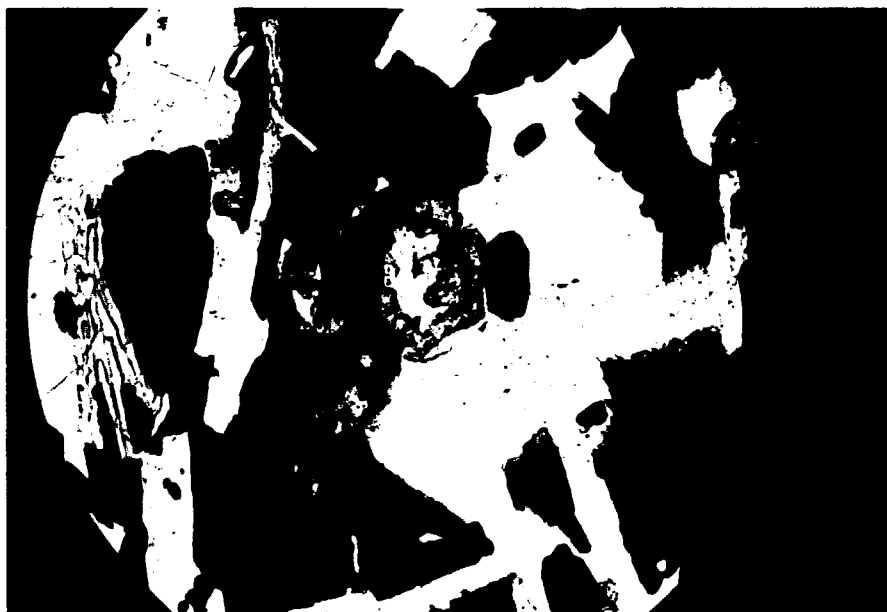


Fig. 18. Completely altered steenstrupine, type Ad.
Magnification 120x.

The type of extreme alteration varies from section to section. The usual type of alteration is replacement by very dark rusty brown material, nearly opaque in thin section. Original inclusions are still present in this case and, except for eudialyte they remain unaltered. In other cases the rusty patches in the altered grains of steenstrupine alternate with analcime. Even in the cases where the original grain disintegrated into

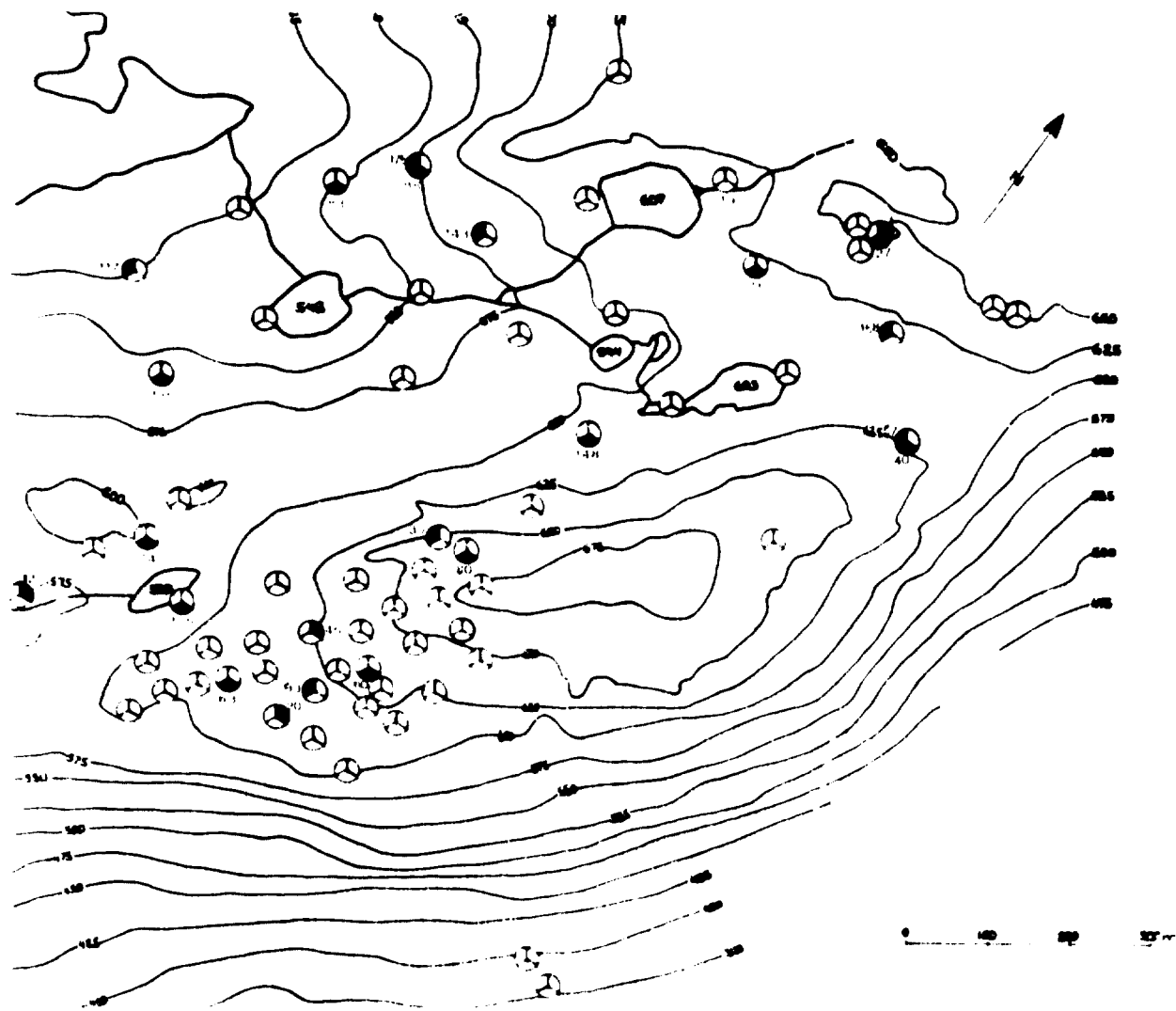


Fig. 19. Distribution of completely altered steenstrupine,
type Ad.

nebulous relics the original inclusions can still be seen. In this case arfvedsonite is usually replaced by aegirine. The rusty alteration product will in these cases change into a loose gray network. Rocks with this type of steenstrupine alteration occur scattered among the rocks with altered zoned and unzoned steenstrupine in the old mine area. Our results (drill holes 54, 46 and 70) suggest that they might form an uninterrupted area in some portions of the northern part of the examined region (Fig. 19).

The shape of the crystals of B type steenstrupine and the inclusions in them have already been described (part 3.3, § 4).

The fresh anisotropic type of steenstrupine, Ba, is very rare. It occurs mainly in the metamict isotropic grains as rims or isolated parts. Anisotropy is usually weak and not easy to observe. As an example we can quote No. 18/78.60.

The metamict B type of steenstrupine, Bb, is not so abundant in the studied area as the A type. Colour in thin section varies from light yellowish to light brown. In this case the brown colour does not represent an alteration feature although the darker brown portions indicate incipient alteration. This type of steenstrupine is isotropic (Fig. 20).

The amount of metamict B type steenstrupine varies from section to section, in general it makes 5%, in some cases up to 10% of the volume of the rock. Crystals are usually large and they are often interconnected by thin cracks in the surrounding minerals which apparently were formed when the volume of steenstrupine crystals increased on metamictization. In a few cases, namely in the section 37/36, large grains of steenstrupine were replaced in their marginal parts and along fissures by grains of monazite associated with uranothorite and U-bearing Na-Zr silicates. They pseudomorph the shape of the original steenstrupine crystals. Alteration processes which can be locally observed usually start along fissures as well.



Fig. 20. Metamict type of steenstrupine, Bb. Magnification 30x.



Fig. 21. Metamict steenstrupine, type Bb, with the apical parts replaced by monazite (light). The pseudomorph retains the shape of the original steenstrupine crystal. Magnification 30x.

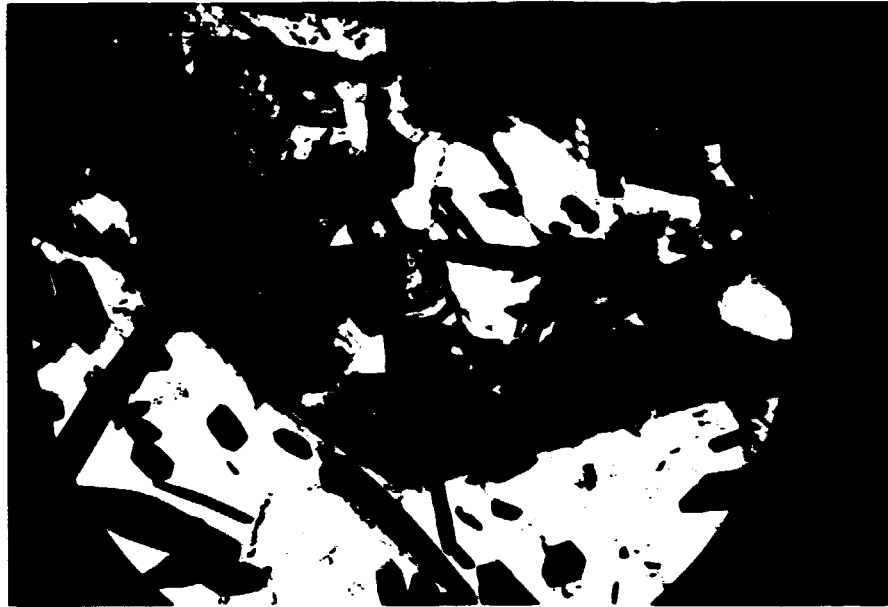


Fig. 22. Metamict steenstrupine, type Bb, partly replaced by monazite. Steenstrupine orange red, monazite dark brown. The light brown mineral in the centre is uranothorite. (Fig. 33 shows the fission tracks of the same section). Magnification 90x.

Fig. 23 shows that this type of steenstrupine is concentrated in the southern part of the "mine area". It is bound to MCG lujavrite and usually occurs in the upper part of the drill holes.

The altered B-type steenstrupine, Bc. In most cases it follows the "metamict" Bb type. In the drill holes 4/107 and 9/67 it occurs in arfvedsonite lujavrite alongside with the A type. In both cases the rock contains veins of MCG lujavrite and of analcime so that we may consider the subhedral, B-type crystals to be of later, metasomatic origin.

The alteration of the B-type steenstrupine proceeded differently at different localities. The replacement by monazite has already been mentioned (Fig. 21, 22). In other cases (18/79, 4/107, 30/47) the alteration has a similar character to that in the Ab type. The altered portions are slightly to strongly ani-

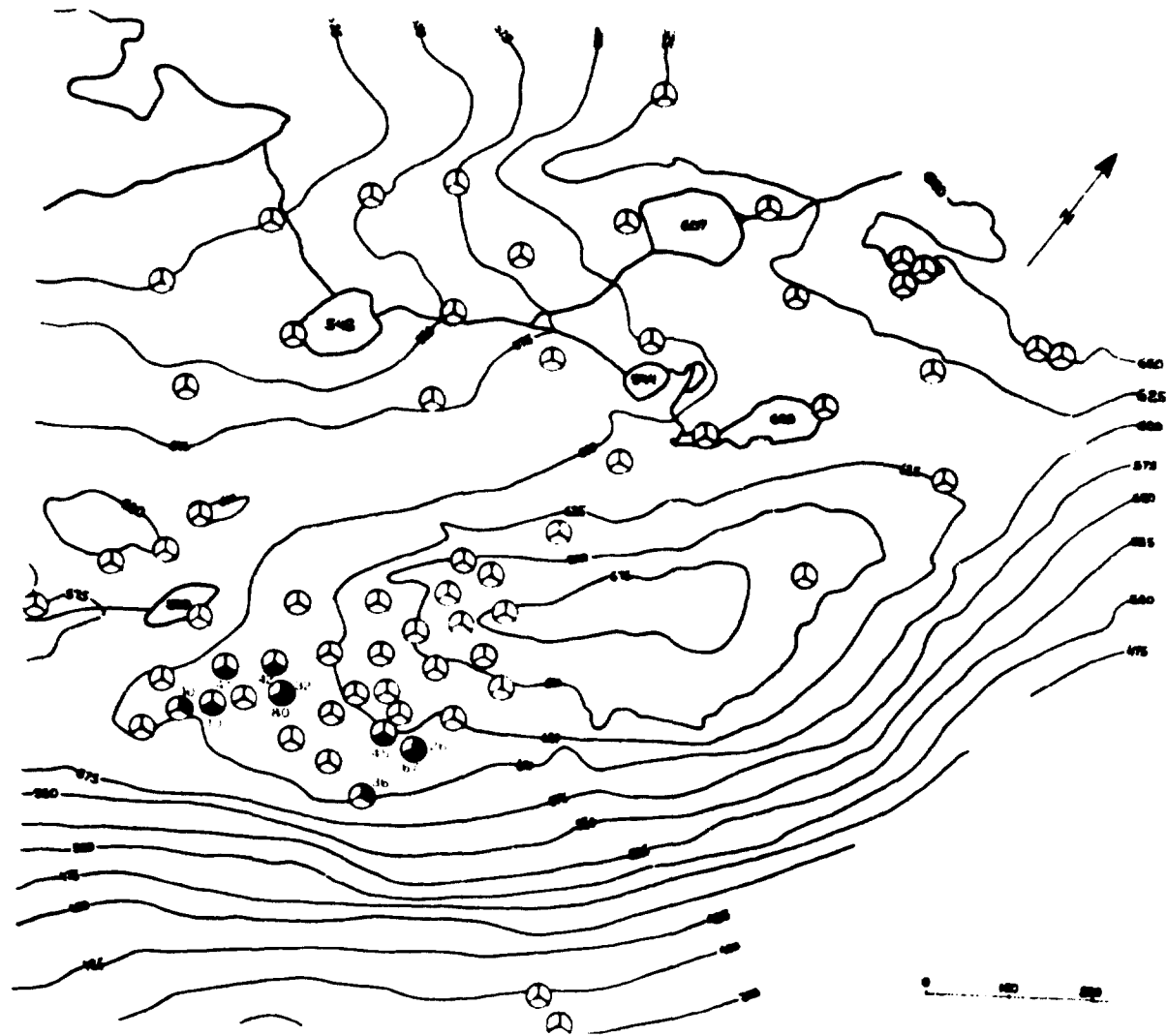


Fig. 23. Distribution of metamict type of steenstrupine, Pb.

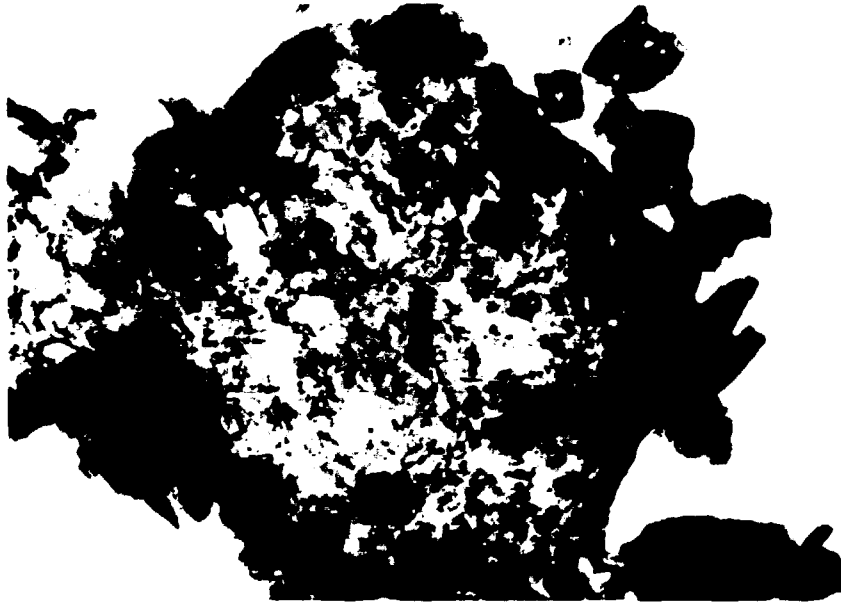


Fig. 24. Strongly altered steenstrupine, type Bc. Magnification 120x.

sotropic and besides the dark components they most probably contain natrolite and analcime. In the case of strong alteration some parts of the original steenstrupine grains are replaced by neptunite (Fig. 25).

When the frequency of different types of steenstrupine is plotted against the studied rock types the following conclusions can be drawn (Table 8):

- 1) The degree of alteration of steenstrupine cannot be considered as a function of the rock type for all the three principle rock types bearing the A type steenstrupine, arfvedsonite lujavrite, naujakasite lujavrite and deformed lava.
- 2) As mentioned above, the B type steenstrupine ranges from fresh to metamict and altered and is practically limited to MCG lujavrite.
- 3) Intensity of alteration of steenstrupine is not a function of the intensity of hydration of the rock. Thus completely altered steenstrupine frequently occurs in weakly hydrated

rocks, and fresh or weakly altered steenstrupine can frequently be found in completely hydrated rocks.

The geographical distribution of different steenstrupine types has already been discussed. The trend of the completely altered steenstrupine and especially of the "barren rocks" to occur in a distinct area along the NW and N margins of Kvanefjeld should again be stressed.

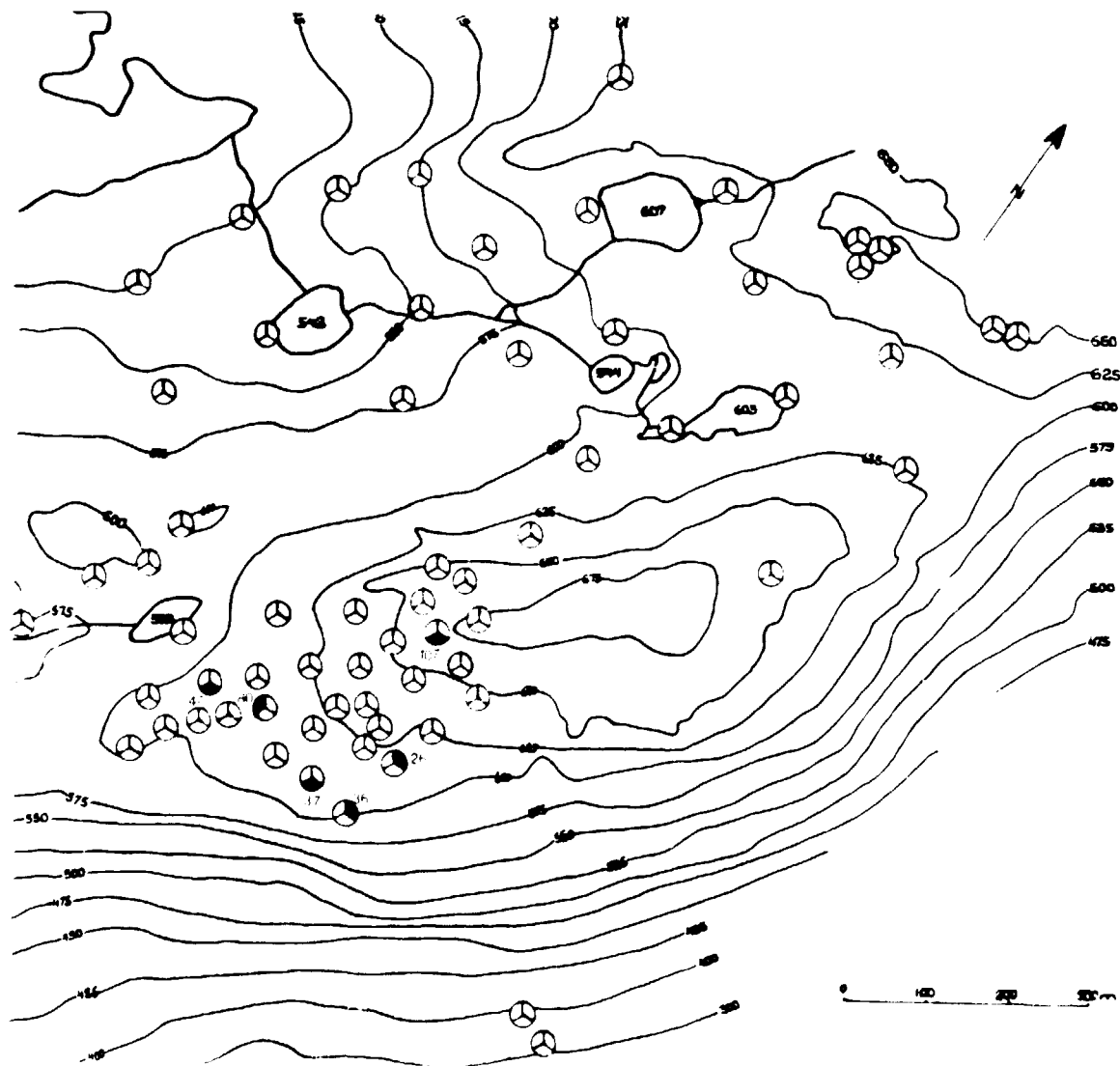


Fig. 25. Distribution of altered metamict steenstrupine type Bc.

4. FISSION TRACK INVESTIGATIONS

4.1. Techniques, scope of work

For the location and determination of U-bearing minerals in thin sections of the studied rocks, the fission track method was used. The method was developed by Fleischer et al. (1965). It was applied to the Ilímaussaq rocks for the first time by Wollenberg (1971) whose modification of the method is followed to some extent in the present study.

As a solid state fission-track detector we used lexan polycarbonate plastic 0.75 mm thick. A lexan slide is firmly attached to the surface of the polished thin section in such a way that two edges of the lexan slide and of the section exactly coincide. A pack of up to 6 "sandwiches" is irradiated by thermal neutrons in the facility at the DR 3 research reactor at Risø. After some experimenting an irradiation time of 1 minute was chosen. Uranium standards are placed at the front and rear ends of the package.

The standards represent the Ca-Al-Si glass with the eutectic composition in the $\text{CaO-Al}_2\text{O}_3\text{-SiO}_2$ system, to which uranium oxide was added in order to obtain the following U_3O_8 concentrations:

0 ppm	2 500 ppm
500 ppm	5 000 ppm
1 000 ppm	10 000 ppm

The glasses were prepared by weighing out components and each of the mixtures was melted at 1500°C and homogenized in a mortar three times. The method was developed by Gamborg-Hansen (unpublished). They were all checked by delayed-neutron counting (for 10 sec) after neutron irradiation at the research reactor DR 3 at Risø (for 20.3 sec). The results (463, 2417, 5047 and 9776 ppm U_3O_8 for the respective glasses) confirm that the original U contents were preserved during preparation.

The fission tracks in the detectors were developed by etching them with 6N NaOH at 75°C for 10 to 15 minutes. Because of the large amounts and frequent inhomogeneity of the radioactive grains, the uranium content in them was estimated by comparing the density of tracks produced by a grain (or by its part, or a zone in it) with the uniform track densities produced by the six standard glass compositions. We used lower magnifications and worked in the same way as if using the empirical blackening curve on X-ray films. It should be noted that the total U contents of the rocks have been determined by gamma spectrometry of the drill cores (Table 1).

A sliding table (machine work by the workshop of the Geological Central Institute, University of Copenhagen) was constructed for use under the microscope for the fast comparison of the fission track record on the lexan slide with the mineralogy of the original polished thin section. The lexan slide and the thin section are placed side by side on this table and can be centered using the two edges they had aligned in common during their exposure. Thus swinging the table back and forth, the grain and its fission track image will be brought into the same position in the microscope field of view. In this way we avoid the problems in locating and determining the radioactive minerals in the fine grained rocks which contain large amounts of dark minerals. The use of Wollenberg's (1971) method (i.e. observations on the detector-and-rock section sandwiches) would slow down the work considerably.

4.2. Associations of U-bearing minerals

The fission track studies enabled us to localize and determine all the uranium-bearing minerals in the studied rock samples. It was found that in general steenstrupine represents the most important U-bearing mineral and that the contents of uranium in steenstrupine are in direct relationship with its preservation/in situ alteration. In some rocks steenstrupine is associated with other, quantitatively less important U-bearing minerals, or it is decomposed and recrystallized into an association of secondary products.

The following associations include the types of primary mineralization, its alteration as well as the most typical secondary products. The following associations were recognized:

a) Rocks with steenstrupine of the type A

- 1) rocks with metamict and/or altered steenstrupine, $Aa+Ab$.
- 2) rocks primarily with zoned steenstrupine, Ac .
- 3) rocks with all types/degrees of steenstrupine alteration, $Ab+Ac+Ad$.
- 4) rocks with extremely altered, recrystallized and replaced steenstrupine, Ad .
- 5) rocks with metamict and altered steenstrupine (as 1) and with a metamict high-uranium Y-Zr silicate.
- 6) rocks with extremely altered steenstrupine which displays accumulations of U-rich phases.
- 7) naujakasite lujavrites with zoned steenstrupine and a low-U "naujakasite replacement product".

b) Rocks with steenstrupine of the type B

- 1) rocks with metamict and altered, and recrystallised steenstrupine. Among secondary products are monazite, uranothorite, thorianite, neptunite. In some cases it associates with extremely altered steenstrupine A, i.e. $Bb+Bc+Ad$.
- 2) rocks with altered steenstrupine, Bc .
- 3) metamict and altered steenstrupine and an U-bearing Zr-Al silicate.

c) Impregnations of fine to coarse grained metamict to altered steenstrupine of uncertain type in the altered lava.

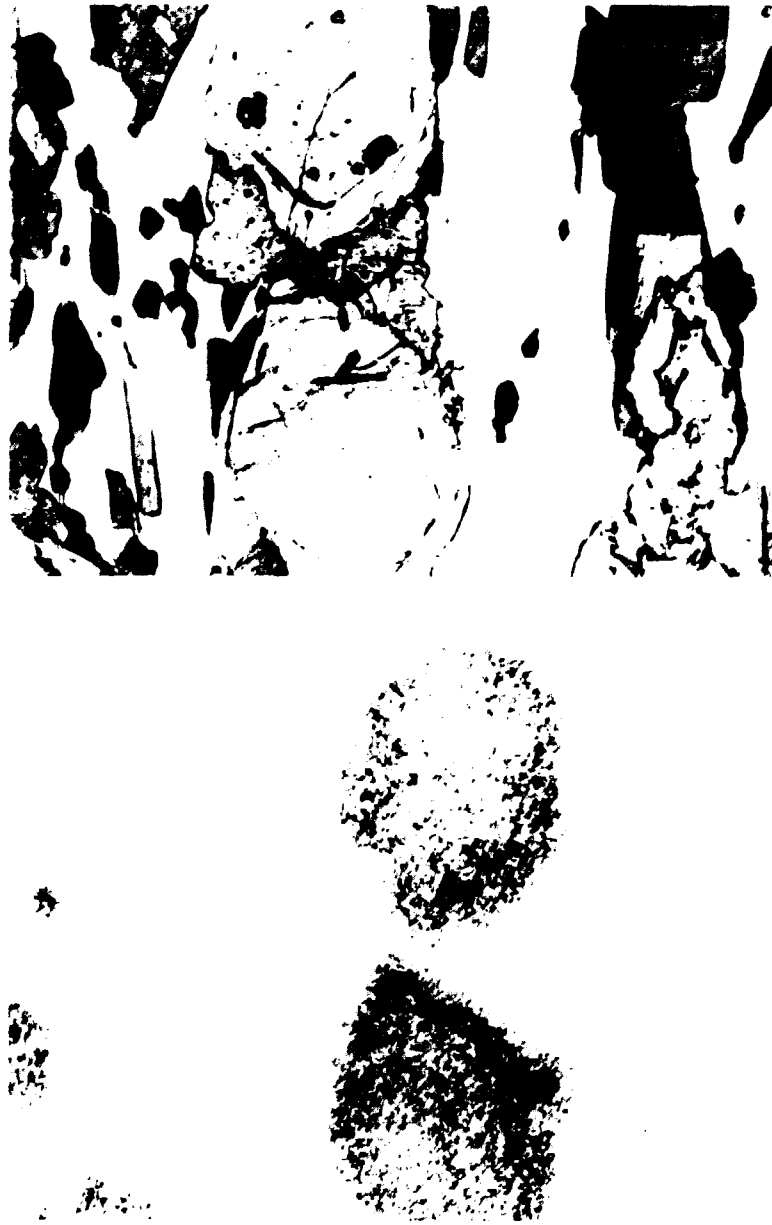


Fig. 26. Microphotograph of the thin section and fission track image of metamict steenstrupine, Aa. Magnification 120x.

4.3. Description of individual associations and the uranium contents in the minerals.

A-1 Rocks with metamict and/or altered steenstrupine (Aa and Ab) as the predominant U-bearing mineral

The Aa steenstrupine usually forms small isotropic grains with fission track density corresponding to 2000-4000 ppm U_3O_8 in some rock samples, and to 3000-5000 ppm U_3O_8 in other samples (Fig. 26). In general, the metamict A steenstrupine does not exceed 5000 ppm U_3O_8 . In most cases it alternates with altered unzoned steenstrupine Ab with higher fission track densities, usually between 5000 and 7000 ppm, sometimes in more altered parts up to 10000 ppm U_3O_8 . In some sections, a characteristically twinned Zr-Al silicate with the same U concentration as in the Aa steenstrupine occurs.

Individual sections (all data ppm U_3O_8):

Sample No.	Aa	Ab	Notes
57-109.00	2500-4000	5000-7500	Aa < Ab
58-93.00	3000-4500	5000-7500	Aa < Ab
56-157	3000-4500	5000-7500	access.silicate 3000-4500
70-16.10	2000-4000		Aa < Ab, access.silicate 2000-3000
60-147.70	2000-3000	inhomogeneous	Aa < Ab 5000-7000 up to 10000
27-29	~ 5000	> 5000 in alt.parts	Aa (Ac)

A-2 Rocks primarily with zoned steenstrupine

In this group zoned steenstrupine, Ac, in which metamict and altered zones alternate, represents the principal U-bearing mineral. Smaller amounts of Ab or Ad steenstrupine may also be present. Differences in uranium contents between the zones are well expressed in fission track images for the cases with broad zones or with simple zonation. (Fig. 27, 28). However, only



Fig. 27. Microphotograph of the thin section and fission track images of altered zoned steenstrupine, Ac in arfvedsonite lujavrite. Magnification 30x.

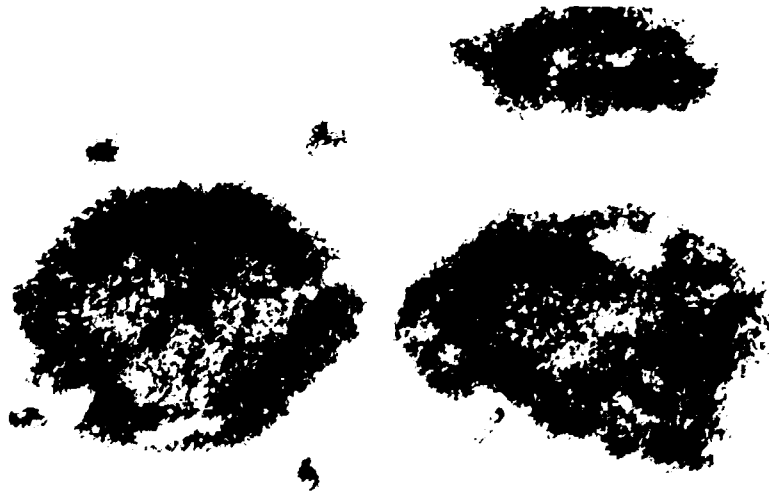


Fig. 28. Detailed view of steenstrupine Ac from Fig. 27.
Magnification 120x.

average U contents over the zoned parts can be obtained in the cases with narrow, repeated zones. For some samples an association of Ac crystals with abundant very fine-grained now altered (Ab or Ad) steenstrupine, dispersed throughout the rock, is typical.

Individual sections (all data in ppm U_3O_8):

Sample No.	Ac	Notes
33-48.00	7000-10000	Numerous small steenstrupine grains in arfvedsonite etc., < 7000. Britholite (creamy yellow, high n , often altered) ...1000. Wavelength scan indicates Si, P, Ca, Th, ? K, La, Ce and Fe as major elements whereas Y, Na, Mn, Nd, Sm and Pb as minor elements.
5-121.30	ppm U_3O_8 8000-10000 dark altered core	
16-52.00	isotropic 8000. Often only just observable light zonation in metamict steenstrupine. Altered zones/parts ≥ 10000	In aegirine-natrolite matrix: numerous small Ad crystals with inhomogeneous distribution of tracks 4000-7000
61-77.05	Pronounced multiple zonation, narrow zones: average: 2500-5000. Broader zones: light zones 2500-4000; highly altered zones 5000-7000.	Small amount of Ab, Ad; in the natrolite-rich zone: very abundant small grains of steenstrupine-strings of grains Ab to Ad 4000-5000
22-120.30	≥ 5000-6000; most altered parts ≤ 10000	A few Ad grains with high U- accumulations occur
6-44.90	Essentially metamict with just observable zonation. Light zones ~ 2000; darker zones ~ 3000	

7-112.20 As the previous one
43-105.20 Light zones 5000;
altered zones \geq 7000

A-3 Rocks with all types/degrees of steenstrupine alteration -
Ab+Ac+Ad

The range of fission track densities reflects the broad range of alteration types present in the same rock. Density of fission tracks in the altered Ab type of crystals corresponds to 4000-5000 ppm U_3O_8 in less altered, lighter parts and 7000-8000 ppm U_3O_8 in altered parts. In the latter, but primarily in the extremely altered Ad grains U-rich accumulations with over 10000 ppm U_3O_8 are found. The Ad type otherwise displays from 500 to 2000 ppm U_3O_8 .

Individual sections (all data in ppm U_3O_8):

Sample No.	Ab,c	Ad
46-73.85	Large inhomogeneously altered Ab crystals: less altered 4000-5000, more altered 7000-8000; high-U accumu- lations 10000; rare zonation	5000-2000
30-12.50	Large Ab as above; cracks with low U-content around Ab	Numerous small Ad crystals with U- rich accumulations 2000-5000; "erikite"/ monazite 500-1000
29-29.85	Ab, c as 46-73.85	

A-4 Rocks with extremely altered, recrystallized and replaced
steenstrupine

The grains of steenstrupine are completely altered into a mixture of secondary phases among which mostly natrolite and monazite, sometimes neptunite can be discerned. In other cases

a gray irregular network results. The shapes of the grains are obliterated, and sometimes their cores are completely replaced by non-radioactive material. As a rule their fission track records are very irregular, mostly 2000-3000 ppm U_3O_8 , in a few instances 5000 ppm U_3O_8 . Monazite shows 2000-3000 ppm U_3O_8 .

Individual sections

Sample No. 46-157.75, 66-87.55, 69-117.05, 21-59.55,
59-61.85, 13-80.00.

A-5 Rocks with metamict and altered steenstrupine (as A-1) and with a metamict (high-uranium) Y-Zr silicate.

In the majority of cases, metamict isotropic, Aa, which already has small altered parts or patches, and smaller amounts of altered, Ab, steenstrupine represent the conspicuous U-bearing components. However, in all sections of this type numerous small randomly distributed grains and strings of grains occur which change state from metamict to highly altered. They probably represented small steenstrupine grains or they might be products of steenstrupine decomposition.

As a rule the U content of the Aa steenstrupine is 4000-5000 ppm U_3O_8 and that in the Ab type (or altered portions) is mostly 7000-8000 ppm U_3O_8 . The fission track densities from the small grains suggest 1000-3000 ppm U_3O_8 although the accuracy is low due to their size commensurate with the length of the fission tracks.

A metamict mineral is disseminated in all samples, consisting of highly decomposed, usually shapeless, darker brown, isotropic grains. High fission track densities suggest concentrations > 10000 ppm U_3O_8 . Some parts show black opaque portions. Although not so abundant as the steenstrupine grains, they may carry a considerable portion of the total U-content in these rocks (Fig. 29). Microprobe scans show Si, Y, Zr, Na and Sn as the main elements and Th, U (~ 1.9 wt%), Fe, K, Ti, Al as minor elements (section 49-139.35).



Fig. 29. Microphotograph of the thin section and fission track image of the metamict U-Y-Zr silicate (dark in the centre; the dense fission track image) associated with metamict and altered steenstrupine in arfvedsonite lujavrite. Magnification 120x.

Individual sections:

Sample Nos. 49-139.35, 25-78.35, 15-22.05, 17-111.10 (the latter with predominantly Ab (8000-10000 ppm U_3O_8)).

A-6 Rocks with extremely altered steenstrupine which displays accumulation of uranothorite

This group is closely related to A-4 but differs from it in important spot-like accumulations of uranium in the extremely decomposed grains of original steenstrupine. The low and very irregular U-contents in the steenstrupine remnants lie in some cases in the range of 1000-2000 ppm U_3O_8 whereas in the other, better preserved, cases between 4000-5000 ppm U_3O_8 . In such grains, one or several accumulations occur with, or far above, 10000 ppm U_3O_8 . It is difficult to assess the nature of the phases but they might represent uranothorite or thorianite (Fig. 30, 31).

Microprobe scans gave the following results for the high-U accumulations: main elements: Si, Th, minor elements: U, ? K, Y, Al, Na, Pb, S. The Th:U ratio \approx 5:1.

The alteration may assume all forms, from a grey fine-grained network to monazite-(and neptunite-) containing recrystallized "ghosts" i.e. accumulations of secondary phases. Microprobe scans also confirmed two darker grains in monazite as uranothorite with Si, Th > U as the main elements, Al, Na, Ce and Y as minor elements.



Fig. 30. Microphotograph of the thin section and fission track images of completely altered steenstrupine, Ad. Accumulations with or far above, 10.000 ppm U_3O_8 might represent uranothorite or thorianite. Magnification 30x.

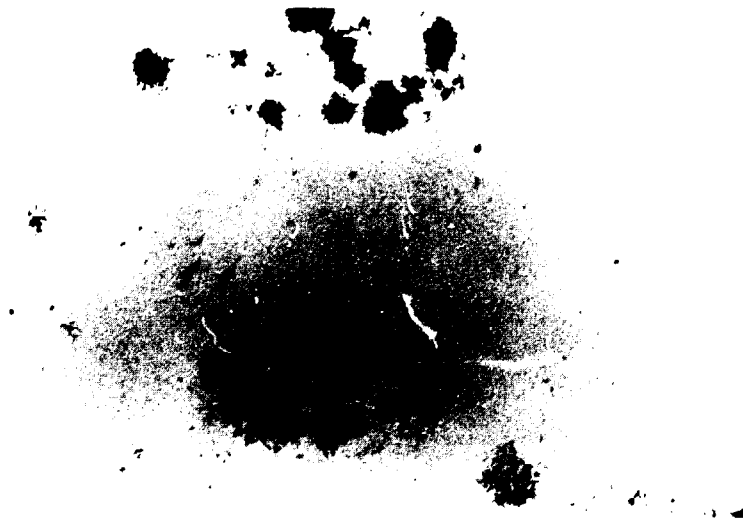
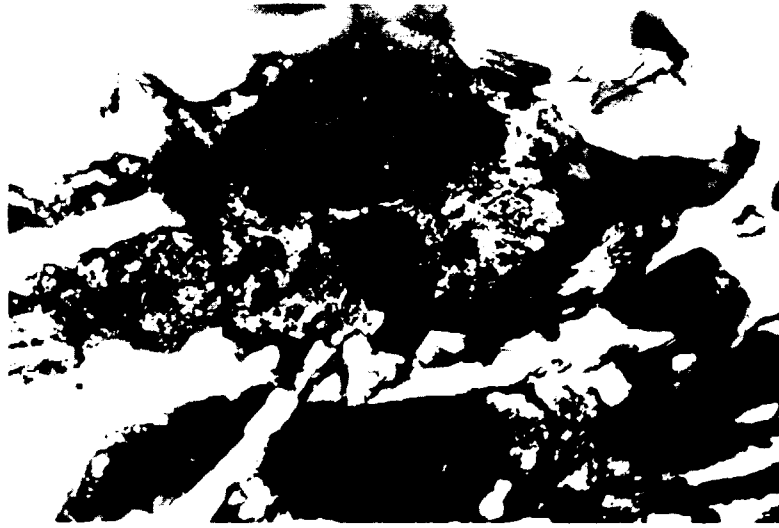


Fig. 31. Detailed view of steeplestrupine Ad from Fig. 30.
Magnification 120x.

Individual sections (contents in ppm U_3O_8):

Sample No.	Ad	high-U spots	Note
39-81.00	~ 5000	10000	
54-57.00	4000-5000	multiple accumulations	
56-13.00	as 54-57.00	not abundant	Few spots in (altered) naujakasite 1000-2000
43-179.00	4000-6000	not abundant	
62-67.83	5000-6000	present	"Ghost" with neptunite
63-135.30	1000-2000 (5000)	"	Often "hollow ghosts" or monazite 1000-2000
69-11.05	3000-5000	"	"Ghosts", also monazite
64-29.85	5000 (outlines)	7000->>10000	Usually "hollow"

A-7 Naujakasite lujavrite with zoned steenstrupine and an uranium-bearing replacement product of naujakasite

Steenstrupine in naujakasite lujavrites is typically nicely zoned (Fig. 32). Zonation also can be followed on the fission-track records. The lighter (metamict, slightly altered) zones with 5000 ppm U alternate with highly altered zones and portions with 7000, rarely up to 10000 ppm U_3O_8 .

Naujakasite, always altered to some extent, is partly replaced by a light yellow (light brown) isotropic mineral which encroaches both from the grain surface and as veins along the cleavage of naujakasite. The aggregates are too small to be analyzed quantitatively by the microprobe, but their wavelength scan suggests Si, Al, K, Na and Fe as the main, Ca and Mn as the minor elements. P is absent, as well as any appreciable amounts of rare earths. All the elements are already present in

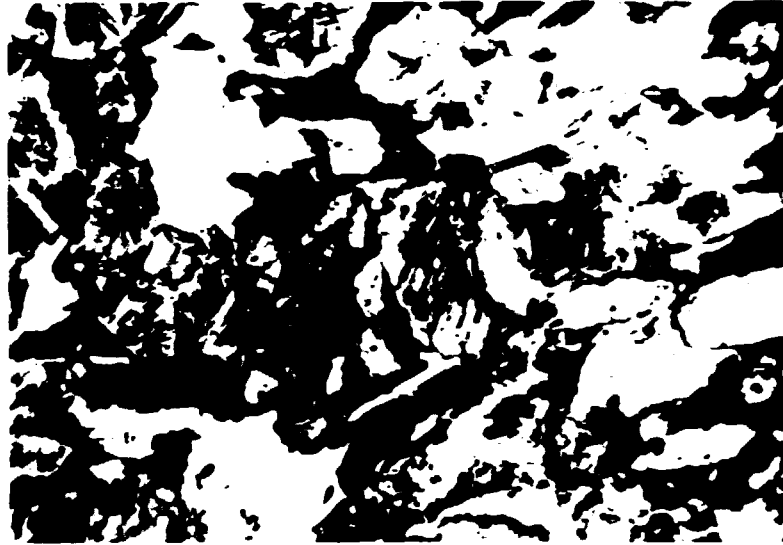


Fig. 32. Microphotograph of the thin section and fission track image of altered zoned steenstrupine, Ac in naujakasite lujavrite. The dark and more altered zones yield high fission track densities. Magnification 120x.

the parent naujakasite. This replacement phase consistently displays fission tracks which suggest an U_3O_8 content of 500-1000 ppm, sometimes slightly more.

In some of the sections numerous, highly altered grains occur replaced by intimate mixtures of secondary minerals, which still preserve, albeit in a very irregular fashion, the original U content. Fission track densities suggest a range of 1000-2000 ppm U_3O_8 , although there are cases with ≥ 3000 ppm U_3O_8 present. The microprobe scan of the aggregates suggests that they represent alteration products of eudialyte.

Individual sections:

Sample Nos. 49-71.30, 5-128.45, 25-78.35, 46-59.00, 28-90.70,
and 3-68.65.

B-1 Rocks with metamict and altered steenstrupine B; sometimes together with extremely altered steenstrupine A (or with a microscopically identical product) - Bb+Bc+Ad.

The metamict and altered grains of steenstrupine B are often associated in the same sample. In some cases the extremely altered steenstrupine A is also present, disseminated in the rock among (or close to) the large grains of steenstrupine B. It should be noted that in this stage, Ad, the fine-grained aggregates after an altered steenstrupine grain may be virtually indistinguishable from similar aggregates after several other primary components, and might require a complete microprobe (bulk) analysis for their characterization.

The Bb steenstrupine which forms large subhedral crystals usually gives a more or less homogeneous fission track image with densities indicating 4000-6000 ppm U_3O_8 in the majority of cases. Occasionally it may reach above 7000 ppm U_3O_8 . Incipient alteration is connected with the latter uranium concentrations (7000-10000 ppm U_3O_8).

Besides the cases where the alteration products are fine-grained and remain essentially in situ (U content drops in the extremely altered cases of this type to 2000-3000 ppm U_3O_8), a complete recrystallization and replacement of steenstrupine B is common.

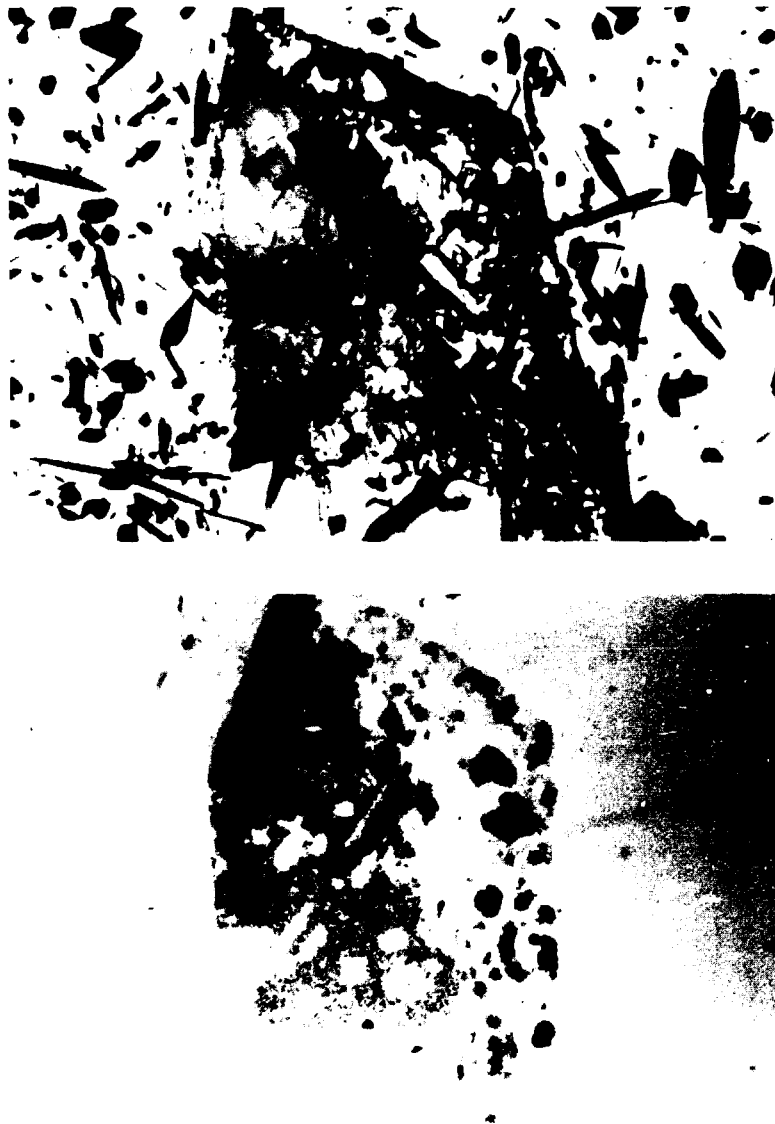


Fig. 33. Microphotograph of the thin section and fission track image of metamict steenstrupine, Bb, partly replaced by monazite, uranothorite and other phases. Homogeneous track density represents steenstrupine. Weak track density represents monazite and dense black spots the tracks from uranothorite and the Na-Zr-Si phase. Magnification 30x.

The products recognized are (concentrations from the unpublished microprobe analyses by J. Rønsbo and M.M.; sample 37-36.0): crystalline monazite (fission track densities show 1000, rarely up to 3000 ppm U_3O_8), metamict uranothorite (U contents ~ 22 wt %U)

two distinct U-bearing Na-Zr silicates (with 5.9 and 2.3 wt %U respectively and no Th present), neptunite. These aggregates preserve the shape of the original steenstrupine grain and mix together with all the original crystals which were enclosed in the poikilitic B steenstrupine. Parts of original steenstrupine, however, are dissolved and substituted by common rock-forming minerals of the MCG-lujavrite (Fig. 33). Dark skeletal crystals of a decomposed, highly inhomogeneous, Si-Zr-Ti-Nb-Na-Ca containing mineral in steenstrupine B from the sample 37-36.0 contain 3-7 wt %U and no Th (M.M. & J.R.).

When the Ad type is present, the lighter portions of the fine-grained product show 4000-5000 ppm U_3O_8 whereas the darker brown parts have densities between 6000-8000 ppm U_3O_8 . Often the fission track image shows spots with $\gg 1\%$ U in these grains, which probably represent uranothorite (or thorianite).

In this group (MCG lujavrites with Bb+Bc(+Ad)) eudialyte in radiating clusters represents a typical additional U-bearing mineral. Its fission track densities suggest 1000-2000, rarely ≥ 3000 ppm U_3O_8 .

Individual sections (all data in ppm U_3O_8):

Sample No.	Bb	Bc aggr.	Ad aggr.	Note
26-20.00	5000-6000	Recryst. U-thorite $\gg 1\%$; rest 7000-8000 monazite 1000-3000	4000-5000 (light parts); 6000- >8000 (dark parts); leached-out parts; high U-spots	
18-8.55	4000-5000	Network 1000-2000 with high U-spots + neptunite		Abundant small Bc or Ad aggregates 1000-2000
18-32.60	5000-6000	No U-thorite or monazite	≤ 7000	Bb > Bc "eudialyte" 4000-5000

8-45.30	5000-9000		"eudialyte" 4000-5000
16-73.9	5000-6000	Only incipient alteration, > 7000	Many small grains 5000-6000
14-100.30	\geq 7000	\sim 10000; high U-spots	
37-36.00	\pm homo-geneous 8000, > 10000	Monazite, U-thorite, the Si-Zr-Na-U phases, etc.	Large grains

B-2 Rocks with predominantly altered steenstrupine, Bc

This group of MCG-lujavrite samples contains only, or predominantly, altered to very altered steenstrupine B. Typically, steenstrupine crystals are altered and replaced, sometimes obliterated or partly dissolved. Monazite may be concentrated in the pseudomorphs or in the surrounding rocks. Furthermore, the pseudomorphs contain neptunite, (? natrolite), metamict uranothorite, or are represented by a brownish-grey fine-grained network. The density of fission tracks is lowered, between 2000 and 4000-5000 ppm U_3O_8 . Commonly the high-U spots occur (uranothorite) with \gg 10000 ppm U_3O_8 (Fig. 34, 35).

Individual sections (all data in ppm U_3O_8):

Sample No.	Bc	Note
20-20.10	Recryst. to dissolved; tracks heterogeneous 2000-5000, monazite 500	Few Bb grains 5000-7000
1-91.45	In arfvedsonite felt 2000-4000	"Eudialyte" (fresh) 1000 High-U spots up to 10000
27-62.00	Replaced 2000-3000; in less altered 4000-5000	Eudialyte 1000-2000
23-37.40	Obliterated to U-thorite \geq 1% U monazite, neptunite	

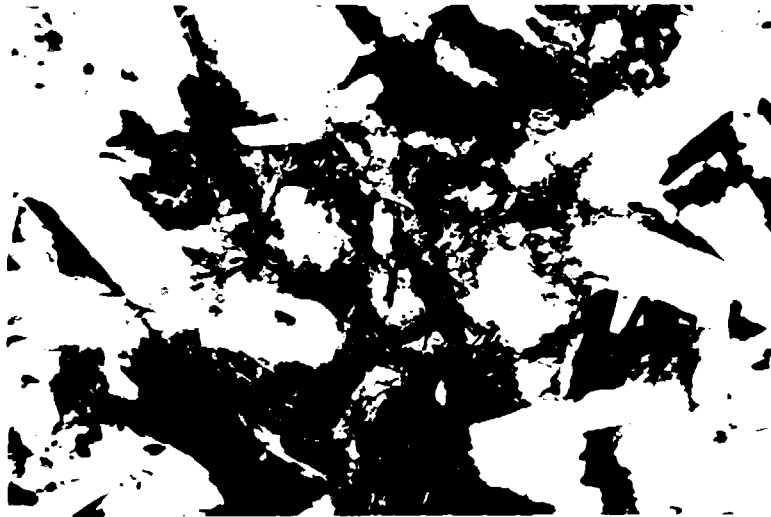


Fig. 34. Microphotograph of the thin section and fission track image of predominantly altered steenstrupine, Bc, in MCG lujavrite. Magnification 30x.

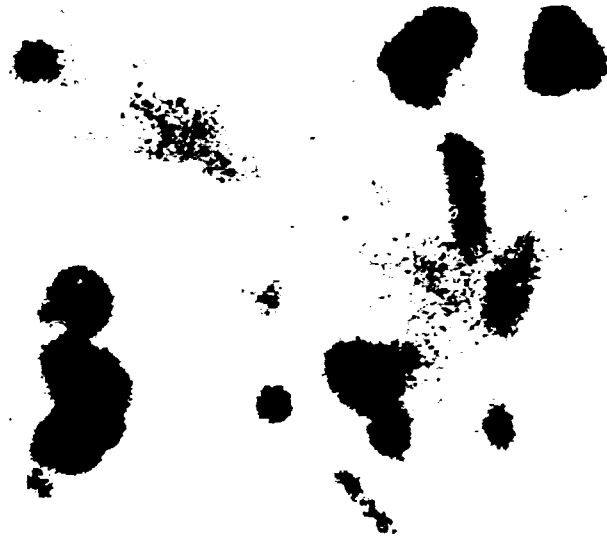


Fig. 35. Detailed view of steenstrupine Bc from Fig. 34.
Magnification 120x.

B-3 Metamict and altered steenstrupine B associated with an
U-bearing zircono-aluminosilicate

This is a subtype of the above Bb+Bc type, which contains appreciable amounts of fresh, twinned and slightly poikilitic U-bearing mineral with low birefringence. Microprobe data

indicated substantial amounts of Si, Al, Zr, Na and Ca, minor amounts of Y and ?Sn. The mineral shows in fission track 3500 ppm U_3O_8 . Drill hole No. 31.

C-1 Altered lava with impregnations of the fine to coarse grained metamict to altered steenstrupine of uncertain type

The type is represented by section 61-22.30 which is an inhomogeneous rock, altered from lava, with vein-like, predominantly felsic impregnations between darker, arfvedsonite-rich portions.

In the darker portions large steenstrupine (?Bc) crystals are abundant, with fission track image indicating 10000 ppm U_3O_8 or greater. Another U-bearing component in these darker, arfvedsonite-rich parts is represented by small grains. They are highly altered so that they acquired irregular outlines. Although difficult to estimate because of their size, their U content seems to be low, only ~ 1000 ppm U_3O_8 .

In the light, narrow, impregnation vein, fine grained, disseminated to agglomerated, light brown, slightly anisotropic steenstrupine is associated with natrolite crystals. Locally steenstrupine is heavily altered into fine grained, anisotropic, dull brown, shapeless pigment. Fission tracks show, for the majority of grains, contents above 10000 ppm U_3O_8 . Light minerals enclose disseminated minute grains of brownish altered steenstrupine. The U content is estimated for them as 5000 ppm U_3O_8 .

5. CHEMICAL AND MINERALOGICAL STUDIES OF STEENSTRUPINE

5.1. Microprobe analyses

Microprobe analyses were carried out using the Hitachi XMB-5S microprobe at the Institute of Mineralogy, University of Copenhagen. A data reduction programme by Springer (1967), modified by J. Rønsbo after Sweatman & Long (1969) was used. The analytical lines and the standards used are listed in Table 9. The peak positions used, except for those of U and Nd, were not influenced by interferences with other spectral lines. Background problems were encountered for Pr and Al.

5.1.1. The measurement problems for U and Nd

Quantitative work on uranium was effectively made impossible by the interferences of other lines (Th and K) with the rather insensitive lines of uranium. The problem was aggravated by the unusual background yielded by steenstrupine in the wavelength regions of interest and by the low U contents to be determined.

The $L\alpha_1$ line of neodymium at 2.365Å, and the cerium $L\beta_1$ line at 2.351Å lie very close to each other. At higher Ce or Nd contents the lines of the two elements would appreciably overlap but at the concentrations encountered the overlap is minimal.

5.1.2. Analytical procedures

Sodium, and especially H_2O easily evaporate from the analysed spot in the steenstrupine sample under the impact of the electron beam. Therefore the lowest possible acceleration voltage, 10 kV, was used for the sodium analyses. 15 kV was used for the other elements, 30 kV for Th.

The analyses for each element are based on 6 to 10 counts, each over a period of 10 seconds. During each determination the

sample was slowly moved to prevent excessive heat accumulation and sample decomposition at the analysed area.

The analytical results, in wt %, are given in Table 10. Because of the variable valency of Fe and Mn in steenstrupine, the values for oxygen are tentative.

5.1.3. The analysed materials

The analysed samples from Kvanefjeld

- 6-72.88 Zoned steenstrupine, Ac, in hydrated arfvedsonite lujavrite. It displays a rather thick metamict outer zone and a variably altered core with small crystals of arfvedsonite. Analyses Nos. 51, 55, 56, 59, 65 represent the outer zone; No. 53 the less common metamict deeper zone. Nos. 52, 58, 59 and 62 represent the slightly altered, Nos. 50, 63 and 66 the altered, and Nos. 54 and 57 the strongly altered cores of various grains.
- 9-66.65 Crystals of unzoned metamict steenstrupine B which contains numerous arfvedsonite needles. Steenstrupine occurs among arfvedsonite and light minerals. The latter have fractured on metamictization.
- 11-134.90 Zoned steenstrupine, Ac, in naujakasite lujavrite. Analyses Nos. 17, 25, 32 and 35 represent the slightly altered metamict (and No. 23 the altered) outer zone whereas those with Nos. 18, 24 and 34 the highly altered cores of the same grains. A small independent metamict grain yielded the analysis No. 22.
- 18-79.65 Subhedral, mostly metamict steenstrupine C in the analcime - steenstrupine vein.

- 48-163.00 Slightly hydrated naujakasite lujavrite which contains small crystals of steenstrupine A. Both the metamict, unaltered and, close to them, the unzoned altered to highly altered grains commonly occur in the rock and were analyzed.
- 29-15.00 Subhedral crystals and accumulations of extremely altered steenstrupine B. The resulting products are separated on microscopic scale thus yielding highly heterogeneous microprobe results. The studied sample represents a strongly hydrated MCG lujavrite.
- 39-140.00 Weakly hydrated arfvedsonite lujavrite with small crystals of steenstrupine A. Altered, unzoned crystals occur in the rock next to the accumulations of unaltered, metamict ones.
- 54-39.85 Altered, sheared weakly hydrated lava. The crystals of steenstrupine are altered into weakly translucent aggregates of secondary products. Their outlines remain preserved.
- 61-127.85 Zoned steenstrupine, Ac, in weakly hydrated arfvedsonite lujavrite. Analyses Nos. 7, 12 and 13A represent the highly altered outer zone, Nos. 8, 11, 13 a broad crystalline zone, and Nos. 9, 10, 14 and 15 the highly altered core. Analysis No. 16 represents patches of altered steenstrupine in indistinctly zoned highly altered grains.
- 65-51.10 Weakly hydrated arfvedsonite lujavrite. Altered steenstrupine A displays inclusions of arfvedsonite and indistinct zonation. The locally developed metamict rim is represented by the analyses Nos. 37 and 43. The remaining analyses represent the main portions of the grains, i.e. the altered core parts.

Samples from the pegmatites and veins outside Kvanefjeld

1) Sample No. 199104 (Fig. 36)

A large naujaite inclusion in black lujavrite is cut by numerous hydrothermal sodalite-natrolite veins with sporadic steenstrupine. One of the veins, 10-15 cm thick, is composed of 10-100 vol% of steenstrupine. Lujavrite adjacent to the vein contains several vol% of disseminated steenstrupine.

Steenstrupine in the massive areas is coarse crystalline, fresh and distinctly anisotropic. When isolated among silicate minerals, the crystals are euhedral each crystal having a narrow, well defined rim of anisotropic steenstrupine. Parts of the crystal interior may be replaced by a secondary, strongly anisotropic steenstrupine which does not affect the rim material.

2) Sample No. 199115 (Fig. 36)

Sodalite veins in naujaite are up to 10 cm thick and contain microcline, aegirine, natrolite, eudialyte and several vol% of steenstrupine. The crystals of steenstrupine are zoned metamict, optically isotropic. At the margins and along the cross-cutting fractures they are replaced by a light to dark brown semitransparent isotropic steenstrupine variety.

3) Sample No. 199146 (Fig. 36)

Irregular sodalite-aegirine veins with abundant steenstrupine, situated in naujaite. Steenstrupine is isotropic, metamict and is partly altered into an extremely fine-grained secondary material. Some crystals have transparent margins and "dusty" altered central areas.

Another isotropic steenstrupine variety is the light to dark red brown "steenstrupine" developed along the margins and fractures in the earlier steenstrupine varieties.

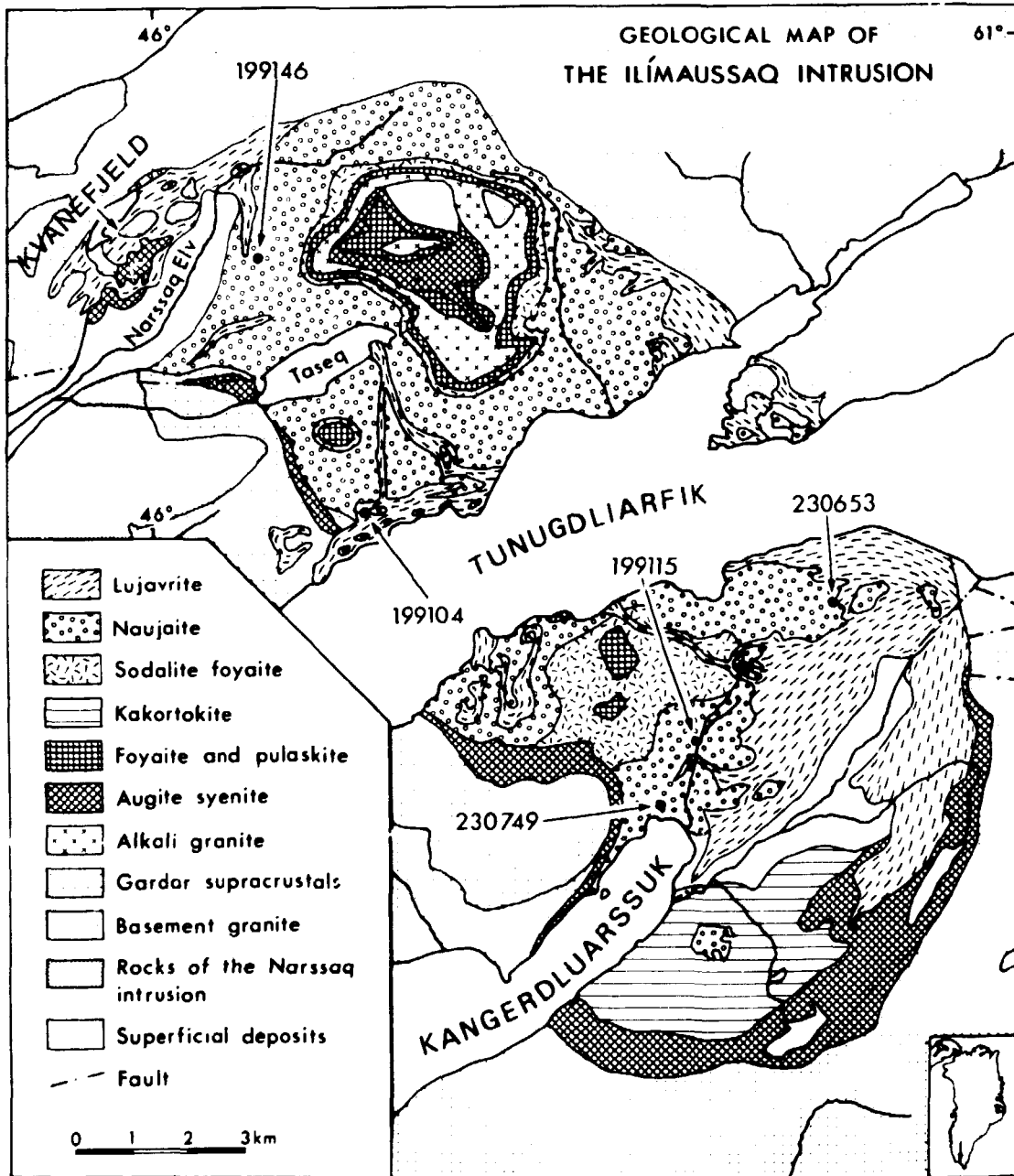


Fig. 36. Sample locations for steenstrupine samples from the pegmatites and veins outside Kvanefjeld area.

4) Sample No. 230653 (Fig. 36)

Up to 5 cm thick massive steenstrupine vein in naujaite. Steenstrupine crystals are composed of an intergrowth of isotropic, metamict steenstrupine with a distinctly anisotropic variety. The latter has the character analogous to the replacement steenstrupine phase in sample 199104. Metamictization of the primary steenstrupine apparently took place after the partial replacement of it by the distinctly anisotropic variety. Metamict steenstrupine contains disseminated extremely fine-grained anisotropic alteration products.

Katapleite and a red-brown micaceous mineral occurs among the steenstrupine grains.

5) Sample 230749 (Fig. 36)

The sample represents the albite rich zone of a complex naujaite pegmatite. "Steenstrupine" is characterized by an anisotropic rim (as in 199104) with central areas completely altered to dark brown, isotropic material. Katapleite, a red-brown micaceous mineral and natrolite occur among the steenstrupine grains.

5.2. Scanning electron microscopy

Because of the fine grain size of the common alteration products of steenstrupine, a scanning electron microscope was used to investigate selected samples. The apparatus used is the Cambridge Stereoscan 180 microscope at the Inst. of Historical Geology and Palaeontology equipped with a Link energy-dispersive X-ray analyser. The radiation range recorded was 0 to 10 keV, in some cases 0 to 20 keV. Samples were coated with aluminium.

The method gave additional insight into the fine-scale mineralogy of the analyzed material. However, it has some limitations and procedural difficulties which prevented its large-scale use for the study of the steenstrupine alteration:

- 1) Some important elements (primarily P vs. Zr) cannot be distinguished from each other in the spectrum. Problems are also caused by partial overlap of U and Th, those among various rare earths, and of Fe and Mn by subsidiary peaks. In the present experimental arrangement Na could not be recorded.
- 2) Ion etching of thin sections over extended periods did not thin the steenstrupine alteration phases sufficiently to become transparent for the electron beam although the surrounding rock-forming minerals were virtually etched away and the sections disintegrated. Thus, the transmission microscopy could not be performed.
- 3) In the reflection arrangement many mineral grains had to be distinguished only by analyzing them or by a scan of the examined rock fragments at a particular X-ray wavelength, making the work tedious. With increasing magnification, contamination of the spectrum by stray radiation progressively increases.

The following results were arrived at by critical examination of the studied samples:

17-62.00 Hydrated lava, steenstrupine A with very altered brown core and unaltered, crystalline rims.

In the scanning electron microphotograph, the grains of steenstrupine show compact, grey to black rims with simple to conchoidal fractures, and an altered core of earthy or fine-grained appearance (Fig.37).

In grain 1 (Fig. 37) the grey to black rim represents siliceous steenstrupine with $Si \gg P$ and with only minor amounts of Th and U. Immediately adjacent to the altered core is a black massive layer, apparently a metamict steenstrupine layer. It is somewhat richer in Th and U. It has a fairly sharp contact with the altered core composed of a fine-grained, uniformly looking mass of an alteration product.

The bulk analysis of an uniform area in the core gives a steenstrupine spectrum with slightly higher contents of Ca and Fe and the highest contents of Th, U (and K).

Alteration processes are limited to the high Th and U areas.

The low-Fe spots in the core, picked up using the characteristic Fe line, give $P > Si$ and a very high Ca content (Fig. 37). Rare-earth contents remain high while Mn is somewhat lower (Zr cannot be discerned from P).

The high-Fe spots show nearly pure Si and elevated K, indicating that they represent enclosed mafic minerals (arfvedsonite).

A grain of galena has been located between the metamict and altered parts (Fig. 38).

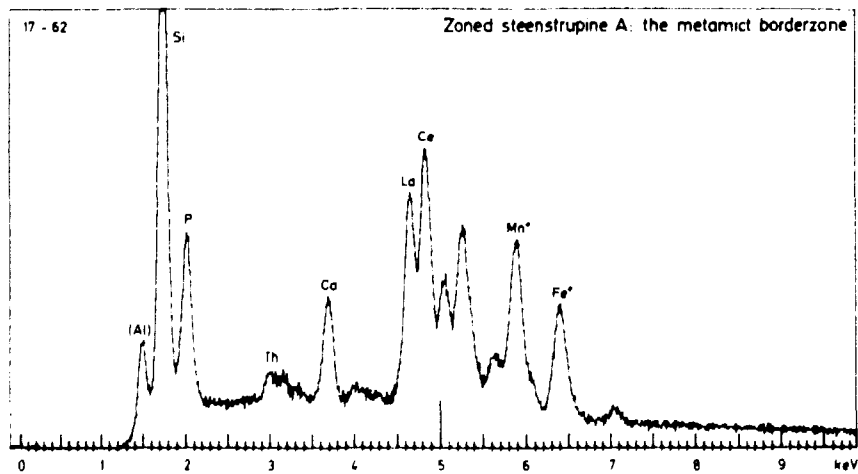
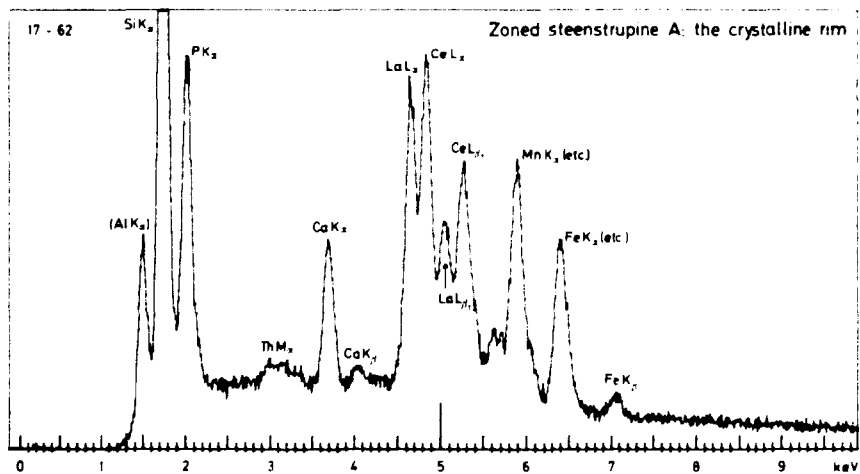
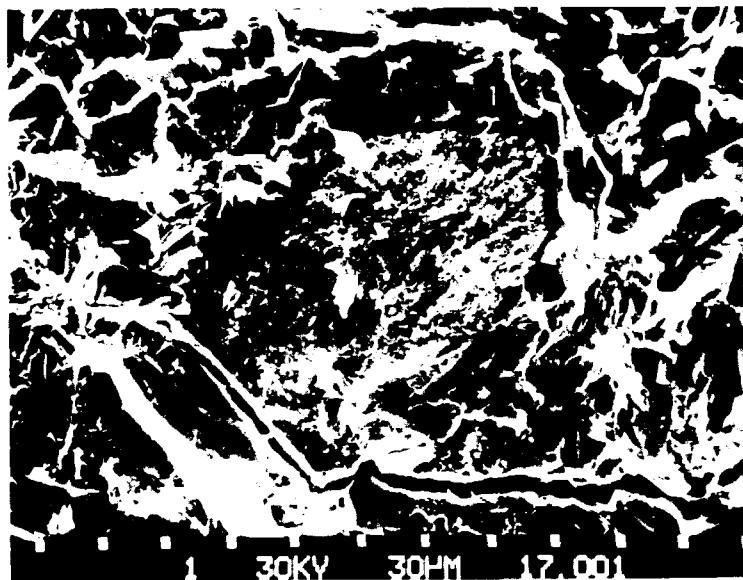
The other grains indicate a similar pattern, with somewhat lower P contents in the core, less Mn, and U & Th large in the core and almost absent in the rim. For all examined grains the La/Ce ratio is significantly smaller in the cores and larger (peak heights about equal) in the rims.

Remnants of a cubic or tetragonal mineral with pyramidal shape in the mass of the steenstrupine core gave:

$P > Si$, very high Ca, RE; higher Fe, low Mn, and very small amounts of U and Th (Fig. 39).

55-155.35 Arfvedsonite lujavrite with very altered steenstrupine.

Again, steenstrupine grains with ?metamict massive rims and altered cores were located and examined (Fig. 40). The rims display slightly smaller P contents and very low contents of Th and U. The core, both immediately below the rim and in the crystal center is more siliceous, with Th & U content so high that the Th peak is commensurable with the Ca peak. Again, as in 17-62.0, in the rim the La/Ce ratio is distinctly higher than in the core.



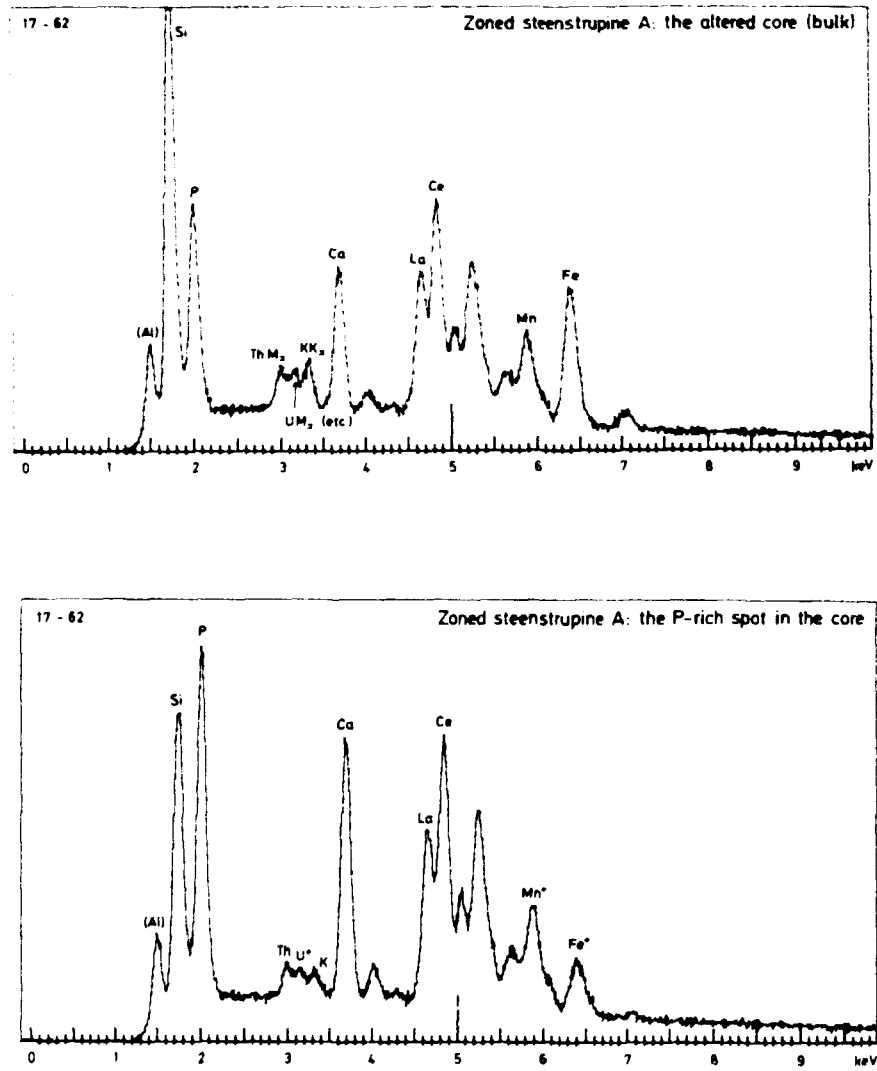


Fig. 37. Scanning electron microscope photograph of zoned steenstrupine 17-62.00 and the energy dispersive X-ray spectra of four analysed spots in the steenstrupine grain (numbered 1 to 4 in the order of the above recordings). The spectral lines present are decoded in the first plot; "+" in the remaining plots means contributions from other, not enumerated lines of the elements present. Aluminium coating.

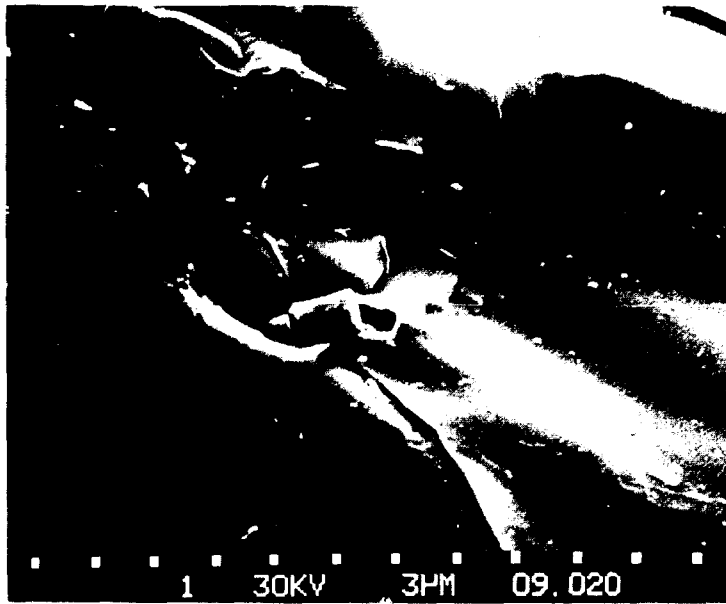
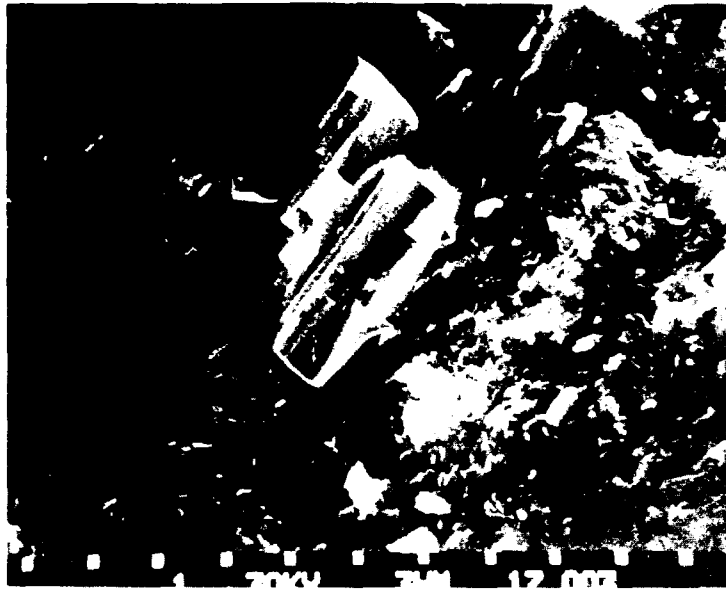


Fig. 38. Grains of galena crystallized inside steenstrupine. Top: sample 17-62 (zoned steenstrupine A); bottom: sample 37-36 (metamict steenstrupine B).

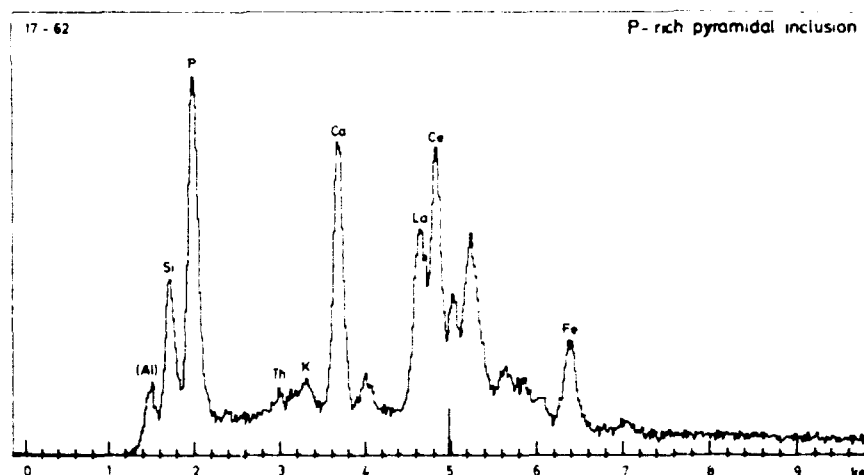
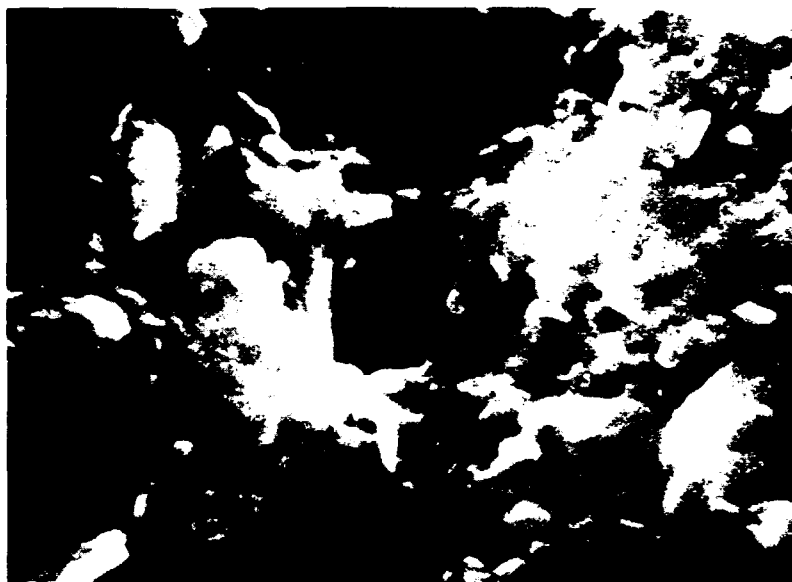


Fig. 39. The SEM photograph and EDA recording of a minute pyramidal inclusion in the core parts of the grain of steenstrupine 17-62.00 shown in Fig. 37.

The core is filled with small crystals of arfvedsonite and it contains white "specks" which are Ca- and P-rich, with less Th(U) and Mn (Fig. 40).

Steenstrupine was also found as imperfectly developed crystals (combinations of basal pinacoid and rhombohedra), exposed on the fracture surface of the rock. Typical spectra of steen-

strupine, sometimes contaminated by arfvedsonite (Si, Fe, K) were obtained.

Loose crystals in the vugs are always aluminosilicates or in one case a Nb silicate. An undefinable spot in a complex aggregate yielded a very high P content with lower Si amounts,

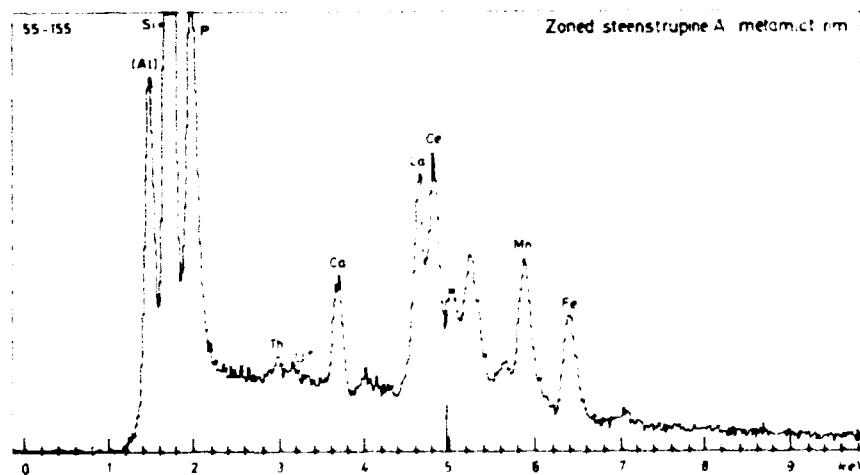
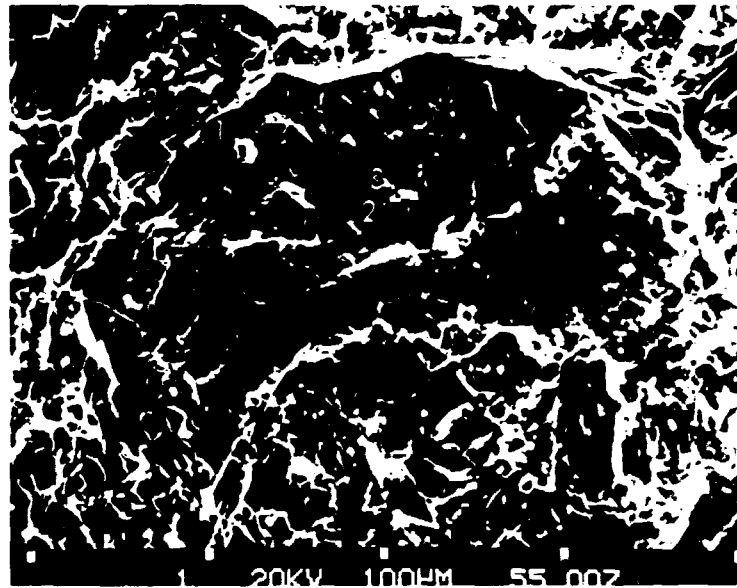
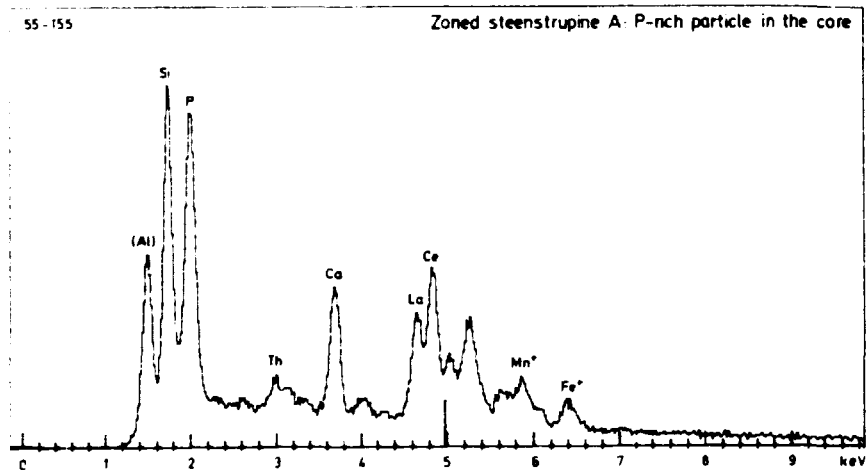
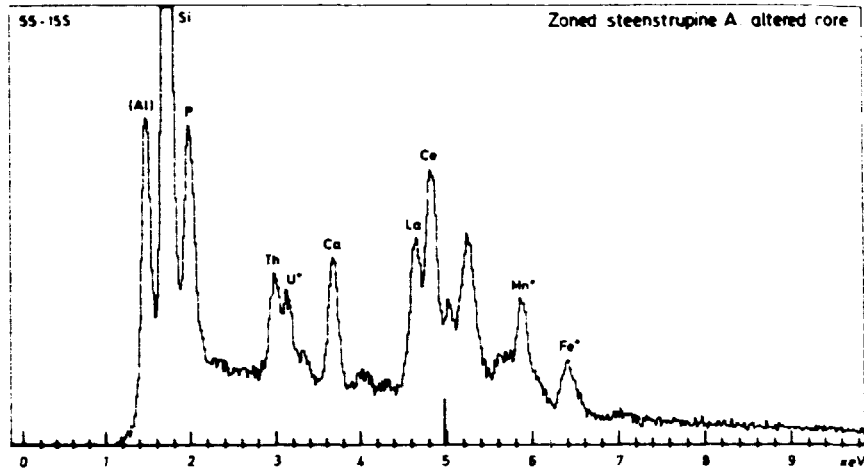


Fig. 40. The photograph and EDA recordings from zoned steenstrupine 55-155.35. For explanations see Fig. 37.



a very high Ca content, traces of Fe and no REE, U or Th. This Ca (?Na) rich (silico)phosphate indicated a possible explanation for the high P-high Ca spots in the altered steenstrupine cores. However, the presence of other, Ca- and REE-rich silicophosphates cannot be excluded.

37-36.00 Medium to coarse-grained lujavrite with metamict and recrystallized steenstrupine B.

The metamict steenstrupine B again shows strong predominance of Si over P. It shows Ce peaks distinctly higher than those

of La, higher relative contents of Mn and distinctly higher contents of Th and U (no K). The metamict mass is compact, uniform dark grey with conchoidal fracture (Fig. 41).

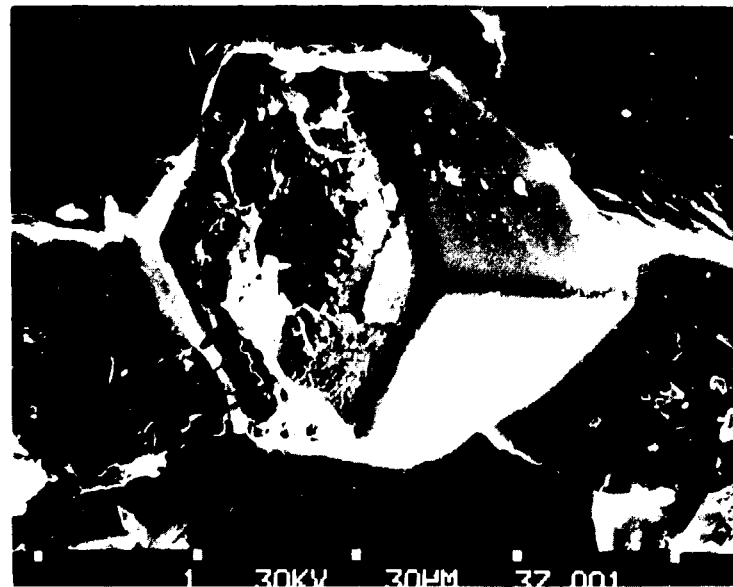
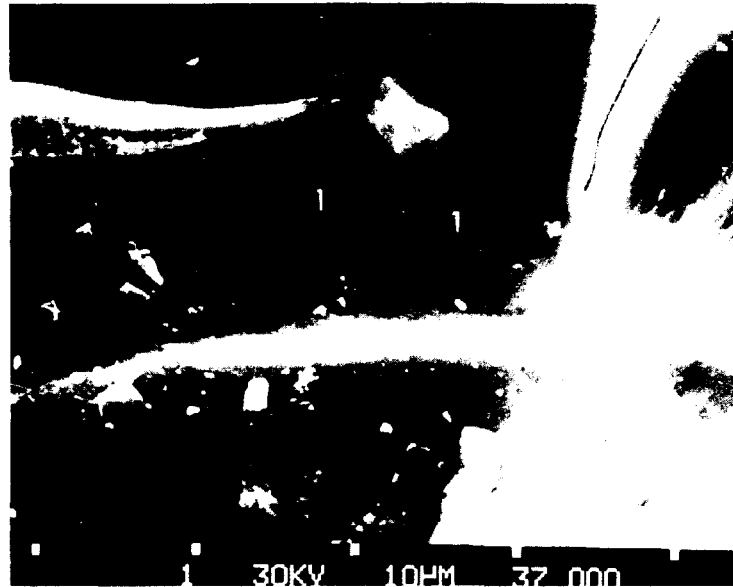


Fig. 41. Top: uranothorite (1) replacing metamict steenstrupine (bulk) along fine fissures. Bottom: negative of an arfvedsonite crystal in MCG lujavrite. Sample 37-36.00; the SEM images.

Irregular minute grains of uranothorite were found in the metamict mass, with shapes indicating their formation by replacement of steenstrupine along fine fissures (Fig. 41). Their analyses show $Th > U$, Si and appreciable amounts of Pb from radioactive decay. Spectral patterns contain low peaks of all major elements from the surrounding steenstrupine.

Bundles of subparallel crystals of monazite occur next to steenstrupine, together with light silicates and uranothorite (Figs. 42, 43). Uranothorite in this case gives a pure spectrum. Monazite is siliceous, with $P \gg Si$, with practically no Ca, Mn and Fe in the pattern, with the $Ce > La$ peak ratio as in steenstrupine B. There is a definite content of Th and U. An indistinctly layered oval grain in monazite (Fig. 44) displays high-REE contents, small amounts of Th, and low concentration of $P > Si$ (ratio as in the surrounding monazite). The data are not sufficient to specify the mineral unambiguously.

Fine-grained subparallel intergrowths of monazite (after steenstrupine), associated with ?neptunite (main K, Ti, Fe, Si, no Zr, Nb) are more siliceous than the previous monazite bundles, with higher Th (and U) contents (Fig. 45).

9-23.7 Medium to coarse grained lujavrite. Patches and nests of metamict to extremely altered steenstrupine B.

Steenstrupine again is siliceous, $Si \gg P$, with somewhat higher Fe/Mn ratio than the previous ones. Typically the La peaks are much lower than the Ce peaks, and the Th (& U) peak is high, often almost equal to that of Ca (Fig. 46).

The strings of newly formed particles along the fissures show the spectrum identical (in intensity ratios!) to that of surrounding massive steenstrupine. An irregular grain of monazite developed in steenstrupine shows a low Th(U) content and low Si content (?contamination).

The layered, grey and black steenstrupine with still compact appearance may, besides the typical steenstrupine spectra,

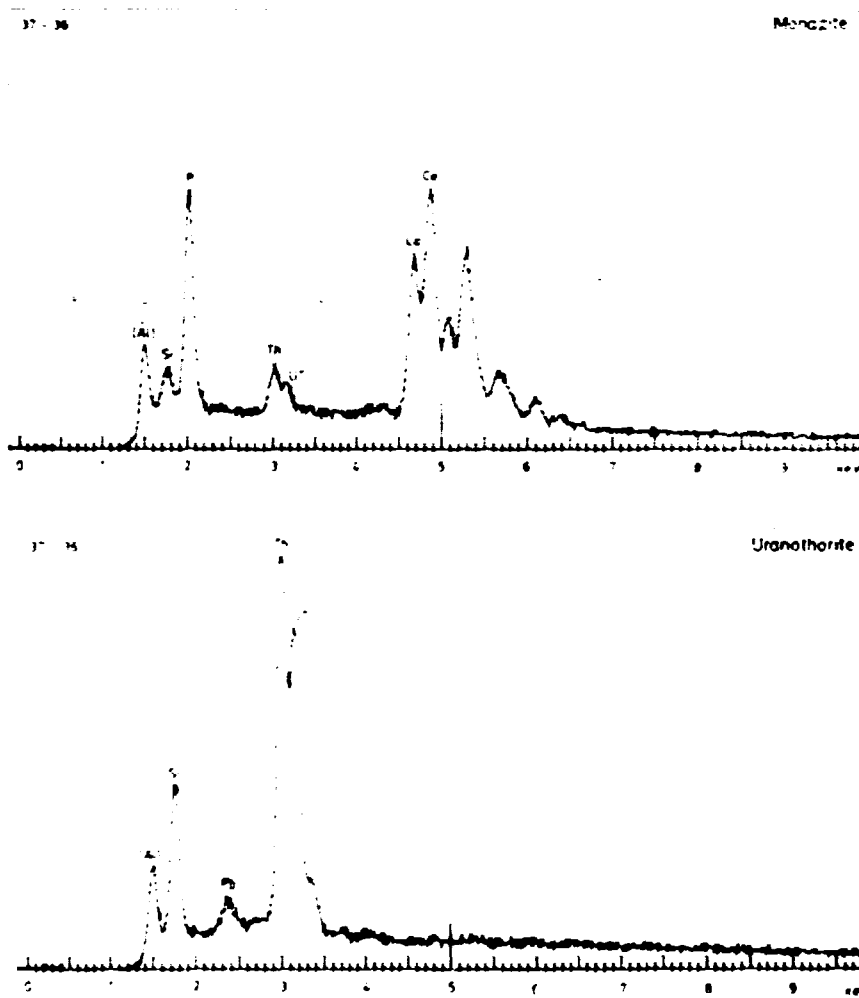
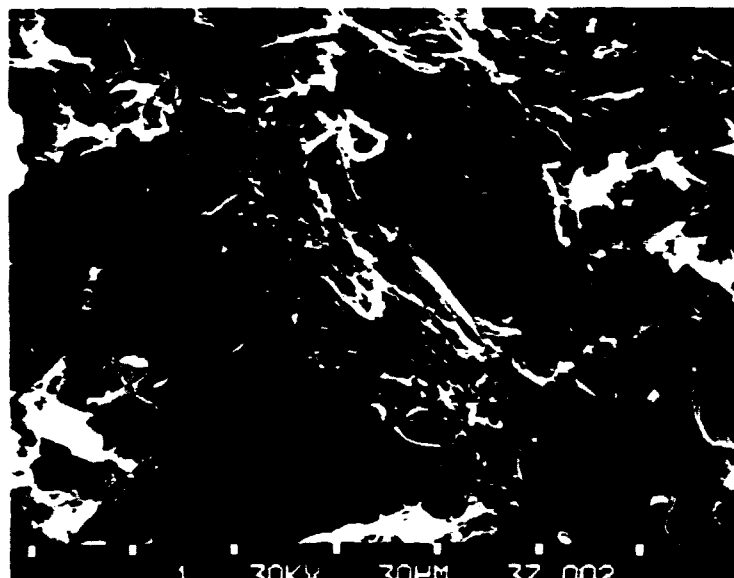
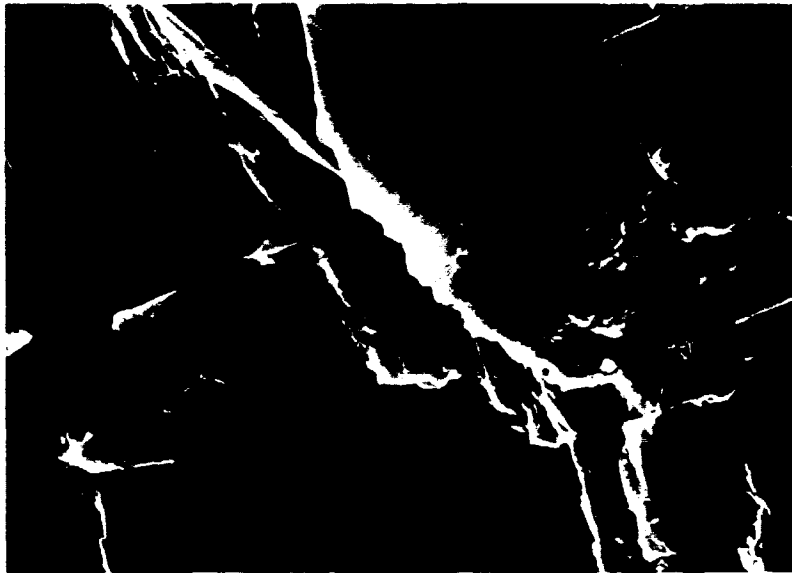
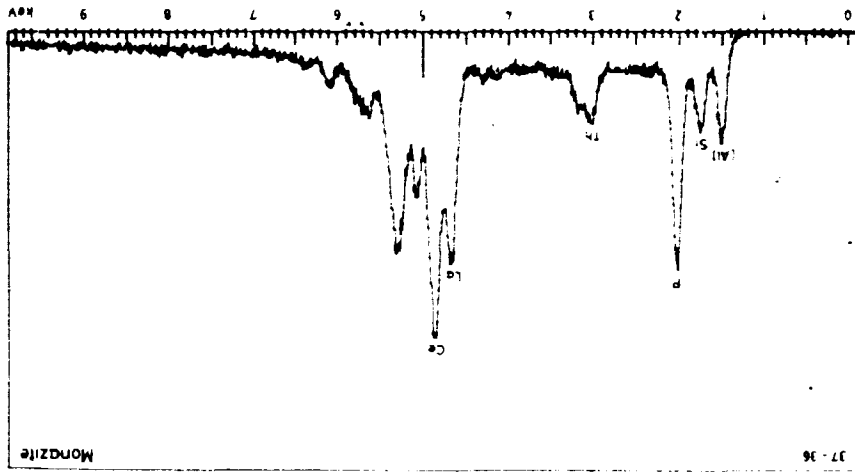


Fig. 42. Aggregate of crystalline siliceous monazite (1), uranothorite (2) and light rock-forming silicates after steaming in B in the sample 37-36.00. For explanations see Fig. 37.

Fig. 41. The SEM image and EDX recording of a crystal of siliceous monazite in light rock-forming minerals in the sample 37-36-001.



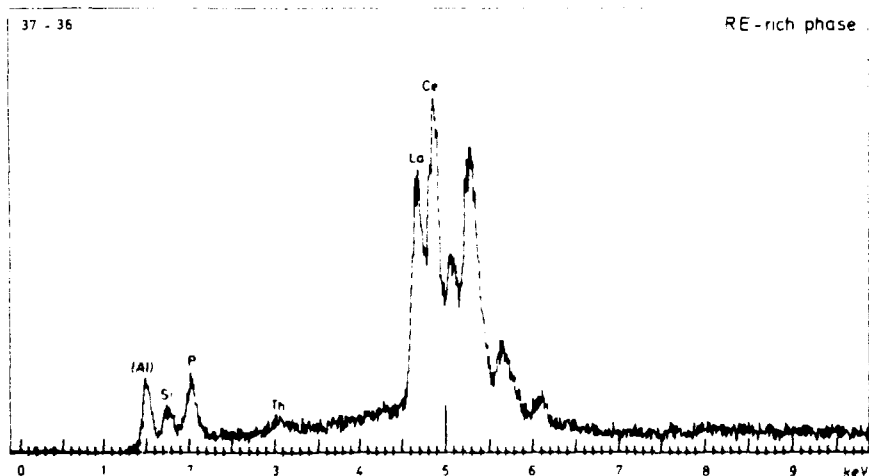
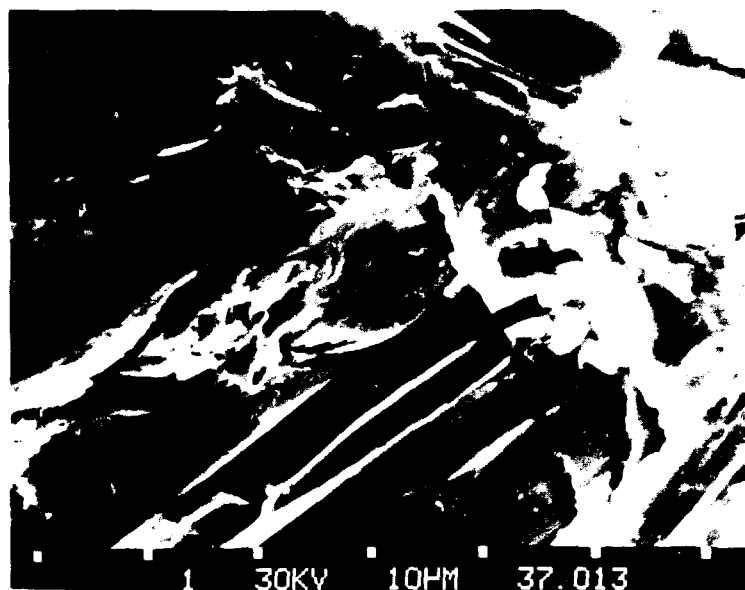


Fig. 44. The SEM image and the EDA recording of a phase rich in rare-earths from the sample 37-36.00. The grain of the phase (center) is enveloped by crystalline, siliceous U-Th containing monazite similar to that in Figs. 42 and 43.

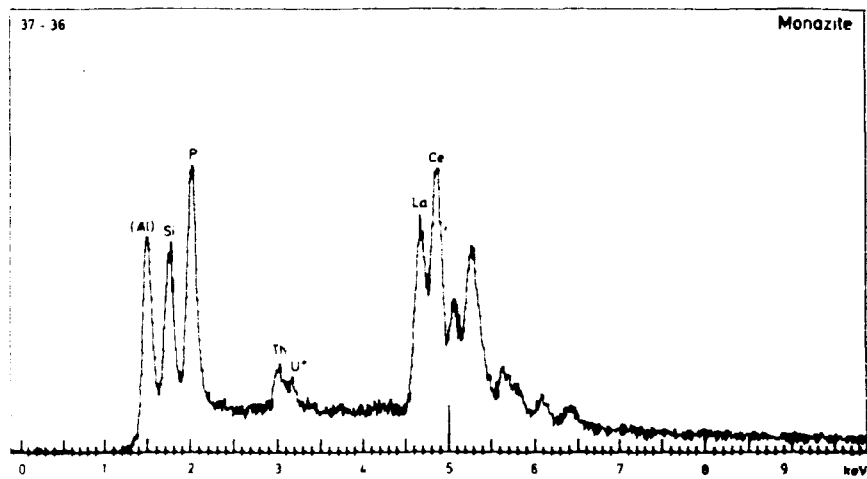
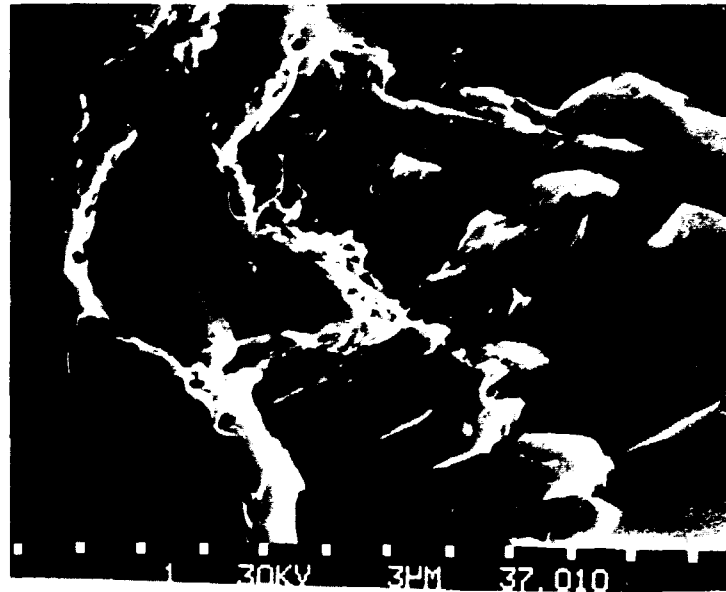


Fig. 45. Highly siliceous crystalline monazite (center) with (?) neptunite (right-hand portions) replacing metamict steenstrupine B (left-hand parts) in the sample 37-36.00. SEM image of a fracture surface and EDA recording.

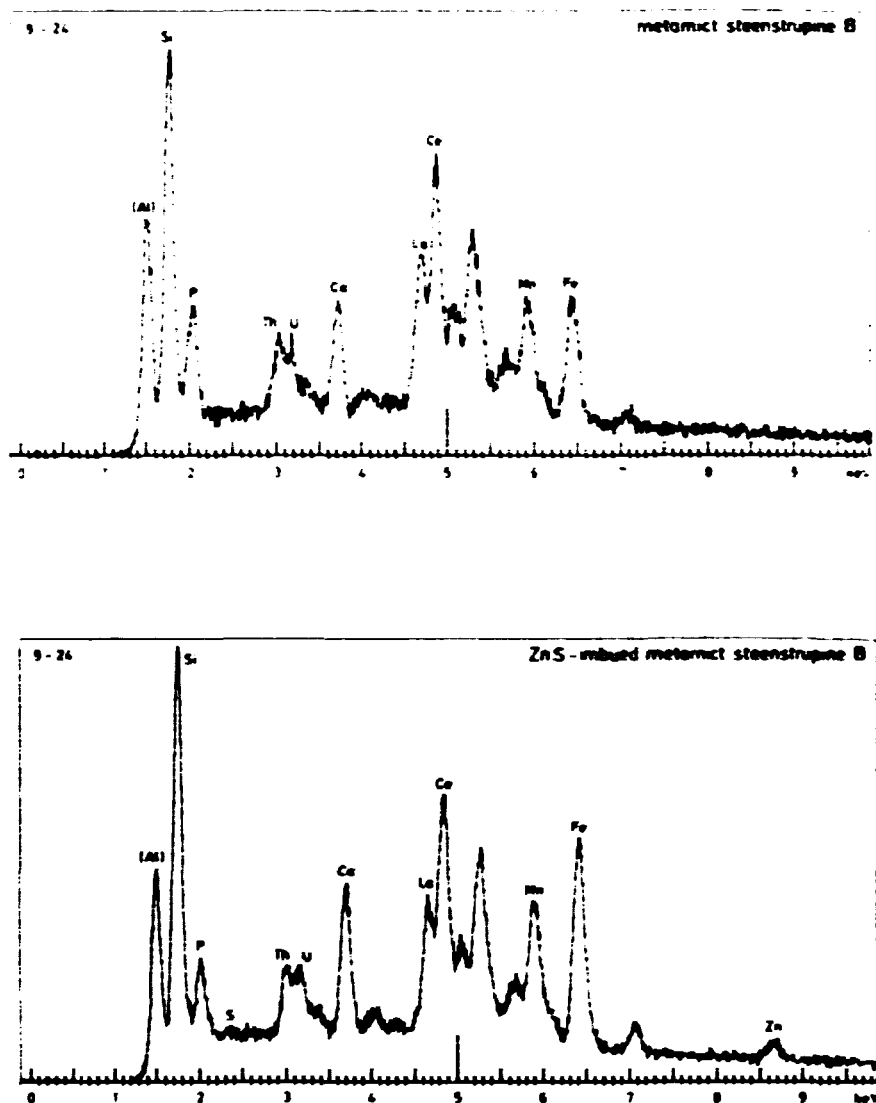


Fig. 46. EDA recordings from the steenstrupine B sample 9-23.70. The upper spectrum comes from a massive uniform aggregate of metamict steenstrupine; the lower one from a layered portion with frequent compositional changes and an overall ZnS content (see paragraph 5.2).

locally yield the low-Si & P, high REE or high-P & Ca (?REE) compositions similar to those above. It also may constantly give distinct Zn and S contents, indicating its internal contamination in (predominantly) metamict state (Fig. 46).

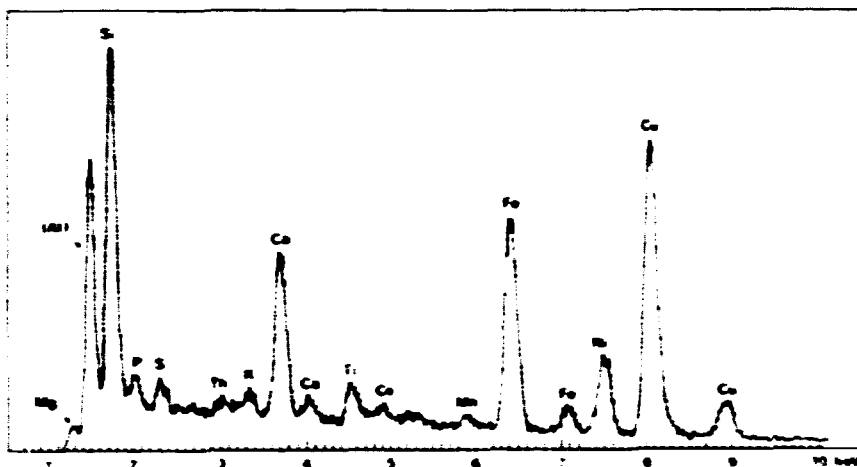


Fig. 47. Energy dispersive X-ray spectrum of a portion of flaky cavity fillings in altered steenstrupine B from the sample 9-21.70.

Cavities in steenstrupine are generally coated by subparallel aggregates of flaky minerals with irregular to polygonal grain outlines. They did not yield a unique type of spectrum. In general, away from the cavity walls the spectra of these flaky minerals reveal Si (no P) with Ca, K, Fe, elsewhere only with K or Si (+?Na). Occasionally, high REE-contents also occur, without P. Visible amounts of Zn and S can occur throughout the cavity, indicating presence of dispersed ZnS. Locally, the single grains of the flaky cavity fillings may yield very exotic spectra (e.g. Fig. 47), without the possibility of distinguishing single phases in them (Pb coincides with S and Ag with Th).

5.3. Mineralogical studies on the crystalline steenstrupine No. 199104 from Tunugdliarfik, the Ilímaussaq Complex.

Practically all the steenstrupine in the Kvanefjeld ore occurs as small to microscopic grains which cannot be effectively obtained as a clean fraction for more detailed mineralogical investigations. Moreover, the portions which are crystalline always occur as parts of composite grains and cannot be separated. Although steenstrupine from veins occurs in larger

masses, as a rule it again is predominantly metamict or altered into secondary products.

Thus a find of masses of only weakly metamictized (or altered), still crystalline steenstrupine at Tunugdliarfik (Fig. 36) enabled us to undertake detailed mineralogical investigations of the "original steenstrupine". The results of such investigations are then critically applied to the study of the main mass of steenstrupine which occurs in the rocks of Kvanefjeld. Detailed report on steenstrupine from Tunugdliarfik will be published elsewhere (Makovicky & Karup-Møller, 1981). A summary of all important data is given below.

The locality is described in part 5.1. The examined crystals contain small to medium large homogeneous cores, darker in transmitted light, and thick, finely zoned outer parts. The microprobe composition of these, as well as those of the thin outer rims and of the anisotropic replacement steenstrupine mentioned in 5.1 are given in Table 11.

The fluorine content of the bulk steenstrupine 199104 was estimated by J. Kystol (Geological Survey of Greenland) using a fluoride-specific ion electrode to be 0.27 wt% F.

The uranium content of this sample was determined by L. Løvborg (Risø) using delayed-neutron counting following neutron irradiation in the research reactor at Risø. The mean value obtained is 0.46 wt% U. The fission-track densities (see 4.1) suggest ~ 5500 ppm U_3O_8 in the cores and ~ 7000 ppm U_3O_8 in the thick, zoned areas of the crystal. They are fairly uniform within the limits of either area.

The emission spectral analysis of the bulk steenstrupine 199104 was performed by H. Bollingberg (Inst. of Petrology, Univ. of Copenhagen) on a Hilger quartz spectrograph. The following minor and trace elements were found (in ppm): Zr 4400, Y 4700, Mg 3400, Al 2700, Ti 780, Ba 550, Ni 300, Sn 220, Cr 190, Sc > 100, Be 86, B 63, Co 60, Nb 85, Ga 40, Cu 12, V traces. They were estimated using prepared mineral standards.

Mössbauer spectroscopy of the bulk steenstrupine 199104 (Albertson et al., personal comm.) revealed that practically all iron in the mineral is trivalent. This, however, should not be considered a general phenomenon because another steenstrupine sample from veins in the Ilímaussaq complex was found to contain substantial amounts of Fe^{2+} (besides Fe^{3+}) by the same method.

In cooperation with J. Bailey (Inst. of Petrology, Univ. of Copenhagen) the approximate valency of manganese in steenstrupine 199104 was determined from the $M\alpha$ - $K\beta_{1,3}$ - $K\beta'$ X-ray emission peak profile (Urch & Wood, 1978) as approximately $\text{Mn}^{2+}/\text{Mn}^{3+} = 2:1$.

Infrared spectra of steenstrupine 199104 were taken on a Beckman IR9 double-beam spectrometer at the Mineralogical Inst., Technical University of Denmark (DTH). KBr pellets with 0.2% of steenstrupine, and of steenstrupine partly dehydrated at 350°C , were used.

The spectrum is dominated by three strong absorption bands: one below 700 cm^{-1} and two between 750 - 1400 and 2500 - 3700 cm^{-1} . It is complicated by numerous small to medium peaks. The complex band centered on 950 - 1100 cm^{-1} reflects stretching frequencies of the $[\text{PO}_4]$ and $[\text{SiO}_4]$ tetrahedra. It lies in the region of condensed tetrahedra and its great simplification plus shift to higher frequencies on dehydration at 350°C show the pronounced influence of hydrogen bonds on these tetrahedra.

The composite bands at 1655 cm^{-1} and at 2500 - 3700 cm^{-1} represent the bending and stretching frequencies of structurally bound water. The material heated at 350°C still shows H_2O frequencies. They suggest tighter structural bonding than that observed for the water released at lower temperatures. No bands indicative of strong $\text{OH}-\text{Me}^+$ interactions were observed.

The DTA and DTG/TG analysis was performed on the Mettler Recording Vacuum Thermoanalyser at DTH, Lyngby. Pure steenstrupine, dried at 50°C , was run against the Al_2O_3 standard with temperature increase of $10^{\circ}\text{C}/\text{minute}$ in dehumidified air.

Dehydration starts above room temperature and can be divided into three stages characterized by the broad maxima at 95-100°C, (the principal peak) at 150°C, and at 190°C. Another small endothermic peak occurs at 330°C. After a slightly wavy portion of the DTA curve, a pronounced exothermic reaction follows at 720°C. The DTA curve remains essentially horizontal afterwards, except for a small exothermic maximum at 1020°C.

The total weight loss between 25°C and 720°C is 10.5 wt%. Until 230°C 7.3 wt% are lost, between 230 and 340°C the loss is 1.6 wt%, and subsequently additional 1.6 wt% are lost until 720°C. The weight loss up to 720°C primarily represents the loss of variously bound H₂O.

The X-ray studies confirmed that the symmetry of steenstrupine is rhombohedral, with $\underline{a} = 10.46(1)\text{\AA}$ and $\underline{c} = 44.99(3)\text{\AA}$. The X-ray and morphological data (Moberg 1898) indicate the space group $\bar{3} 2/m$. Powder data of steenstrupine are given in Table 12.

On annealing between 25°C and 900°C (the X-ray photograph taken by G. Roed, DTH, on a Nonius high-temperature Guinier camera) steenstrupine persists unchanged, except for continuous shrinking of the lattice, until $\sim 102^\circ\text{C}$. The first changes in the powder pattern are soon followed by a pronounced "collapse" of the structure at $\sim 180^\circ\text{C}$ which produces an altered pattern of X-ray lines with typical "doublets". At 250°C all these lines vanish and only the 003 reflection of the original steenstrupine persists, with the steadily decreasing \underline{d} value. It fades out at $\sim 535^\circ\text{C}$ with the \underline{d} value of only $\sim 13.7\text{\AA}$. After very diffuse lines have appeared at $\sim 250^\circ\text{C}$, as premonitions of the phase change, at $\sim 850^\circ\text{C}$ (or already below 750°C on protracted annealing) new phases with very diffuse X-ray lines crystallize. They represent a mixture of monazite, a cubic CeO₂-like phase ($\underline{a} = 5.50\text{\AA}$) and an unidentified phase with the principal \underline{d} spacing of 4.26Å. These results conform well with those of Gamberg-Hansen (1977) and earlier investigations.

The measured density of crystalline steenstrupine 199104 varies widely from between 3.16 g/cm³ to above 3.31 g/cm³ as estab-

lished in heavy liquids during the mineral separation by J. Frederiksen, Inst. of Petrology, Univ. of Copenhagen. These variations are caused by numerous gas-liquid and solid inclusions contained even in the best steenstrupine fraction.

The REE content of steenstrupine 199104 was analysed by J. Bailey using X-ray fluorescence. A Philips PW 1410/20 spectrometer, with a tungsten anode operated at 80 kV and 30 mA, and allanite as a REE standard was used. The following lanthanides were measured: La 8.58 wt%, Ce 13.90%, Pr 0.82%, Nd 3.40%, Sm 0.11%, Gd 0.08% and Er 0.057%. Y content is 0.55 wt%. Taking into account the different hydration of the bulk sample and of the thin sections analysed by the microprobe, the agreement is very good except for Pr. The REE fractionation plot (see below) suggests that the microprobe values for Pr are too high whereas those from X-ray fluorescence are lower than a smooth distribution curve predicts. The other samples analysed by microprobe yield values more in line with the fractionation curve.

5.4. Discussion

In order to obtain a better understanding of the chemistry of steenstrupine, and of its variations, the weight per cents of elements (Table 10) were recalculated into atomic proportions (Table 13). In agreement with the trigonal symmetry of the mineral, and with its density (Makovicky and Karup-Møller, 1981) the atomic proportions were normalized so that the sum of tetrahedrally coordinated cations Si and P is equal to 18. No evidence could be obtained concerning the structural role of the minor amounts of Al in steenstrupine, or on the possible substitution $[\text{SiO}_4]^{4-} \leftrightarrow 4[\text{OH}]^-$ in the metamict material. Consequently, both were excluded from further consideration. Finally, the individual analyses were lumped together according to the alteration types within each sample (Table 14).

5.4.1. Statistical studies

Table 15a and Figure 48 show the mean value, standard deviation and the extreme values for each element in the entire studied material. It includes both steenstrupine as well as its metamictization and alteration products with the exception of the coarse-grained products, which contain microscopically recognizable phases. The tabulated values reveal that

- 1) The alteration process, from the crystalline through metamict to the altered material, is nearly isochemical for all stages with the exception of the most intense alteration. This statement is corroborated by the more detailed analyses which follow.
- 2) The Si/P ratio concentrates about the value of 13.8/4.2 atoms in a cell in what is practically an unimodal distribution.
- 3) Ca and REE+Y are concentrated in a rather narrow range around their respective averages of 1 and 6 atoms in the original unit cell. The variety of distributions of the individual measured rare earths, La, Ce, Pr and Nd, is much larger, but only the skew of the individual La and Ce distributions projects into the REE curve.
- 4) Th, Y, Mn and Fe have broader, symmetrical and close to unimodal distributions whereas the small amounts of Ti, Zr and Al are biased towards low concentration values.
- 5) Na has a very complicated, at least bimodal distribution curve over an extremely broad range of values from 0 to 13 atoms in an original unit cell. The average of ~ 6 Na atoms represents the least populated value.

The potential differences in the composition of steenstrupines of different petrological or genetic types were studied by the same means as the total composition. The plots of the frequency distributions were again used but will not be illustrated here.

The comparisons of the genetic types of steenstrupine, named A, B and C in part 3.3, are partly influenced by the lower number of analyses on the metamict B variety (Table 15b). Thus, the deviations of the B type in Table 15b from the values charac-

teristic for the A and C type may not always be statistically significant.

The average Si/P ratio, the REE value and the bulk of Ca concentration values are practically identical for the A and C types. The values for the C (vein) type in Table 15b are partly influenced by the presence of a special high-Ca, low-Na variety in the vein material. The distribution curve confirms that the bulk of the Ca values are concentrated around 1.0 also in this case.

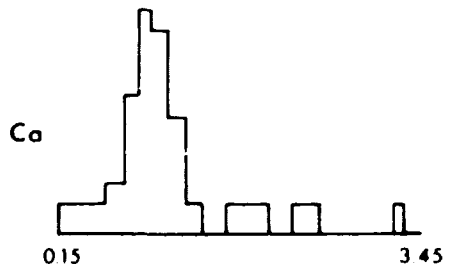
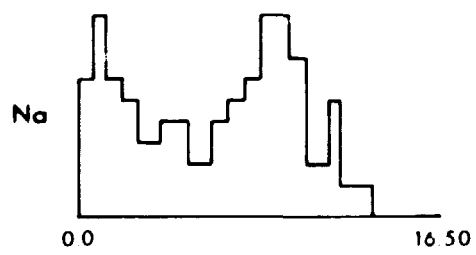
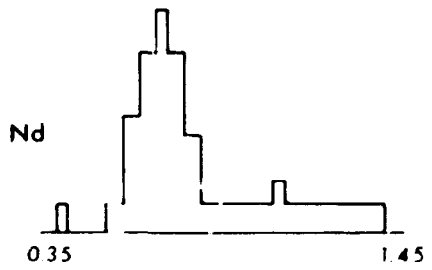
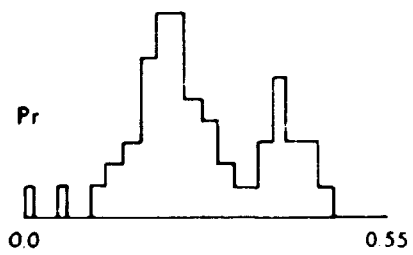
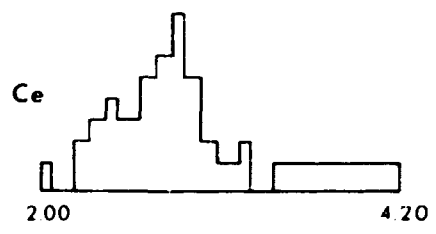
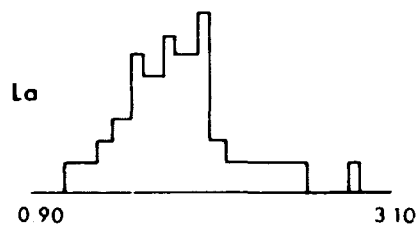
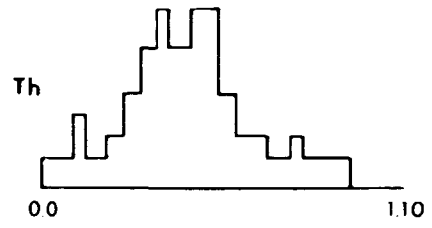
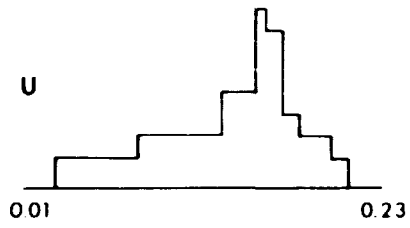
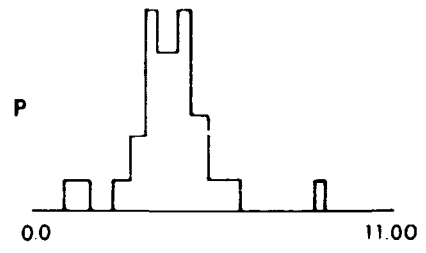
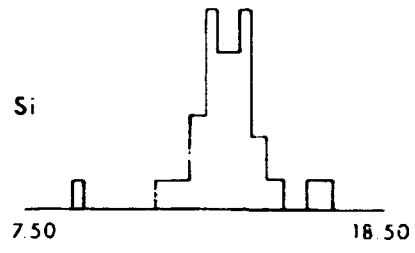
Among the rare earths, the bimodal La distribution, and unimodal Ce and Nd distributions do not show significant differences among the steenstrupine types.

Among the elements which increase slightly from the A type towards the C type are Th (0.33 → 0.51 at./cell), Pr, Mn (in the C type) and Zr; all of them usually display unimodal distribution. Aluminum decreases towards the C type as does yttrium. Fe shows a small increase in the B-type of steenstrupine where it might arrest the expected increase in Mn.

Steenstrupine from three principal petrological categories is available for chemical comparisons: arfvedsonite lujavrite, naujakasite lujavrite and from veins/pegmatites (Table 15d).

The average Si/P ratio is identical for all three petrological types. The same holds for the mean value and distribution of REE+Y. The distribution of La is bimodal, that of Ce unimodal, whereas Pr and Nd are more scattered over their concentration ranges. The averages are nearly identical, and the standard errors similar for La, Ce and Nd in all the above types.

If we disregard the high-Ca outliers in the veins and pegmatites (see above) the Ca values are identical (approx. 1 Ca atom in the original cell) for all the categories. However, those for steenstrupine from lujavrites are broadly distributed about the average whereas in the vein material they are sharply concentrated about 1.0.



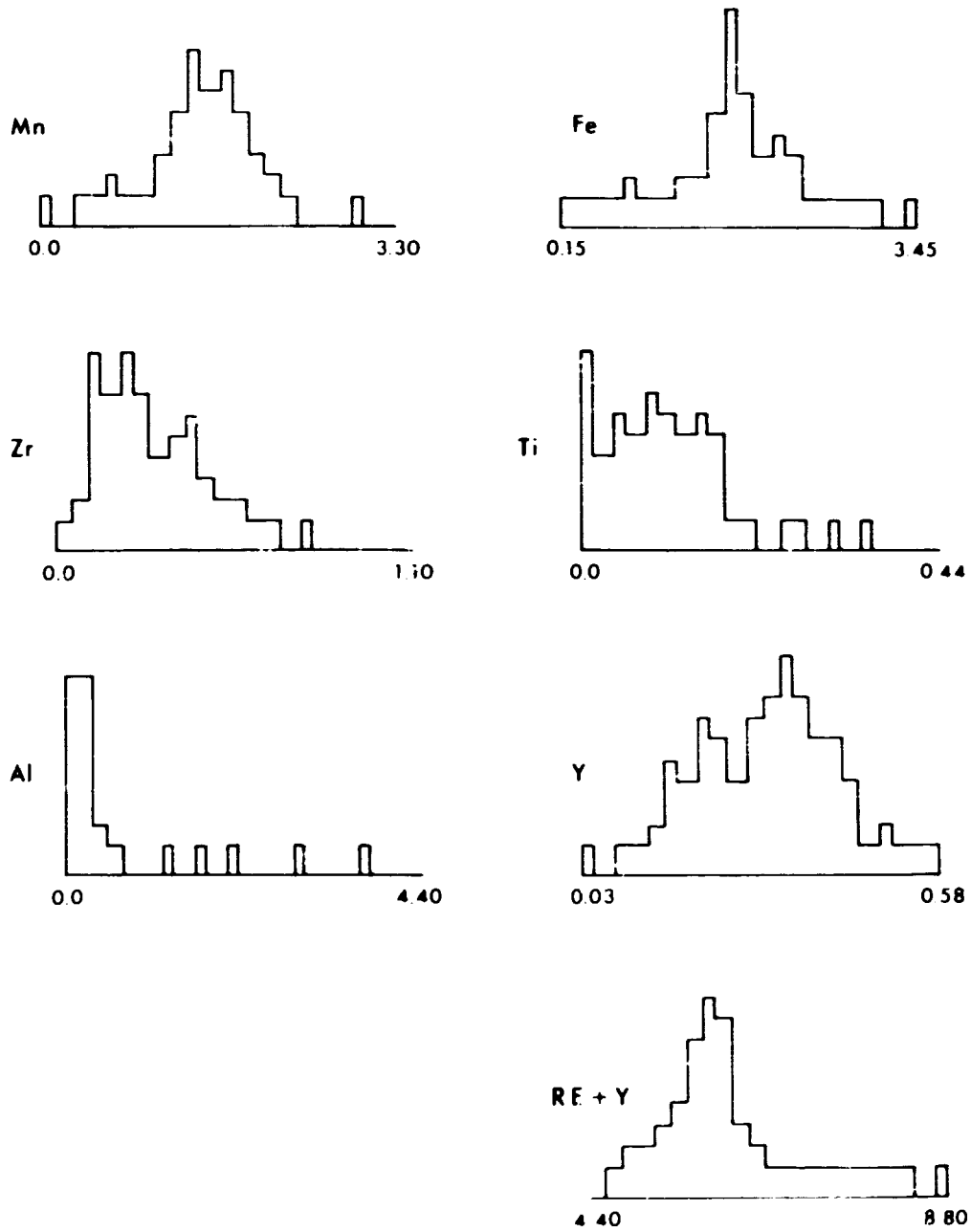


Fig. 48. Frequency histograms for the normalized (Si+P = 18.00) atomic proportions of individual chemical elements in the analysed steenstrupine material. The values of the end points of abscissae are indicated for each element.

The distribution of Na is strongly bimodal, or for the vein material even trimodal. Whereas in the rocks the higher Na contents prevail and result in higher averages (7.5 and 9.75 Na atoms/cell), a new and large frequency maximum appears at very low Na contents in the vein material.

The Mn, Th, Pr and Zr contents are markedly higher in the vein material whereas Y and Al are higher in the steenstrupine from lujavrites. The iron content remains stable.

The compositional data for the steenstrupine from different rock - hydration types (Table 15c) are best documented for the weakly hydrated rocks on one hand and for the intensely hydrated rocks on the other hand. Thus, the deviations observed for the medium hydrated rocks cannot be considered statistically significant.

Across the entire scale of hydration intensities the Si/P, REE+Y and Ca values remain unchanged. The same is true for Pr, Y, Mn, Fe, Zr and Ti. The small decrease in the La contents, connected with the small increase in the Ce and Nd contents with increasing hydration cannot be considered significant.

The elements displaying slightly decreasing values with hydration are: Th (from 0.36 to 0.27 atoms/cell) and Na (from the average of 8.5 to that of 7.1 atoms/cell). Al shows very low contents in highly hydrated rocks, reminiscent of the similar trend observed for the steenstrupine material from veins.

The potential chemical changes on steenstrupine alteration were studied using the statistics in Table 15e. Steenstrupine from both the rocks and veins was divided into six categories related to the descriptions in parts 3.3 and 4.3. These are: 1) crystalline, 2) metamict, 3) slightly altered, 4) altered, 5) extremely altered (fine grained) and 6) completely altered into a heterogeneous mixture of individual minerals. The individual zones of zoned steenstrupine were distributed among the relevant categories of this classification.

Two more categories were defined for the steenstrupine from veins: 7) Anisotropic steenstrupine which replaces the crystalline (or now metamict to altered) steenstrupine from veins. It forms lobes reaching from the periphery deep into the crystals; 8) Isotropic brown-red "steenstrupine" which replaces the vein types along fractures. These types were first optically described by Euchwald & Sørensen (1961).

The basic question is the interpretation of the differences found in this particular statistical study. The observed characteristics might be primary, formed during the crystallization of steenstrupine, or secondary, representing element transport during alteration.

Almost all of the categories defined here span various genetic and petrological types. This is the reason why the metamict and slightly altered steenstrupine display broadly distributed values when compared with crystalline steenstrupine which primarily comes from veins. As mentioned above, the statistical estimates for this type are influenced by the presence of the variety with 8 REE atoms per 18 tetrahedrally coordinated atoms.

The other factor causing spread of concentration values around their statistical mean is the differentiation process which takes place with advancing alteration (cf. part 4.3). It is well illustrated in Table 15 for the sequence from the altered via the extremely altered to the microscopically heterogeneous assemblage.

The presumably primary trends in the contents of Si, Th and REE between the different zones of the simply-zoned grains of steenstrupine A from some samples (part 5.2 and Table 14) are in the total statistics obscured by the differences between the rock/genetic types. Thus, no significant overall correlations with the degree of alteration could be established for the Si/P ratio, for the concentrations of Na, Ca, Th, Mn, Fe, Zr, Ti, REE as well as for the amounts of individual rare earths, with a possible exception of Co.

The only potentially significant trends are: 1) the marked decrease in the Mn content in the stage of extreme alteration. The same is true for Na which still occurs in high concentrations in altered steenstrupine. 2) an increase in the Al content in the analysed fine grained mixture representing the altered and extremely altered steenstrupine. The same is possibly true for the content of cerium but it could also be a primary compositional feature of these steenstrupines.

The results of this study show that, unlike the individual cases (part 5.2 and Table 14), no overall values of Th concentration exist which would be typical for each degree of alteration of steenstrupine.

The alteration types 7) and 8) ought to be compared with crystalline steenstrupine which primarily represents a vein material.

The replacement phase is generally richer in P, poorer in Th (also to some extent in Ca, Al and Y) and largely isochemical with the parent crystalline steenstrupine in the rest of the elements.

The brown-red phase, however, is not chemically homogeneous. The less intensely coloured portions, closer to the parent steenstrupine (No. 199115) still represent a variety with 5-6 REE atoms per 18 tetrahedral atoms. The portions in the central parts of the cross-cutting veinlets are darker and represent an isotropic product with 3 REE atoms per 18 tetrahedrally coordinated atoms. The latter phase also displays significantly higher contents of Ca, Fe, Al, Ti and Th. It contains practically no sodium. The crystalline phase and its alteration products from the vein specimen 230749 display very similar characteristics. These "steenstrupine varieties" somewhat alter the average characteristics of the crystalline and/or vein steenstrupine types. These exceptional "steenstrupine varieties" will be the object of further mineralogical studies.

5.4.2. The interelemental correlations in steenstrupine

The compositional varieties of, and the coupled substitutions in steenstrupine were studied by means of statistical methods and compositional plots. After excluding the measurements on highly altered and/or coarsely recrystallized steenstrupine as well as those on steenstrupine with 8 REE atoms in the steenstrupine unit cell, 133 measured points were left for processing. For the normalized atomic proportions covariance and correlation matrices were obtained as well as the principal component factor analysis performed. Furthermore, analysis of variance was performed by calculating the portions of the variance of each element covariant or contravariant with the variance of each of the remaining elements, i.e.

$$\text{variance (A) } \times [\text{correlation coefficient (AB) }]^2,$$

A and B running over all combinations of chemical elements, a sort of a mass balance sheet of all substitutions and compositional variations in the mineral. This scheme was modified into a charge balance sheet with the entries:

$$\text{var (A) } \times [\text{correl. coeff. (AB) }]^2 \times [\text{valency (A) }]^2.$$

The latter sheet is only approximate due to the uncertainties in the valences of Fe and Mn in the bulk of steenstrupine. Finally, an assessment of the, sometimes appreciable, residual variances was attempted - either as specific variances perhaps connected with the inestimable variations in the H^+ contents or in the valencies of Mn and Fe or as error variances due to the measurement problems and calculation approximations. Both kinds of residual variances have pronounced influence on the usability of the balance sheets.

The multiple linear regression equations were calculated for the chemical elements involved. Some caution has to be exercised in their interpretation because of the probable interactions of the not-entirely-independent x_i variables.

Throughout section 5.4, numbers in parentheses will denote one standard deviation of the preceding value in terms of the last digit. Both the entire data set and selected groups of data points were treated by the above procedures. Due to the action of the above mentioned unmeasurable factors, and especially of the differently weighted multiple substitutions in different samples which also have somewhat different bulk compositions, the correlation coefficients derived from all data are usually low to medium-high. The same is true for the unrotated and rotated factor loadings in the principal - component factor analyses (Tables 16 and 17).

The problem has been partly alleviated by analysing the sets of data (Tables 18-21) selected after genetic and alteration criteria. Among themselves they clearly indicate that in different samples or under different conditions different substitution and variation patterns will prevail.

In the unaltered or little altered steenstrupine from all genetic categories the normalized Si content varies between approximately 12.8 and approximately 14.9 atoms in the unit cell, leaving 5.2 to 3.1 positions for P. Except for the variations of the Na content this represents the largest change in the charge equal to $2.1 e^-$.

Ca displays variably pronounced positive, and (REE+Y) zero-to-pronounced negative correlation with Si. The positive correlation between Th and Si is most expressed in steenstrupine A (Table 18 and 19). The same holds for the positive Fe/Si correlation whereas the negative Mn/Si correlation equally occurs in all the samples. Ti and Zr show no distinct correlation with Si in the bulk sample. No reliable trends can be traced for the much dispersed Al and Na vs. Si plots. For all these elements individual assemblages show highly differing correlation patterns (Tables 18-22). In general, both the Si-rich and the P-rich steenstrupine can be alternatively Na-rich or Na-poor.

The multiple linear regression equation reads:

$$\text{Si} = 14.53 + 1.20(32)\text{Th} - 0.59(11)(\text{REE}+\text{Y}) + 0.05(1)\text{Na} + \\ 0.79(11)\text{Fe} + 3.74(72)\text{Ti}$$

with 0.46(25)Ca, 0.50Al, as well as Mn and other x variables not accepted in the F test because of large spread.

In the vein material 199104 there are no significant correlations of Si with other elements except for Ti (Table 22).

$$\text{Si} = 12.68 + 6.83(1.03)\text{Ti}$$

with 0.55 Ti, 0.36 Ca and other variables not accepted in the F test.

The other major component, rare earths with rather arbitrarily added yttrium, range in steenstrupine from about 5 to 6.2 (REE+Y) in the unit cell. Already Table 14 reveals some differences in the relative amounts of different REE, which are well expressed in the Tables 16-22 in the form of correlation coefficients La/REE and Ce/REE of the distinct sample groups. These trends will be discussed below in terms of the REE differentiation patterns.

The indistinct negative correlation between Ca or Th, and (REE+Y) can be up to reversed in some sample groups. The Na/(REE+Y) correlation is insignificant for the total of the samples as also are the correlations Ca/Na and Ca/Mn.

For all the material

$$(\text{REE}+\text{Y}) = 8.88 - 0.28(4)\text{Si} - 0.63(20)\text{Th} + 0.87(29)\text{Zr} \\ + 1.05(46)\text{Ti} + 1.20(18)\text{Al} + 1.71(40)\text{Y}$$

with the standard deviations approximately inversely proportional to the F values of the individual coefficients of the above variables; 0.24Ca and 0.15Mn as well as the other

elements were omitted because of the low F values. For the vein specimen No. 199104 the equation simplifies to

$$(REE+Y) = 5.37 + 0.09(2)Na + 2.29(44)Y$$

with 0.32Ca, 0.32Mn, etc. again omitted.

The correlation tables reveal, and an extended regression equation for Si in the entire material describes the different behaviour of La against Si on one hand and of Ce against Si on the other hand. The equation reads:

$$\begin{aligned} Si = & 13.00 + 1.39(34)Th - 0.00La - 0.90(18)Ce - 2.31(61)Pr \\ & + 1.12(45)Nd + 0.04(1)Na + 0.88(11)Fe + 3.92(70)Ti \\ & + 1.02(32)Al \end{aligned}$$

where La is uncorrelated whereas Ce distinctly negatively correlated with Si. The analytical problems with Pr and Nd have been mentioned. Below acceptability levels, - 1.03Y ought to be noted. The Ce/Si dependence is clearly marked in the zones of zoned steenstrupine A, discussed below.

From the fairly tight and distinctly unimodal concentration of the sum [REE+Y+Th+(Ca - 1.0)] about 6 atoms in the "REE" position as opposite to the scattered and spread distribution of ΣREE we conclude that the partial substitution of (REE+Y) by Th and Ca (and maybe even vice versa) takes place in all steenstrupine types. Tables 1.-22 show that this substitution ought to be most important for the sample 6-72.88 whereas least important for the vein sample 199104.

The other trend conspicuous in the correlation tables is the correlation of the Si and Th contents. With the increasing substitution of P^{5+} by Si^{4+} , Th^{4+} might replace REE^{3+} or also structural positions occupied by other cations. For the entire material:

$$Th = -0.65 + 0.07(2)Si - 0.02(0)Na + 0.25(6)Ca$$

with -0.05(REE+Y), -0.05Fe, etc. below the acceptance level.

For the sample No. 199104:

$$\text{Th} = 0.92 - 0.32(10)\text{Mn} + 0.80(15)\text{Y}$$

with 0.05Si, -0.01Na, etc. below acceptance level.

The composition plot of Th vs. Si shows that the Si/Th correlation in the entire material has genetic connotations; it is the (on average) more siliceous vein steenstrupine (the C type) that displays higher Th contents.

Microprobe sums of cations are not sufficiently reliable to indicate distribution of Th between the REE and the (Mn, Fe, Zr, Ti, etc.) positions. For the sample 199104 they suggest that a sizable portion of Th might reside in the latter position, in agreement with the altered equation above. Involvement of Mn with Th can also be observed in the metamict steenstrupine A and in the sample 6-72.88 (Tables 18-20).

In the latter two cases Mn is contravariant and Fe covariant with Si. However, the most important is the inverse relationship of Mn with Fe:

$$\text{Mn} = 2.29 - 0.29(5)\text{Fe} - 0.03(1)\text{Na}$$

$$\text{Fe} = -0.91 + 0.27(4)\text{Si} - 0.44(9)\text{Mn} - 2.31(47)\text{Ti} - 0.61(30)\text{Y}$$

for the entire sample, with all the other elements below acceptance level; and

$$\text{Mn} = 2.41 - 0.40(18)\text{Th} - 0.25(10)\text{Fe}$$

with -0.06Si, 0.10(REE+Y) and -0.68Ti, etc. below acceptance level;

$$\text{Fe} = 3.08 - 0.77(23)\text{Mn}$$

and 0.48Zr, etc. below acceptance levels, for the sample No. 199104. In the latter, the Mn/Th dependence seems to be only caused by incorporation of the Th rich core in the plot and is not valid over the entire grain.

In agreement with poor communality (large scatter) of Mn all equations, except for the first one for Fe, explain only small portion of variance. The Fe for Mn substitution deviates substantially from the 1:1 ratio.

Interesting Y/Zr correlations exist in steenstrupine samples from different genetic types. The correlation is positive in the zoned sample 6-72.88, close to zero in the metamict steenstrupine A and negative in the bulk sample due to the presence of vein material with a distinctly negative Y/Zr correlation. The Th/Y correlation is negative in the first samples whereas it changes to positive in the vein material. The Zr/Th correlation is negative in most cases although the magnitude varies widely.

For the entire sample:

$$Y = 0.18 + 0.05(2)(\text{REE}+Y) - 0.49(4)\text{Zr} - 0.21(4)\text{Al}$$

with 0.07Th, 0.003Na and -0.01Ti, etc. below acceptance level, whereas in the vein sample No. 199104

$$Y = -0.95 + 0.32(10)\text{Th} + 0.17(3)(\text{REE}+Y) - 0.22(1)\text{Na}$$

with -0.13Zr, etc. not taken up into the equation because of the low F values.

For the entire material:

$$\begin{aligned} \text{Zr} = & 0.26 + 0.19(6)\text{Th} + 0.07(2)(\text{REE}+Y) - 0.005(3)\text{Na} \\ & - 0.13(5)\text{Ca} - 0.23(5)\text{Al} - 0.89(9)\text{Y} \end{aligned}$$

with the statistical importance of individual contributions decreasing in the order Y, Al, REE, Th, etc.

With a much poorer explanation of variance of Zr, in the sample 199104:

$$\text{Zr} = -0.03 + 0.03(1)\text{Na} + 0.19(8)\text{Fe}$$

whereas -0.35Y , -0.16Ca , etc, were omitted.

The changes in the Zr/Y correlation and the Th/Y correlation might indicate changes in the structural role of Th and Y in steenstrupine with changing conditions, from steenstrupine A to steenstrupine C. In this direction also the Th content increases and the Y content decreases as indicated in 5.4.1. These two correlations perhaps suggest that in the vein material, C, a part of Th and Y might occupy the Zr-containing position to a greater extent than it does in the steenstrupine A. Although the Y content does not significantly exceed the values expected from the REE differentiation pattern (see 5.4.4) its rather independent behaviour in a number of regression equations confirms its structurally ambiguous role.

The charge balance charts show that the mutually correlated portions of charge variances for the major substitutions in steenstrupine do not balance out. For the case of (REE+Y) covariant with the relative increase in P they even add up. This confirms the role of the Na^+/H^+ charge balancing and of the potential changes in the valency of Mn and Fe, mentioned above.

For the very loose correlation of sodium with the other elements in the entire material:

$$\begin{aligned} \text{Na} = & -9.37 + 1.44(35)\text{Si} - 9.98(1.68)\text{Th} - 2.36(85)\text{Mn} \\ & + 14.34(2.54)\text{Y} \end{aligned}$$

Below significance level are -3.45Zr and -4.45Ti whereas Fe and (REE+Y) are uncorrelated.

In the sample No. 199104:

$$\text{Na} = -12.26 + 3.63(98)(\text{REE}+\text{Y}) - 11.70(4.19)\text{Al} - 15.69(2.87)\text{Y}$$

with 2.99Zr , 5.99Ti , etc. below significance level, and Ca, Mn, Fe uncorrelated.

Inspection of compositional plots shows that many of the Na-involving correlations have genetic and/or sampling causes: e.g. the bulk Na/Si relationship is again caused by abundant sampling of more siliceous C steenstrupines from veins. The (variously pronounced) Na/Th, Na/Mn, Na/Y, Na/Zr and Na/Al correlations in the sample 199104 come from the accumulation of respective elements either in the core or in the rims of the grains whereas in the bulk of the sample no correlations can be traced.

Ca is poorly correlated with the majority of elements. For the entire material:

$$Ca = 0.89 + 0.54(9)Th - 0.31(11)Zr$$

whereas no correlation exists with (REE+Y) and Na. 0.03 Si is the most important of the variables below acceptance level.

In No. 199104:

$$Ca = 1.03(11)$$

with the most important not accepted contribution being 0.17 (REE+Y), and Th, Na, Mn, Fe, Y practically not correlated.

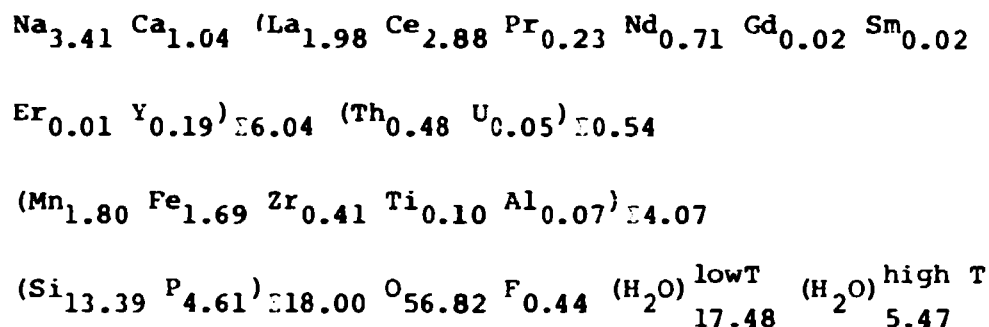
Calcium belongs among the elements with high residual variance in all studied sets (Tables 16-19). It only gets lower in the steenstrupine A where the correlations of Ca with Th and Si become more significant. The same is true for another persistently poorly correlated variable, Mn, which generally also can assume different valency states. Other elements with high residual variances are Si, Na, the individual rare earths, Al, Ti and to a lesser degree Zr.

Experience shows that the error variances of Nd, perhaps Ca and of the "small elements" (Pr, Al, Ti and Zr) might represent contributors to their residual variances. For Na, Ca, ZREE, Mn and Si (vs. P) the presence of variable amounts of H^+ in the structure allows variations which are uncorrelated with the variations of the other elements detectable by the microprobe

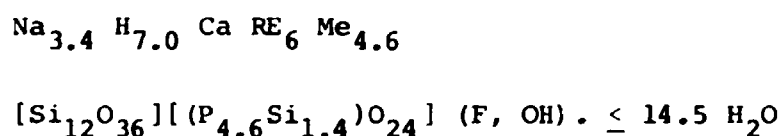
and surely account for a part of their residual variances. In this connection it should be stressed that the generally non-integral sum of "metal atoms" (Mn, Fe, Zr, Ti, Al, ...) and the rather large, not fully accounted for, variation in REE (below 6.0) suggest presence of cation vacancies in the original and the metamictized steenstrupine.

5.4.3. The chemical formula of steenstrupine

The empirical formula of steenstrupine 199104 was proposed by Makovicky & Karup-Møller (1981) as follows:

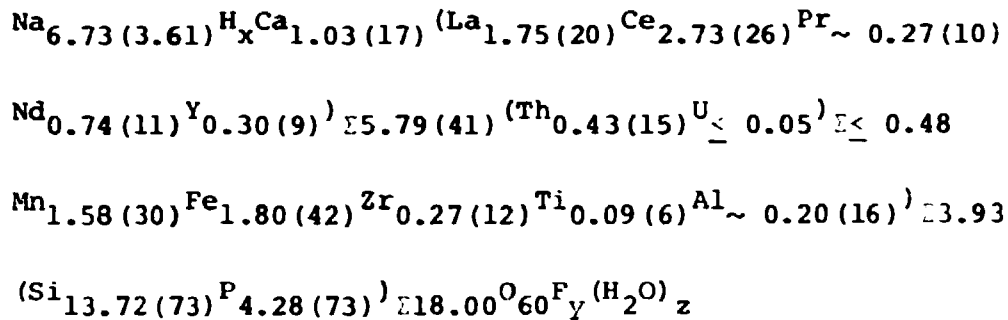


leading to the tentative crystal chemical formula (based on the facts briefly presented in 5.3) in which the "metals" other than REE+Y assume at least two distinct crystal chemical positions:



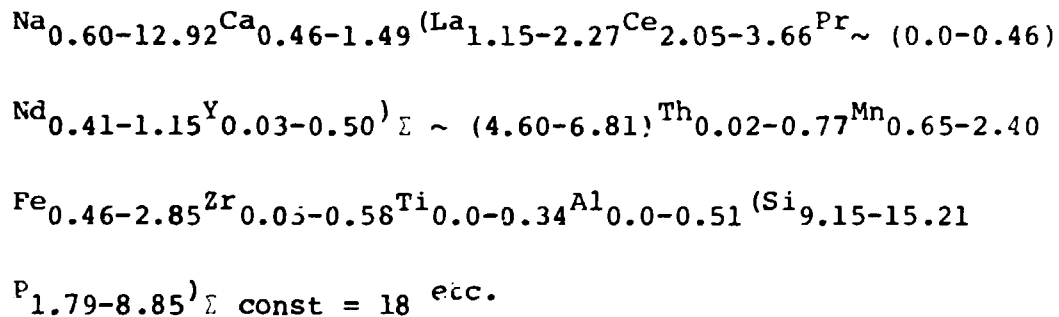
with Na and H variable and contravariant, Y and Th(U) arbitrarily ascribed respectively to the REE and "Me" positions although possibly both are present in either position, at least one (OH, F) position present and vacancies present in at least the "Me" positions.

The material in this study is mostly metamict or altered and does not allow better precision of the formula. Relying upon the above established formula, the average steenstrupine from the 133 accepted and used analyses has the composition:



with the values of x, y, z and the valencies of Mn and Fe not estimable by the present methods. Except for the altered Na/H ratio all the sums in the formula remain remarkably similar to those in No. 199104. Formulae of individual samples and of the alteration types in them are given in Table 14. Na contents are shown in Fig. 49.

In terms of extreme values from the 133 individual data points the formula reads:



As already shown above, part of the variation is due to the experimental problems with multiple measurements performed on small grains which are often zoned and easily decomposed by the electron beam.

In trying to summarize the observed interelemental correlations in the formula, several reasons for compositional variations ought to be tested:

- 1) coupled substitutions to maintain the overall charge balance in the structure.
- 2) covariant or contravariant changes of element concentrations in order to balance out changes in ionic radii of two or more elements in adjacent portions of the structure.

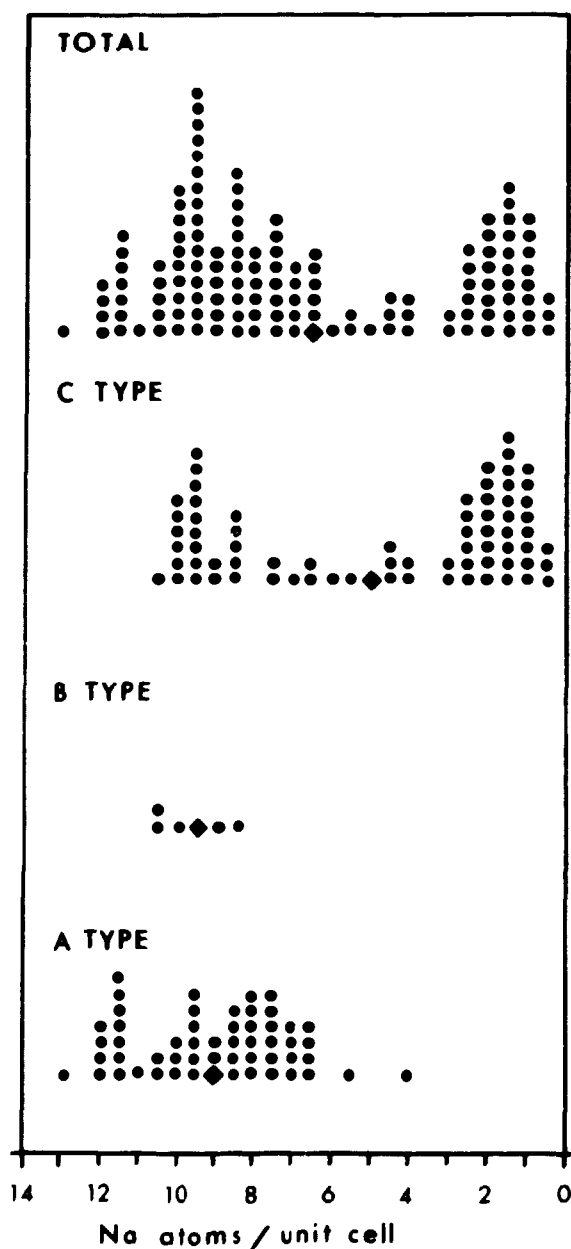
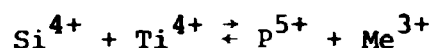
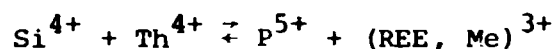
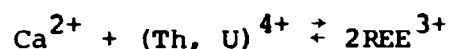
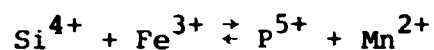


Fig. 49. Frequency histograms of the Na contents in steenstrupine. A, B and C represent the three genetic categories of steenstrupine defined in paragraph 3.3.

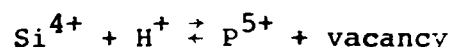
- 3) concurrent changes in concentrations of different elements in the mineral-forming magma or solutions during the crystal growth which do not play structural roles sub 1) and 2).
- 4) selective leaching from the formed crystals.
- 5) changes in structural role (preferred site type) of an element due to changing p-T conditions.

In the first category, the following substitutions can be selected from the statistical studies (schematically, without an attempt to assess their changing weights):



They assume very different importance in different samples and environments.

The substitutions involving Na^+ are undoubtedly present (as seen from the coefficients in Table 18), but they are camouflaged by the variations in Na^+ due to the relatively free substitution of H^+ for Na^+ . Similarly, the residual variances also suggest the substitutions which involve H^+ , e.g.



which are also active for Ca, REE and Th.

With the valency of Ce set to 3+ (as suggested by the ordinary behaviour of Ce in the REE - differentiation plot, 5.4.4) the contravariance of Ce and Si might be ascribed to the second of the above categories. It exists in the bulk of the material and would represent a preference for the larger REE cation out of the two principal ones (cerium rather than lanthanum) when the size of the presumably adjacent tetrahedra $[(\text{Si}, \text{P})\text{O}_4]$ increases due to the incorporation of more phosphorus.

A number of "correlations" between two elements appear to be associated purely with the existence of a distinct growth zone enriched in one element and with a certain concentration of the other element. The two elements are found to be uncorrelated throughout the entire mass of the crystal. As examples, the

Na - involving "correlations" and the Mn/Th relations in No. 199104 may be quoted.

Leaching of Na^+ from the crystals, under its simultaneous replacement by H^+ (and H_2O) has to be assumed for the steenstrupine C from the specimen 199104 because of its extraordinarily low Na contents. The crystallinity of this sample on one hand and the high Na^+ contents of many metamict samples on the other hand suggest that metamictization and the loss of Na^+ do not represent strictly coupled processes.

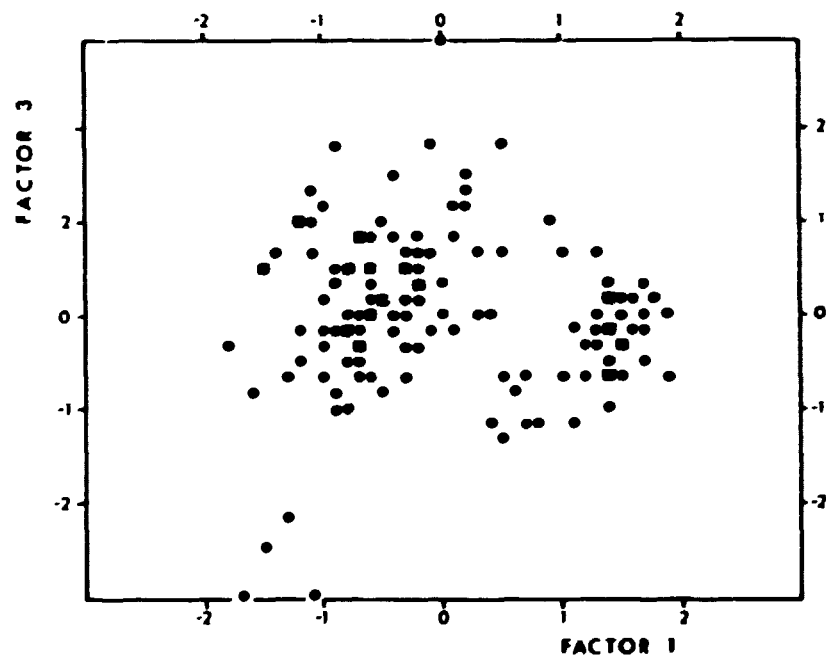
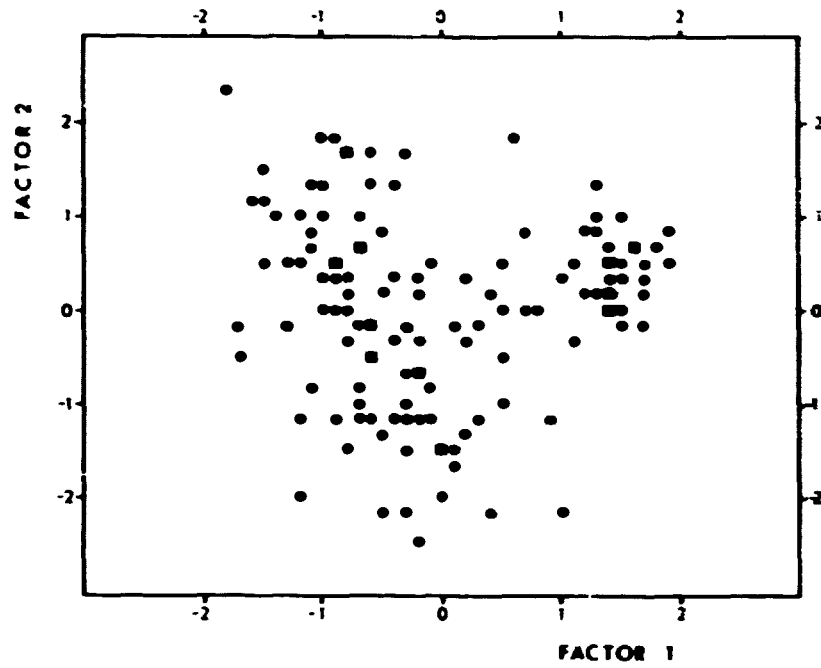
The possibility of the ambiguous, and changing roles of Th and Y - distributed in the REE positions on one hand and in the "Me" (Zr) positions on the other hand - has already been discussed.

In conclusion, we ought to stress that the problem of mutual substitutions and variations of elements in steenstrupine is known only very broadly and imperfectly because of 1) the experimental errors in multiple measurements on the, in the majority of cases, inhomogeneous material, 2) the missing information on the H^+ content and Mn, Fe valencies in the analysed spots.

The factor analysis of the 133 analyses of steenstrupines suggests that all this material represents a chemically homogeneous body, i.e. one broadly isomorphous species. The only separate grouping of points in the factor score plots represents the sample 199104 which differs from the other material by the distinctly larger amount of the (-Na) including complex variable (factor 1) in the data points (Fig. 50). This variety can be denoted as protonated steenstrupine.

5.4.4. The distribution pattern of rare earths in steenstrupine

The REE fractionation plot for steenstrupine was chondrite-normalized, using the REE concentrations given for chondrites by Matsuda et al. (1973) and Taylor & Gorton (1977). All analysed steenstrupine appears to be highly selective for the lightest



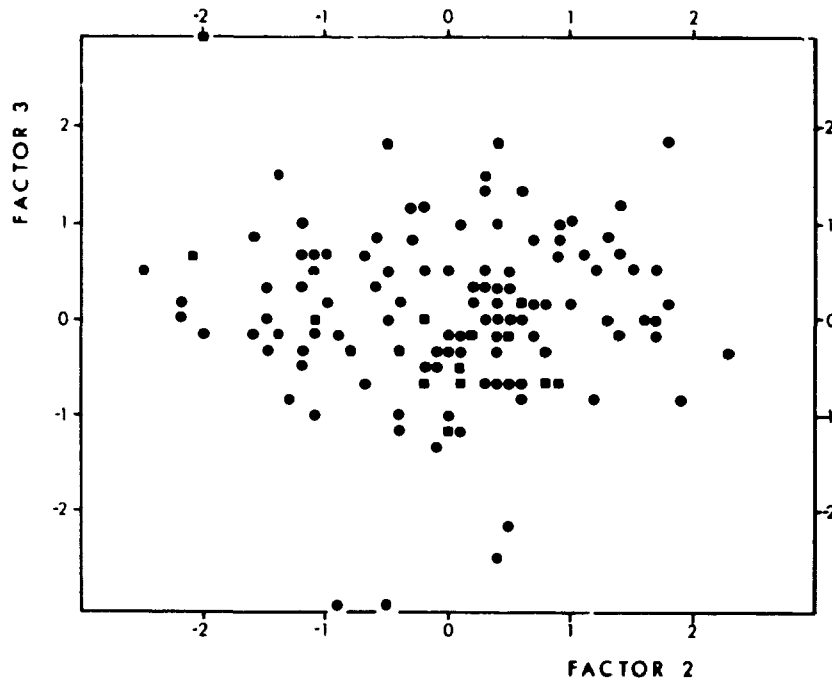


Fig. 50. Factor score plots of the three principal factors for the 133 steenstrupine analyses. Results are rounded to 1/6 and 1/10 on the y and x axis, respectively. Those outside the plotted area are placed on the margins. Overlap of data points is indicated by squares.

rare earths, in particular La itself. For the majority of samples the relative abundancy curve progressively rises from Nd to La. The X-ray fluorescence analysis of steenstrupine 199104 shows that already the contents of Sm are negligibly small and Y does not exceed the relative, chondrite-normalized abundancy of its heavy REE neighbours, i.e. it is not selectively incorporated in steenstrupine 199104. The high-lanthanum pattern is shown by all genetic types of steenstrupine, from A to C.

Two analyses of steenstrupine suites, in the samples 6-72.88 and 11-134.9, show a less pronounced preference for La, with Ce and Nd assuming a more important role in the total REE spectrum, i.e. the light-REE maximum is lower and broader. Except for hydration of the parent rocks, and distinct zonation of steenstrupine, no special chemical and/or paragenetical features were observed which would separate these two specimens from the

rest of the material. In both cases (in a trend opposite to that found in the samples of zoned steenstrupine Nos. 17-62.00 and 55-155.35 analysed in the scanning electron microscope, 5.2) the La/Ce ratio generally decreases towards the metamict rim of the crystals. The La values vary little whereas the other REE (primarily Ce) increase with the increasing total of REE.

The above La/Ce zonation of steenstrupine is attributable to the changing physical - chemical conditions and/or to the concentration (depletion) processes in some rocks of the mining area. In the sample 17-62.0 the outer zones are slightly more siliceous, with the core richer in P, whereas the general trend in Nos. 6-72.88 and 11-134.9 is opposite. (In all cases the fine grained, not quite homogeneous mass of the highly altered parts makes it difficult to determine the overall concentrations). As mentioned above, from all the REE examined, only Ce is distinctly negatively correlated with the Si/(Si + P) ratio, what accounts for the above observed La/Ce zonations. Similarly, Ce is strongly correlated with the REE totals, tying up REE and Si in a negative correlation (Tables 16-21). In the zoned crystals, Ce, Pr and Nd are negatively correlated with Th, whereas La remains uncorrelated or even positively correlated (Table 18).

The data of Bailey et al. (1978) show that in lujavrites selective enrichment in the lightest rare earths takes place against the older rocks of the Ilfmaussaq intrusion. This process increases the relative (normalized) abundance of La against the heavy REE by almost an order of magnitude. Our data appear to confirm that this process is mainly due to the appearance of steenstrupine in the rock. In this mineral the difference in the relative abundances of La and heavy REE spans approximately two orders of magnitude. Interestingly enough, the narrow, La-rich, and the broader, La-poorer, REE distribution patterns observed in the steenstrupine studied by us resemble closely the REE patterns of the lujavrite samples 154397 and 154360 respectively (Bailey et al. 1978), representing perhaps different stages of magma and REE differentiation.

6. RECOVERY OF URANIUM

6.1. General

The uranium deposit at Kvanefjeld consists of a number of different rock types of which distinct types of lujavrites are predominant.

The lujavrite consists of 1) alkali-rich aluminosilicates which are readily dissolved in acid, 2) feldspar, and 3) mafic minerals. In addition to these there are a number of rare minerals, among them steenstrupine which is the main uranium-bearing mineral. Other rare minerals also contain uranium but their contribution to the uranium content of the deposit in most cases is unimportant.

The average uranium content of the lujavrite is in the order of 340 ppm with a cut-off level of 250 ppm. The estimated size of the resource on various cut-off levels is shown in the following table. (For details see Nyegaard et al. 1977).

<u>Cut-off level</u> <u>(ppm U)</u>	<u>Uranium tonnage</u> <u>(1000 tons)</u>	<u>Average grade</u> <u>(ppm U)</u>
50	44	210
250	27	346
300	21	375
350	13	414

For comparison, on a world-wide scale a grade below 800 ppm U is usually considered uneconomic, but with the rapid increase in the demand and price of uranium, grades below that figure are now being re-evaluated.

The principal U-bearing mineral, steenstrupine, its alteration products and the other uranium bearing minerals are described in detail in the sections 3.3 and 4.3. Some types of steenstrupine are readily soluble in 2M H₂SO₄ but most types are insoluble.

6.2. Carbonate pressure leaching

The most widely utilized method of uranium recovery from ores is acid leaching. However, this is unacceptable for steep-slope because of the low recovery values, viz. 30-40%, the large consumption of acid, and the release of silicic acid in the leach liquor which inhibits further processing towards the uranium concentrate. As an alternative to the acid leaching process the so-called sulphating roasting process was tried in a pilot study in 1976-77. However, two results of this study gave rise to pessimism. For the first, the uranium recovery from representative drill core samples was lower than from the large, bulk sample of MGG lujavrite from the old mine adit. This poor result is accentuated with the addition of the bore core material from the 1977 drilling programme which extended the area investigated. Secondly, the investigation of the waste from the pilot study foresaw a continuous, unacceptably high, environmental contamination.

Carbonate leaching is the obvious extraction process with an alkaline rock such as lujavrite. The method had been considered earlier but was of little effect at the moderate temperatures applied. However, recent technological developments have improved the outlook for industrial application in the temperature range 250-300°C, temperatures which laboratory studies indicate could be optimal and economically interesting.

The uranium-containing minerals are decomposed under the influence of carbonate and oxygen at elevated temperatures. The uranium is retained in solution as the stable uranyl-carbonate complex.

The process was first tested in an autoclave of 3 liters capacity in which only two tests could be made per day. By running a number of experiments simultaneously it is possible to obtain the optimum conditions for the important parameters. Therefore, a set of mini-autoclaves were constructed of steel in the shape of a test tube. Up to 34 of these could be rotated in an oven at the same time in a special rack which kept the contents in steady motion during heating.

It was established that the leaching solution should contain 12% of sodium bicarbonate i.e. a saturated solution, and only 2% of sodium carbonate. Oxidizing conditions are imperative. In the mini-autoclaves oxygen was supplied in the form of hydrogen peroxide, H_2O_2 , which is decomposed into oxygen and water. The amount of H_2O_2 added corresponded to 10 bars of O_2 . However, considerable trouble was encountered with samples from the northern region of the deposit. Often the recoveries were very low and non-reproducible. An improvement could be obtained by increasing the amount of H_2O_2 , and also by addition of cupric carbonate, which may act as an oxygenation catalyst. This trouble did not appear in the experiments with the larger autoclaves. Here atmospheric air was used at a pressure of 8 bars, which proved sufficient.

In a pilot plant under construction air will be supplied continuously by a compressor against the working pressure of about 80 bars in the pipe autoclave.

High recoveries require temperatures well above $200^{\circ}C$. The different ore types are not equally sensitive but $260^{\circ}C$ is sufficient for all types.

The actual time of reaction could not be determined because of the rather slow transmission of heat into the oven-heated autoclaves.

For this purpose another oven-type was used, which consists mainly of a pipe-loop immersed in a melted-salt bath. The slurry of ore in carbonate solution is forced through the pipe-loop at a speed of more than 2 m per sec., which ensures violent turbulence.

The fineness of grinding appears to be of prime importance, especially at short reaction times. A grinding level of 90% minus 100 μ has been shown to be appropriate. It allows the leaching to be accomplished in a few minutes and gives no excessive filtration problems at a later stage.

Maximum recoveries have been obtained with slurry densities of up to 700 grammes of solids per litre, but viscosity strongly depends on temperature in the 260°C-region so it may be safer to work at, for example, 500 grammes per litre. On the other hand the capacity of the equipment is fully utilized only at the highest possible slurry load.

In order to process all the 102 drill core samples of interest, a standard testing programme was established, using the mini-autoclaves and designed in accordance with the above findings:

The samples were ground to 99% minus 71 μ . 14 grammes of each were mixed in the mini-autoclave with 14 ml of the solution containing 12% (120 grammes per litre) of NaHCO₃ and 2% of Na₂CO₃, 1 ml of 30% H₂O₂ was added after which the tube was immediately closed, placed in the rotating rack in the oven and heated at 260°C for 30 minutes.

After cooling, the content was filtered and both leach liquor and solid residue analyzed for uranium. The results of the standard testing programme are given in Table 26 and discussed in sections 6.3 and 6.4.

The possibility of running the carbonate pressure leaching continuously on a large scale has been tested in the pipe autoclave, developed and operated by Lurgi, the Federal Republic of Germany. This equipment consists essentially of a long pipe (1 km) through which the slurry is pumped at a speed of 2 m per second. The pipe consists of a heating zone, a reaction zone, and a cooling zone. After the cooling zone the bore is reduced in order to reach atmospheric pressure at the outlet. The material passes the reaction zone in 4 minutes at a flow of 3 m³/h.

A sample of 30 tons of the mine area type (MCG lujavrite) but with a low uranium content (240 ppm) was collected from the loose rock material on the lower slopes of Kvanefjeld in September 1978 and treated in Lurgi's pipe-autoclave pilot plant in Lünen in February 1979.

Three separate runs were made. In each case the ore was ground to 96% minus 75 μ , and the pulp mixing ratio was 1 kg of solid for 1 litre of solution what corresponds to 700 grammes of solid per litre of slurry. The results of the runs are:

- 1) 8% NaHCO₃ 275°C recovery 59%
- 2) 10-12% NaHCO₃ 275°C recovery 61%
- 3) 10-12% NaHCO₃ 250°C recovery 61%

These results are not considered unsatisfactory, since this sample also gave a low recovery in the laboratory tests.

From the autoclave the slurry goes to filtration where the leach liquor is separated out and the residue washed in preparation for disposal. At this stage the mineral villiaumite presents a complication. Villiaumite is a sodium fluoride which is water soluble. It occurs in the lujavrite in quantities up to 1% and hence goes into solution during the extraction and washing processes presenting an environmental hazard from the tailings. Another problem at this stage is the presence of partly dissolved thorium in solution whereas the REE are very little dissolved.

Concentration of the uranium at this stage from the leach liquor presents problems as the ion-exchange method does not work under so high bicarbonate concentrations. As an alternative the precipitation of UO₂ by reduction with hydrogen has been tried. The reduction takes place at 150°C and 15 bar H₂ in the presence of a catalyst. Nickel is a very efficient catalyst, but the UO₂ formed also catalyzes fairly well and has the advantage of not introducing any foreign material.

6.3. Relationship between the U yield and the petrological and mineralogical characteristics.

In order to find the possible factors influencing the yield of uranium from the lujavrites by the standard method described in 6.2, the yield of uranium was compared with the rock types, the

steenstrupine types as well as with the total U contents of the lujavrite samples.

As shown in Figs. 51 to 53, the average U recovery is a function of rock hydration and of the degree of steenstrupine alteration.

The rock hydration: If only the main body of data are considered in Fig. 51 leaving out the outliers, which mostly represent the rock with only monazite + eudialyte, the range of recovery values increases from weakly to strongly hydrated rocks. The upper limit of the yield drops only very little whereas the average and the lower limit drop appreciably with increasing hydration (Table 23).

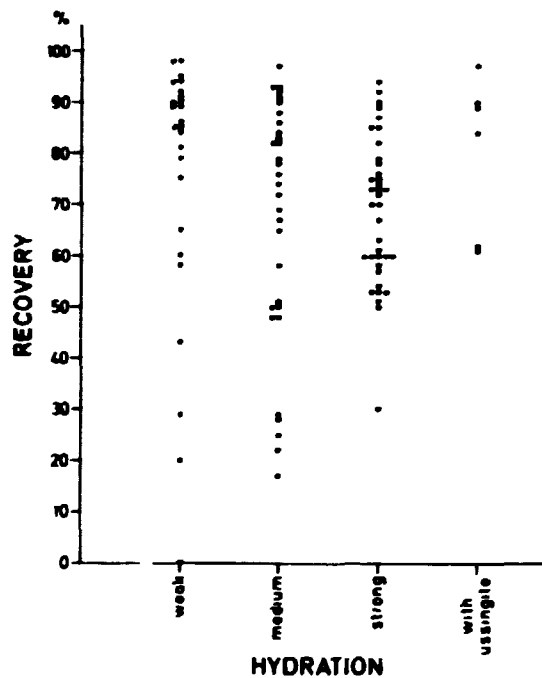


Fig. 51. Recovery of uranium by the standard test procedure (paragraph 6.1) vs. the overall rock hydration for the studied drill core samples.

The type of steenstrupine alteration: For each intensity class of rock hydration, the average yield is controlled by the steenstrupine alteration (Table 24). In Fig. 52 the low and medium hydration groups are given by different symbols whereas the values for the strongly hydrated rocks are featured separ-

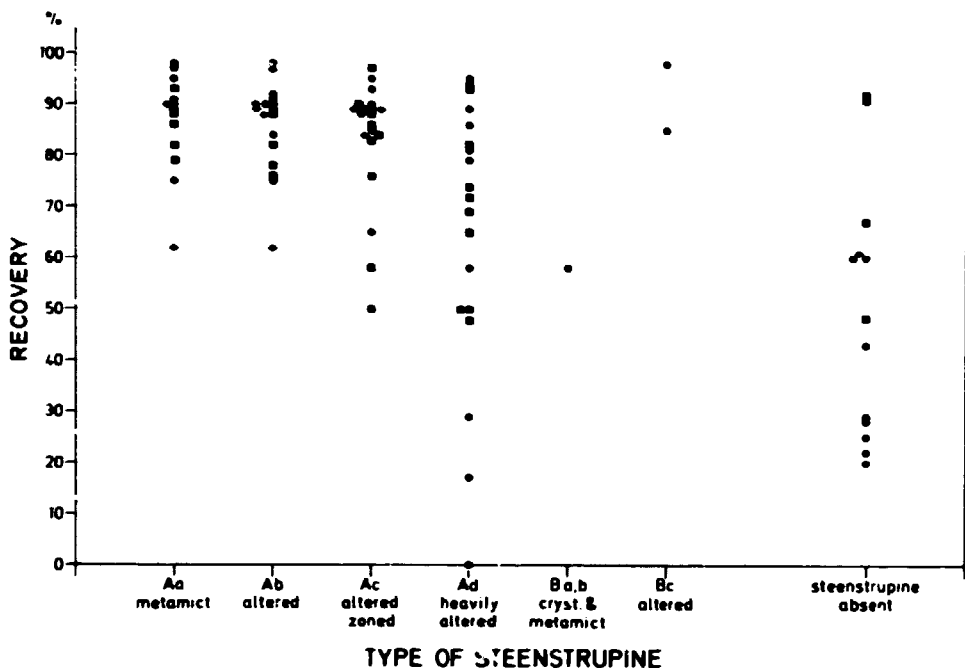


Fig. 52. Recovery of uranium by the standard test procedure vs. the type and alteration of steenstrupine in the weakly hydrated rocks (circles), medium hydrated rocks (squares) and ussingite-containing rocks (diamonds).

tely in Fig. 53. To obtain the impression about the trends described, the values for the rocks with zoned steenstrupine are to be ignored on first inspection. They lie between those for the altered and the metamict steenstrupine, in agreement with the principal components of the zoned grains. Again, considering only the robust estimates, i.e. with the outliers left out (Table 24), the highest yields show a weak decrease with increasing alteration of steenstrupine. However, the lower limit of the commonly occurring yield values drops appreciably with alteration.

This trend is well expressed for the weakly and medium hydrated rock types. In the strongly hydrated rocks both the average and the extreme yield values are substantially lower than in the less hydrated types. Although the average yield values most often decrease with increasing alteration for both A and B steenstrupine, the extreme values show less definite trends (however, often only a small number of samples were available).

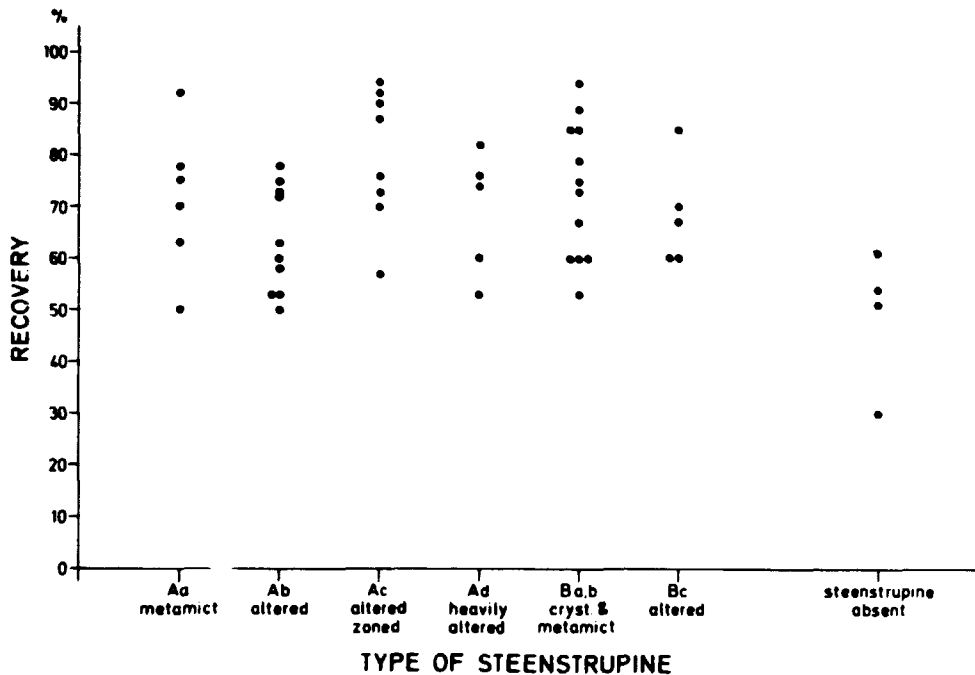


Fig. 53. Recovery of uranium by the standard test procedure vs. the type and alteration of steenstrupine in the strongly hydrated rocks.

Table 24 and the related Figures 52 and 53 can be used in the future extraction operations to estimate the expectancy values for the average yield and for its probable upper and lower limits using the principal petrological and mineralogical characteristics of the processed rock.

In contrast to the above defined relationships no clear connection exists between the yield estimates and the petrological rock types or the total U contents in the rock.

The petrological rock types: With the exception of the low yield estimates for the eudialyte + monazite rocks, the values for all rock types are uniformly spread within approximately the same range (Fig. 54, Table 25). The high standard deviations show that the differences between the mean recovery values for the individual rock types are not statistically significant. Only the values for naujakasite lujavrite are concentrated at the upper limit of the range, representing the typical values for

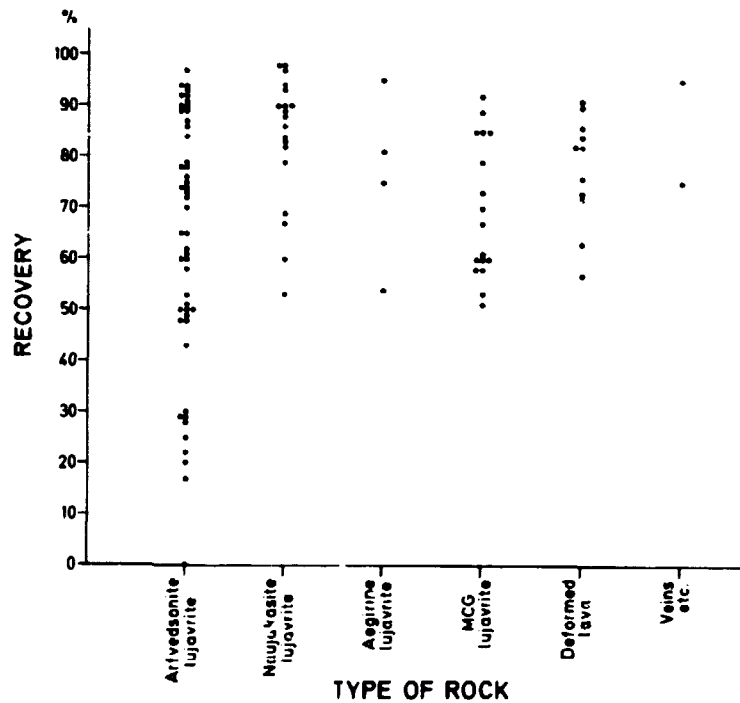


Fig. 54. Recovery of uranium by the standard test procedure (paragraph 6.1) vs. the petrological categories for the studied drill core samples. The low-recovery samples of arfvedsonite lujavrites represent the monazite- and/or eudialyte-bearing rocks.

the zoned steenstrupine, i.e. for a definite steenstrupine type (cf. Figs. 52 and 54).

The total U contents in the rock: The recovery values show no dependence on the total U content in the rock. Except for a few very low recovery values (monazite + eudialyte) and several samples with high U contents, the U contents in the rock are broadly concentrated around 350 ppm, yielding uniformly all values between the 50 per cent and 100 per cent recovery (Fig. 55).

6.4. Regional variations of U yield

The correlations described above between the recovery values and the petrological/mineralogical factors are the cause of the regional variations of the uranium recovery over the Kvanefjeld

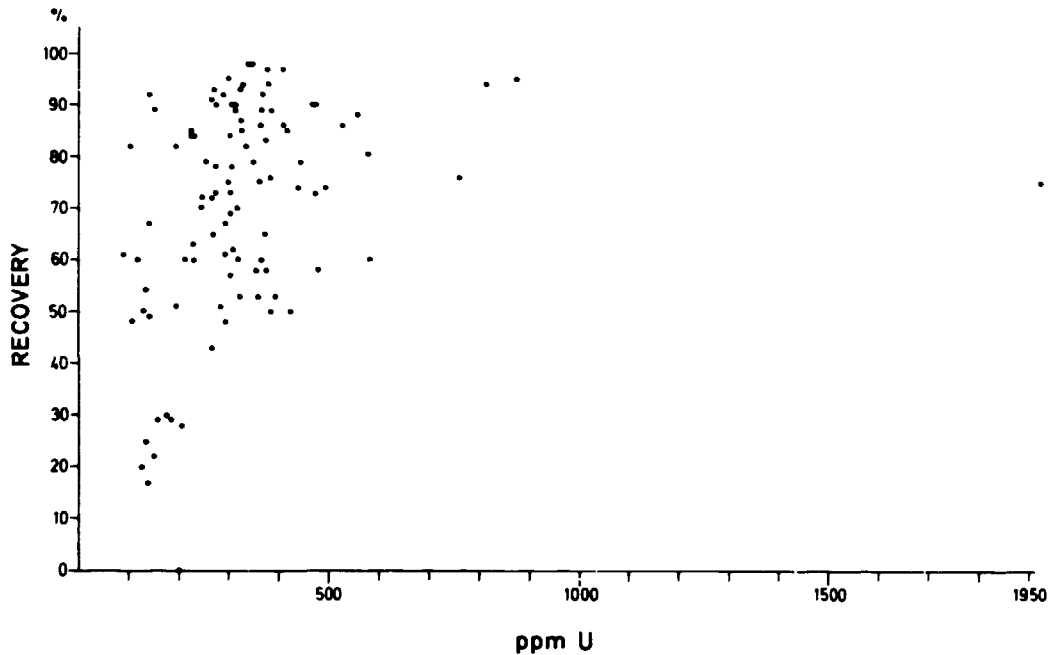


Fig. 55. Recovery of uranium by the standard test procedure vs. the total uranium content in the studied drill core samples.

area. Figures 56 and 57 show both the total uranium content of the studied samples (from wet chemical analyses, Table 26) and its portion recoverable by carbonate leaching under standard conditions (6.2 and Table 26). The samples from veins and contacts with atypical high U contents were excluded as not being representative for the bulk of the ore. For graphical reasons, the densely drilled "mine area" is illustrated separately on a different scale.

On the general background of good to moderate U contents and recoveries, two distinct areas of low recovery values can be outlined:

- 1) The elongated area along the western margin of the Kvanefjeld ore field. It is distinguished both by low total U content in the rock and by the low yield values. At the margin (the drill holes 64, 66, 67, 68, also 62) the recoveries and total contents are poor for the entire lengths of the drill cores. In the (predominantly) inwards situated drill holes

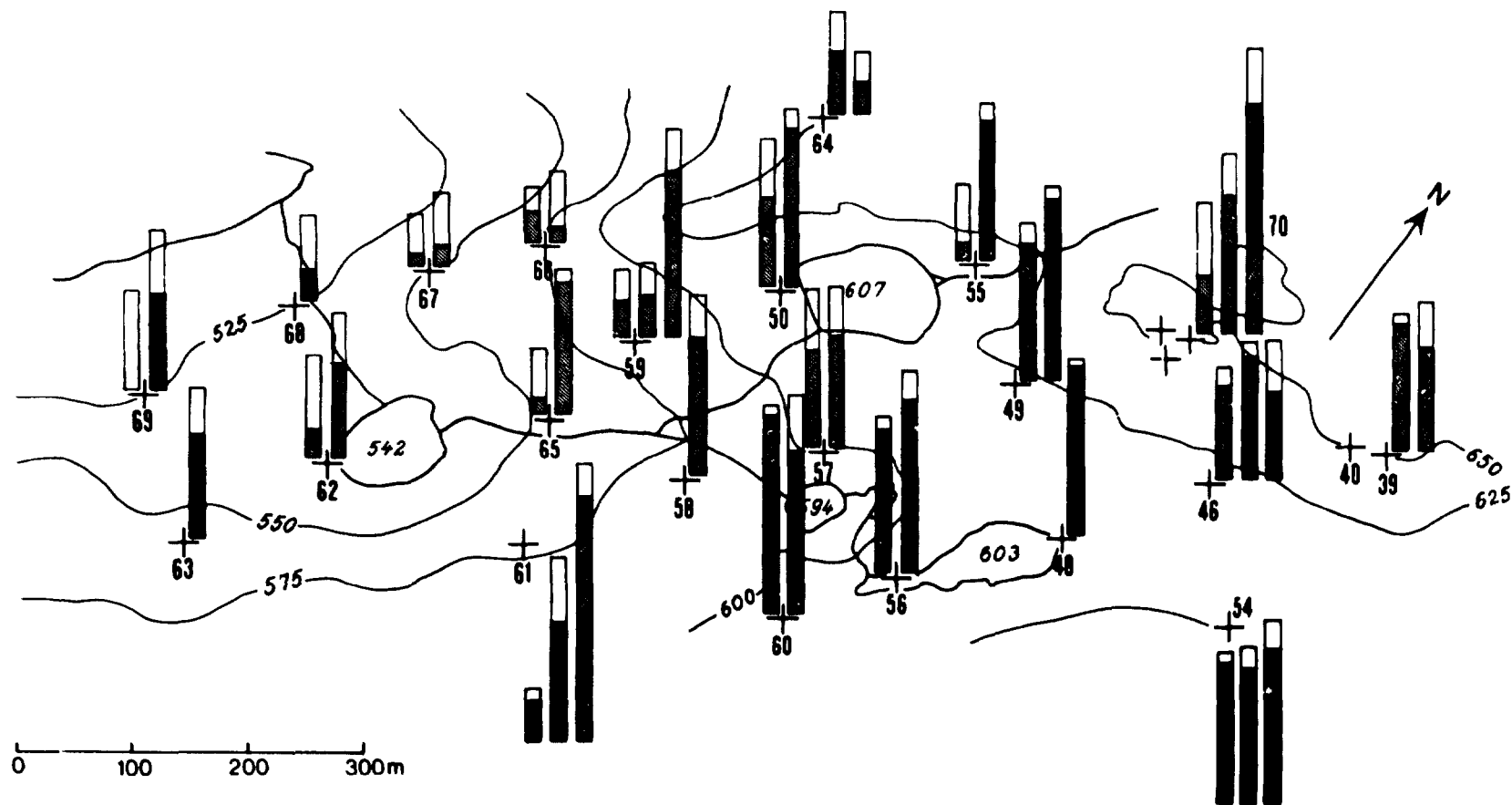


Fig. 56. The contents of uranium in the studied samples from Kvanefjeld (excl. the "mine area" given in Fig. 57). The entire bar lengths express total U contents whereas the shaded portions denote U recoverable in the standard leaching tests described in paragraph 6.1. 100 ppmU = 12.5 mm.

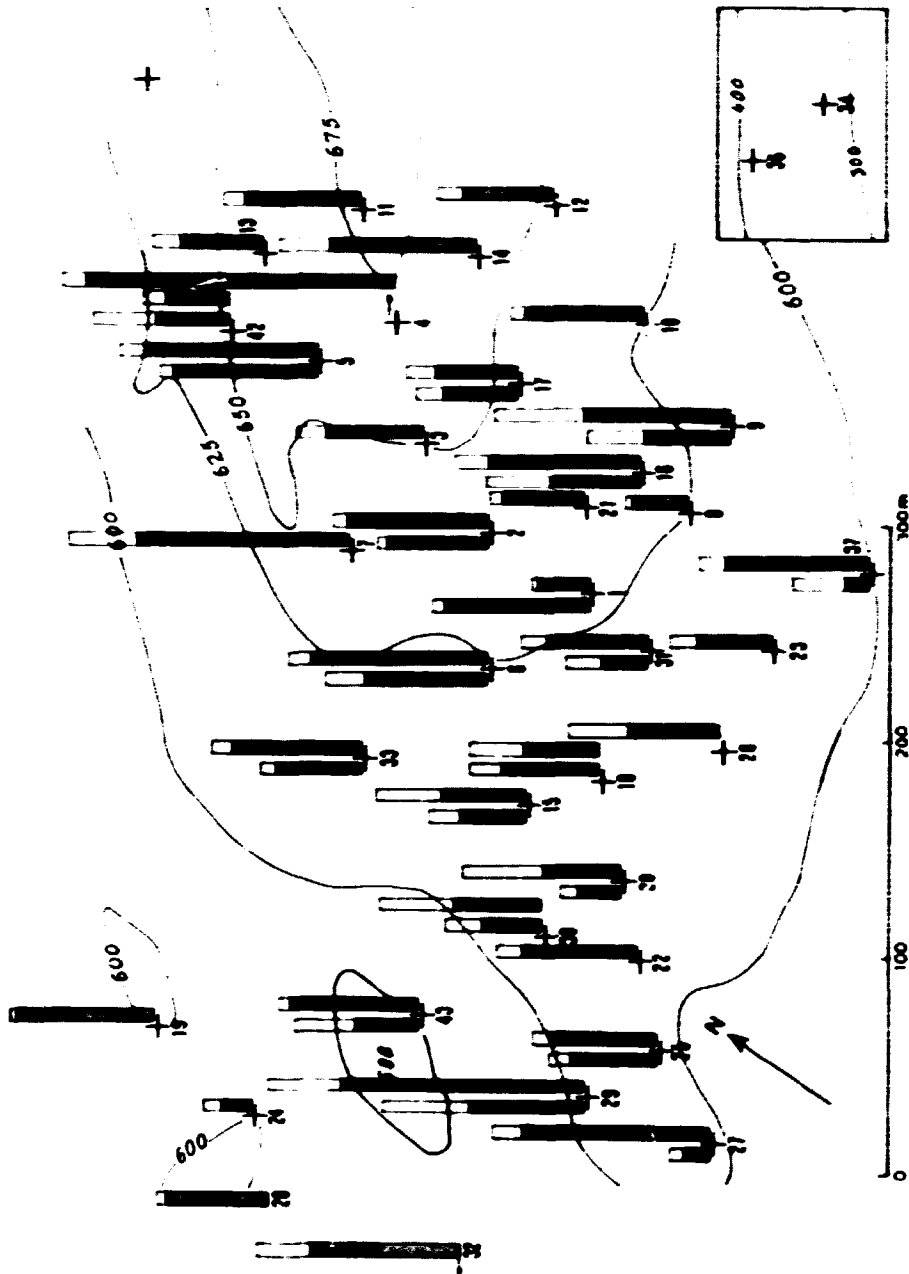


Fig. 57. The contents of uranium in the studied samples from the "mine area" of Kvanefjeld. The entire bar lengths express total U contents whereas the shaded portions denote U recoverable in the standard leaching tests described in paragraph 6.1. 100 ppmU = 1 cm.

(Nos. 69, 65, 59, 50, 55) it is mainly the deeper layers (120-190 m below surface) that yield poor U contents and recoveries. Such an uranium-poor layer continues in depth towards the northern end of the field (drill holes 55, 70 and 46). The autoradiographic and mineralogical studies show that all of these samples either contain only monazite and eudialyte (many of them are "barren" in the autoradiograms) or they also contain intensely altered steenstrupine, i.e. the Ad type. The marginal blocks of the ore field along the eastern side (Nos. 64, 66, 67, 68 resp. 62) should be entirely omitted from tonnage estimates.

- 2) The other region of poor recoveries is in the center of the "mine area". It is elongated in an E-W direction and comprises the drill holes 29, 43, 30, 20, 15, 18, 26, 31. Although the U contents are similar to, or only slightly lower than those in the surrounding portions of the ore field, the extraction yield concentrates around 50-60% in the majority of samples. The common denominator is the high degree of hydration of the majority of the rock samples. Most of the samples represent MCG lujavrite. The remaining ones are distributed between hydrated arfvedsonite lujavrite and hydrated lavas. They contain various type of steenstrupine A, especially Ac and Ad (resp. very similar products), or the Bb/Bc steenstrupine. A small area comprising the drill holes Nos. 16 and 9 (resp. also 17), close to the previous one, displays similar features.

The most stable, relatively high U-contents with good to very good recoveries occur in the central to northern area which stretches out among the drill holes Nos. 10, 5, 60, 49, 56, 54. Unfortunately in the central parts it is interrupted or not documented by drilling.

7. SUMMARY AND CONCLUSIONS

7.1. Geology, petrology

The detailed geological study of the Kvanefjeld area was initiated by H. Sørensen and was summed up in a report issued in 1969 (Sørensen et al. 1969). The various drilling operations over the last decade have greatly contributed to the understanding of the geology and are presented in Sørensen et al. (1974) and Nyegaard et al. (1977).

The area is a megabreccia in which various types of volcanic and sedimentary rocks from the roof of the intrusion and of the plutonic rocks from the early phases of the intrusion form blocks and sheets within the later intrusive nepheline syenite type known as lujavrite.

According to the results of gamma-spectrometric measurements (ibid.), the blocks of naujaite, syenite and unaltered volcanic rocks may be considered of no interest in respect to the radioactive raw materials. The bulk of the ore is represented by various types (generations) of lujavrite. Contribution to the ore mass can also be gained from the altered volcanic rocks interleaved with, or overlying lujavrites. During the processes of alkaline metasomatism these rocks were enriched with radioactive components (Sørensen et al. 1974). Late veins and pegmatites which contributed so much to the mineralogical knowledge of Ilímaussaq are not of economical importance because of their small volume.

In the multiple, complex lujavrite intrusion three types of lujavrite are of principal importance: on one hand these are the arfvedsonite lujavrites and the naujakasite lujavrites, which are apparently the older, magmatic phases; on the other hand it is the medium-to-coarse grained lujavrite which represents a locally important, later formed rock with a presumably pegmatite-metasomatite-like character. Aegirine lujavrites are only of secondary importance in the Kvanefjeld ore profiles.

During the research aimed at developing a suitable uranium extraction technique for the low-grade ore from Kvanefjeld (e.g. Asmund et al. 1971, Gamborg-Hansen 1977) it became apparent that a detailed mineralogical description of the ore and especially of the U-bearing components became essential because of the highly variable extraction yields. In the present research, autoradiography, fission-track investigation of uranium distribution, microscopy, microprobe analyses and other chemical techniques were applied to 102 samples chosen from 9000 m of drill core from the total of 70 drill holes made in the years 1958-1977. The samples generally represent the most abundant rock types in each drill core and were selected from the portions which displayed a reasonably constant, i.e. typical U content over considerable core lengths. Only rarely were the mineralized rock contacts and veins chosen.

The stress was on the statistically (i.e. also economically) important U-bearing associations. This was in contrast to the bulk of the previous work in which mineralogically interesting, selected samples or application of distinct methods were described in detail. Thus, the present research shows the relative (economic) importance of different ore types, of different previously observed or unobserved phenomena and different U-bearing associations throughout the ore body. The statistical approach also allowed the reconsideration of connections between various phenomena which were previously assumed on the basis of (a few) individual observations. Furthermore, the extraction of uranium was studied on the same rock portions as used for the mineralogical research so that direct ties between the respective results could be established.

The overall distribution patterns of radioactive minerals in the studied rocks were recorded by means of autoradiography of rock slabs cut lengthwise from the ore. Five distinct types of these radioactive fabrics were discerned: 1) a homogeneous, fine to medium grained distribution of radioactive grains; 2) veins and layers with radioactive minerals; 3) patches and nests of medium to coarse grained radioactive minerals; 4) individual scattered large radioactive grains, and 5) the autoradiographically

"barren" rocks with no distinct radioactive minerals. In agreement with the above genetic considerations, the type 1 (besides type 2) represents the principal ore fabric type of arfvedsonite and naujakasite lujavrites, the type 4 is typical for the medium-to-coarse grained (=MCG) lujavrites and type 2 the altered, metasomatized volcanic rocks.

The general microscopic description of lujavrites and altered lavas was performed to the degree allowed by the time allotted for the project. Both the principal mafic and felsic components of the rocks were determined together with the most abundant or conspicuous accessory minerals.

During this research it was found that the degree of alteration of primary felsic minerals (nepheline, sodalite, albite, naujakasite, microcline) into hydrated phases (analcime, natrolite, ussingite) transcends the boundaries between various rock types and varies on a regional basis. Thus, all the rocks were classified in the following groups: 1) weakly hydrated, 2) medium hydrated, 3) intensely to completely hydrated, and 4) hydrated rocks with ussingite. These categories are developed throughout the large sections of drill cores. The mafic minerals remain generally unattacked. Thus, this alteration should not be equated with the hydrothermal veins and their alteration zones which are scattered throughout the area.

The weakly to medium hydrated rocks are distributed rather evenly throughout the Kvanefjeld area. However, the intensely hydrated rocks are primarily confined to the "mine area" with the large bodies of MCG lujavrite, being apparently connected with the later stage of their emplacement process. Thus, the entire set of MCG lujavrite samples as well as the arfvedsonite lujavrite and altered lava specimens lying NE of the MCG lujavrite intrusion, below the sheets of roof rocks, are intensely hydrated.

In the other areas, intensely hydrated rocks occur only sporadically. A distinct accumulation of ussingite-bearing rocks occurs in (arfvedsonite) lujavrites overlain by a thick volcanic sheet in the N part of Kvanefjeld.

7.2. Mineralogy and fission-track data

Our studies confirm that steenstrupine and its alteration products represent the principal U-bearing components of the ore. In the Kvanefjeld rocks steenstrupine occurs in two distinct forms, A and B, that differ in grain size, shape and origin.

Type A represents small to medium-large euhedral grains usually with small amounts of inclusions, situated among arfvedsonite needles and felsic components. It appears to be of primary, magmatic origin in both arfvedsonite and naujakasite lujavrites. It is usually distributed homogeneously throughout the rock mass, independent of the hydration.

The type B is less abundant, practically limited to MCG lujavrite. Its generally subhedral crystals are medium to large, often poikilitic, containing all kinds of rock-forming minerals. In many cases they are intimately connected with arfvedsonite felt. Its formation is obviously closely connected with the formation of MCG lujavrite.

Steenstrupine from veins/pegmatites has been denoted as steenstrupine C. Although of no economic importance, its accumulations as pure crystals represent an important source of research material.

In some samples of altered, metasomatized lava the affinities of steenstrupine remain uncertain. The above classification is in good general agreement with that of Sørensen et al. (1974).

Occurrences of still crystalline steenstrupine are rare. In the majority of instances it has either undergone metamictization because of its contents of radioactive elements or, at higher contents of radioactive elements, it was altered (with differing intensity) into a very fine grained aggregate of secondary products. Alternatively, reactions with later solutions caused replacement of steenstrupine A or B by a mixture of crystalline products in which monazite plays the main role.

The metamict steenstrupine, Aa, has a high refractivity index and light creamy colour. Slight alteration on margins or cracks is often observed. Samples with this steenstrupine are spread evenly throughout the area. In many instances it is combined with the unzoned altered steenstrupine, Ab. The latter represents a gamut of occurrences, from the grains with some portions altered to the entire grains altered into fine-grained anisotropic products which are brown in transmitted light.

The uranium content of metamict steenstrupine lies at and above 2000-3000 ppm U_3O_8 but does not exceed 5000 ppm U_3O_8 . The associated altered steenstrupine displays fission track densities of 5000-7500 ppm U_3O_8 , rarely also accumulations with higher contents. The contents typically lie between 0.30 and 0.60 wt% in these two steenstrupine types, depending strongly on the sample location.

Some rocks with the mixture of Aa and Ab steenstrupine contain disseminated numerous minute metamict and altered grains of steenstrupine. Dispersed in these rocks are metamict, dark brown grains of an Y-Zr silicate with substantial concentrations of uranium, Th:U \approx 1:1, which may contain an important portion of total U in the rock. This type occurs in the drill holes 49, 25, 15 and 17.

Zoned steenstrupine, Ac, occurs primarily in the arfvedsonite and naujakasite lujavrite of the "mine area". Types of zonation differ from place to place: cases with altered cores and metamict to crystalline rims are more abundant than those with altered rims. In many instances several altered and metamict zones alternate in one grain. Each locality displays one type of zonation.

This type occurs either alone or it is associated with abundant, very fine-grained disseminated Ab or Ad (see below) steenstrupine. The altered cores display fission track records corresponding to 8000-10000 ppm U_3O_8 , the altered zones at other localities 5000-7000 ppm U_3O_8 whereas the metamict zones 2500-4000 ppm U_3O_8 . The latter two contain respectively 0.25-0.50 wt% and 0.12-0.18 wt% Th.

In some naujakasite luvjarites, naujakasite is replaced by an isotropic, light brown product with the same qualitative chemical composition as the parent mineral except for introduction of uranium. It contains ≤ 1000 ppm U_3O_8 . Associated pseudomorphs after eudialyte, a possible main source of U in the replacement product, display up to, rarely above, 2000 ppm U_3O_8 .

In the case of extreme alteration the shape of the steenstrupine, Ad, grains is gradually obliterated. In most cases steenstrupine is replaced by a very fine-grained, dark brown material, sometimes associated with light hydrated rock-forming minerals. In other cases only a loose, light gray network remains after steenstrupine with occasional darker patches. In still other cases, crystals of monazite, sometimes neptunite and natrolite may be discerned in the pseudomorphs.

The fission track records are, as a rule, very inhomogeneous and the U contents indicated are low, mostly 2000-3000 ppm U_3O_8 . In some rocks spot-like accumulations of uranium occur scattered in the generally low (1000-2000 to 4000-5000 ppm U_3O_8) uranium level of the decomposed grains. The accumulations are far above 1% U and the semiquantitative microprobe scan suggests uranothorite (Th:U \approx 5:1, with a substantial Si content) as the most likely product.

In the cases when the altered and extremely altered steenstrupine A are present in the same rock, the latter may have up to 7000-8000 ppm U_3O_8 whereas the Ad type displays only 500-2000 ppm U_3O_8 with rich accumulations, by far exceeding the 1% U level, still recognizable in the fission tracks.

Fresh, anisotropic steenstrupine, Ba, is rare. It forms parts or rims of generally metamict to lightly altered crystals of B steenstrupine. The metamict steenstrupine, Bb, is isotropic and light brown of various shades. Crystals are usually large and incipient alteration in some zones and in fissures can be observed.

Alteration of steenstrupine B proceeds in two ways:

- 1) leaching and replacement by an aggregate of well crystallized phases: primarily crystalline monazite, metamict uranothorite, an Zr-Na uranium-bearing silicate, neptunite as well as light rock-forming silicates;
- 2) formation of a very fine-grained brown, anisotropic product similar to that formed from steenstrupine A.

The rocks containing steenstrupine B are mostly MCG lujavrites or rocks permeated by veinlets of it. The Bb variety usually gives homogeneous fission track records indicating 4000-6000 (7000) ppm U_3O_8 . Incipient alteration is connected with 7000-10000 ppm U_3O_8 . The coarse-grained monazite in the pseudomorphs only gives 1000 (-3000) ppm U_3O_8 whereas uranium is concentrated in the above mentioned products with several % U. Occasional admixtures of Ad steenstrupine in the hybrid rocks of this category yield 4000-8000 ppm U_3O_8 , again with high U spots.

Eudialyte gives 1000-2000 ppm U_3O_8 . A Zr-containing aluminosilicate sometimes contributes to the U content of the rock.

The altered steenstrupine, Bc, yields 2000 to 4000-5000 ppm U_3O_8 , usually with high U spots >> 1% U and often disseminated monazite with low uranium content.

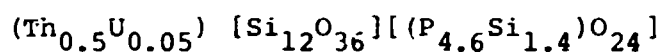
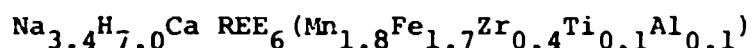
The studied altered, "migmatitized" lava shows steenstrupine crystals both in the darker layers and in the richer, lighter "veinlets". Although of uncertain type, it resembles the B steenstrupine. It contains ~ 1% U and is associated with abundant fine-grained steenstrupine disseminated mainly in light parts (~ 5000 ppm U_3O_8).

The above fission track studies were performed using lexan polycarbonate plastic as a solid-state fission track detector, irradiation by thermal neutrons with U-doped Ca-Al-Si oxide glasses as standards.

7.3. Chemistry of steenstrupine

Steenstrupine represents a complex silicophosphate of sodium, rare earths, calcium, manganese, iron and minor amounts of other metals, including thorium and uranium.

Detailed microprobe, X-ray, infrared and thermal data were obtained on the large occurrence of crystalline steenstrupine from the veins at Tunugdliarfik (Ilfmausaq). For this mineral, with a rhombohedral lattice ($a = 10.46\text{\AA}$, $c = 44.99\text{\AA}$, space group $R\bar{3}2/m$) and observed density varying between $\sim 3.15\text{--}3.35\text{ g/cm}^3$ an average formula

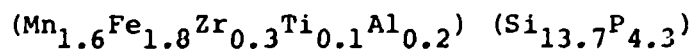
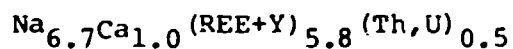


(F,OH) . $\sim 14.5\text{ H}_2\text{O}$ was derived,

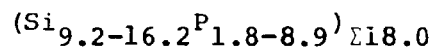
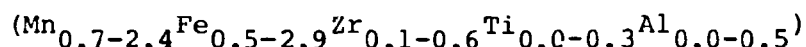
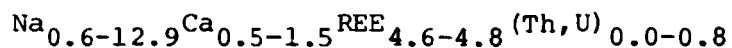
based on $\Sigma (\text{P}+\text{Si}) = 18.0$, with large variations in the Na/H and P/Si ratios (aver. total 4.6 P/13.4 Si).

The present, mainly metamict or weakly altered material enlarges the spectrum of known compositions and mutual replacements. However, the statistical studies show that it represents one, broadly isomorphous mineral species. Only the above, highly protonated steenstrupine can be considered a special variety.

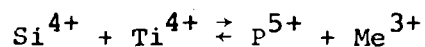
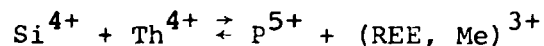
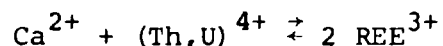
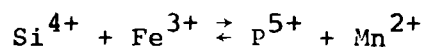
The average cation composition of all analyzed steenstrupines (types A, B, C) is



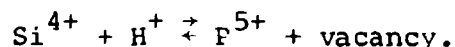
where the composition limits observed are:



No information on water, OH^- or H^+ or F^- contents can be obtained for the A, B and the majority of C steenstrupines. Part of the variation is due to experimental problems connected with multiple measurements taken on the same, often inhomogeneous (zoned) grains which can be fairly easily decomposed by the electron beam. This places some limitations on the derivation of crystal chemical substitutions in steenstrupine. The following coupled substitutions can be considered active, with very variable intensity, in steenstrupines from various localities:



Further substitutions involving Na^+ are undoubtedly present but they are camouflaged by the large variations in Na^+ due to the extensive mutual $\text{Na}^+ \rightleftharpoons \text{H}^+$ substitution, kinetically obviously easy in both directions. Similarly, large residual variances of Si, Ca, REE and Th suggest substitutions involving the non-analysable H^+ component, of the type



The bulk of the material displays negative correlation between Si and Ce which presumably is caused by changing sizes of coordination polyhedra during substitutions. Th and Y might play an ambiguous and changing structural role, on one hand occupying (partly with Ca^{2+}) the REE positions, on the other hand occupying the Zr position.

Variations in chemical composition of steenstrupine of different genetic types, petrological and hydration categories as well as of distinct mineral alteration types are small.

From the A to the C types, the concentrations of Th, Mn and Zr increase somewhat whereas those of Al and Y decrease. Among the rock types, steenstrupine from arfvedsonite lujavrites chemically does not differ from that from naujakasite lujavrites. Higher Na contents prevail (averages 7.5-9.8 Na/cell) in the rocks. Only in the veins was found the low-Na, highly protonated steenstrupine. Variations in Ca and some other elements in the vein material are more restricted than in the rocks, although averages differ little. Rock hydration does not appear to influence substantially the cation chemistry of steenstrupines except for some decrease in the Th, Na and Al values. The first stages of steenstrupine alteration are nearly isochemical; only in intensely altered steenstrupine does the content of Mn, Na and Al decrease. Concentration ranges show increasing differentiation of material on alteration.

In the zoned steenstrupines both the occurrences with the increasing and the decreasing Si/P ratio from the crystal center to the rim were observed. As a rule, the Th and U content decreases towards the rim, continuously or as sharply delineated zones. In numerous cases several high Th, U (= altered) zones alternating with low Th, U (= metamict) zones were found.

The red steenstrupine-like mineral (cf. Buchwald and Sørensen 1961) partly represents metamict steenstrupine and partly a separate, anisotropic to metamict phase rich in REE, Ca, Fe, Al, Ti and Th with only minimal Na contents.

The REE fractionation plot of steenstrupine shows its strong preference for La and the light rare earths. The majority of analysed steenstrupine is highly La-selective. Two samples, however, were found with broader concentration maxima of light REE. These occurrences may represent less REE-differentiated rocks (cf. whole-rock spectra by Bailey et al. 1978). Steenstrupine appears to play an important role in the final (i.e.

lujavrite-stage) differentiation of REE in the Ilímaussaq intrusion. No preferred accumulation of Y in steenstrupine was observed.

7.4. Uranium Recovery

After some unsuccessful experimenting with acid leaching and sulphatizing roasting (Gamborg-Hansen 1977), carbonate leaching of the ore under oxidizing conditions at 260°C was found to give the highest uranium yield. Both oven-heated autoclaves and continuous, pipe-like arrangements were tried. For the precipitation of UO_2 from the uranyl-containing liquor, hydrogen was used in the presence of a catalyst. The major problem of environmental pollution is presented by the fluorides released by the dissolution of villaumite, NaF.

After the basic technology of leaching had been established, a standard testing programme was set up in mini-autoclaves in order to process all the studied drill core samples. 14 grammes of samples ground to 99 μ minus 71 μ were mixed with 14 ml of the 12% solution of $NaHCO_3$ plus 2% Na_2CO_3 . 1 ml of 30% H_2O_2 was added and the bomb was heated at 260°C in a rotating rack for 30 minutes.

The average yield lies between 91 and 63%. It decreases appreciably from the metamict towards highly altered steenstrupine types. In the strongly hydrated rocks the latter trend is less clear because the yields are substantially lowered by hydration.

The rocks with monazite and eudialyte (mostly arfvedsonite lujavrites) represent a special group with very low recoveries (average 42%). Otherwise the recovery values for individual rock types do not significantly differ from each other, each type displaying a fairly large spread of values. Similarly, the recovery values do not depend on the total U content in the rock. The bulk of the data is broadly concentrated around 350 ppm U in the rock, yielding uniformly all recovery values between 50 and 100%.

The above relationships result in certain regional variations of U yield throughout the Kvanefjeld area. On the general background of good to moderate contents and recoveries, two distinct areas of low recovery exist:

- 1) the north-western margin of the Kvanefjeld ore field (comprising 5 blocks) with distinctly low U contents and yield percentages. A layer of lujavrite with these properties extends inwards and also northwards of this stripe. These rocks contain only monazite and eudialyte or also intensely altered steenstrupine.
- 2) in the center of the "mine area" an E-W strip extending over 8-10 blocks. Although the U contents are not distinctly lower than in the surrounding blocks, the yield values concentrate around the values of 50-60%. These rocks are strongly hydrated and most of them are MCG lujavrites. They contain altered or zoned steenstrupines of the A or B types.

7.5. General conclusions and proposals

Several general conclusions and proposals for further research can be drawn from our work:

- 1) Due to the new, extended data the emphasis has been shifted from the MCG lujavrites and associated altered rocks as the principal U ore (with B steenstrupine) to the other lujavrite types with the magmatic steenstrupine A. Similarly, the new drill holes show that the alkaline alteration of lavas is of regional importance and it is not bound to the presence of nearby MCG lujavrite bodies.
- 2) Although in many areas a rather homogeneous steenstrupine of reasonably uniform size represents the principal component of the ore, the potential ore dressing will be complicated in the areas (primarily) with zoned steenstrupine which also have large amounts of fine-grained disseminated steenstrupine in the rock. This association suggests special events taking place in the crystallization processes producing steenstrupine and the associated as-

semblage of rock-forming minerals. Some complications in ore dressing will be encountered with the associations containing the B and Ad steenstrupine varieties as well as with those which contain other, special U-bearing minerals.

- 3) The degree of alteration of steenstrupine is not a function of the rock type for the three principal rock types bearing steenstrupine A.
- 4) Intensity of alteration of steenstrupine is not a function of the intensity of the pervading hydration of the studied rocks. Thus, completely altered steenstrupine or vice versa, metamict steenstrupine, occurs equally frequently in all hydration categories.
- 5) The degree of metamictization and alteration of steenstrupine is connected with the concentration of radioactive elements in it. However, there are not common concentration thresholds which would automatically cause certain degrees of alteration. In general, the alteration processes in the B (and C) steenstrupine appear to take place at higher U and Th values than in steenstrupine A.
- 6) Among the factors causing crystallization of steenstrupine a marked role must be played by the very high concentrations of Na in the parent fluids. Although it has been found to survive, in a crystalline form, an almost complete replacement of Na^+ by H^+ , the case should be considered rather exceptional. Experiments by M. Makovicky, Konnerup-Madsen and Rose-Hansen (unpublished) demonstrate that a variety of hydrothermal solutions will decompose steenstrupine and cause formation of monazite. Such processes probably had a decisive role along the NW margin of the intrusion, giving a low-uranium zone with monazite pseudomorphs after (presumably) steenstrupine. Monazite is refractory to leaching, giving very low yields of uranium. The entire zone (blocks 62,64,66,67,68) should be omitted from resource calculation.
- 7) The statistical estimates of the dependence of the averages and ranges of U yield on rock hydration and on steenstrupine alteration can be used to predict the expected yield values from the petrology and mineralogy of the ore.

Because of the limited time, no detailed mineralogical (i.e. electron microscope and diffraction) studies of the fine-grained (microcrystalline) alteration products of steenstrupine was undertaken. However, one must assume that the alteration products were formed at temperatures which were much closer to those of industrial leaching than the formation temperatures of parent steenstrupine. Thus, they will be more stable and more resistant to leaching than the metamict steenstrupine and will give lower yields.

At this state of knowledge it is not possible to explain unambiguously the strong dependence of the uranium recovery on the rock hydration. As a working hypothesis it is assumed that the U-bearing phases in the hydrated rocks, including the metamict steenstrupine, have already partly adjusted to the pervading hydrothermal fluids and they became more stable to the industrial leaching applied. This hypothesis, however, leaves aside the possible reactions of the hydrated, Na-containing rock-forming minerals during the industrial leaching of crushed rocks.

The low-recovery area in the "mine area" is apparently caused by the intense rock hydration in the "mine" region. Its position does not allow it to be excluded from mining operations.

- 8) The following practical problems appear to be relevant to potential future research in which the principal author would eminently like to continue:
 - a) the fine-scale mineralogical study of the fine-grained alteration products of steenstrupine, which represent a very important portion of the ore;
 - b) the study of the processes taking place when the hydrated steenstrupine-containing rocks are being leached, and possible modifications of the method to counteract the unfavourable phenomena;
 - c) more detailed investigations of the fate of the other important components of the ore (Th, P, REE, Zr) during the uranium leaching processes;

- d) possible modifications of the leaching processes, or experimenting with other leaching agents in order to ameliorate the results of b) and of c), respectively as well as those from monazite-rich rocks;
- e) detailed investigation of concurrent or secondary U-Th minerals in the ore which sometimes carry a substantial part of U in the rock;
- f) ore beneficiation studies based on the knowledge compiled in this report.

ACKNOWLEDGEMENTS

The authors express their thanks to the Director of the Geological Survey of Greenland for permission to publish their work and for his support of the research. The principal investigator (Milota Makovicky) was paid by the funds allotted by the Ministry of Energy of the Kingdom of Denmark. The material investigated is derived from several drilling projects (1958-1977) financed in part by the government of Denmark and in part by the European Economic Community. The microprobe used was purchased by the Danish Natural Science Research Council.

We are particularly obliged to lektors J. Bailey, H.J. Hansen, E. Leonardsen, J. Rønsbo (University of Copenhagen) and J. Gunder Knudsen (DTH) and to the personnel of various laboratories, especially to Mrs. E. Dam, Mrs. G.S. Krarup, J. Lautrup, J. Frederiksen, J. Flyng Petersen, Miss S. Riess, G. Ritnagel and S. Sing for the assistance and/or advice in research as well as to S. Watt (GGU), Mrs. I. Bakø and Mrs. T. Kock for the assistance in the preparation of the manuscript.

From among the authors, Emil Makovicky also served as the coordinating editor for this report.

The interest of Prof. H. Sørensen and of the entire "Friends of Ilfmaussa" group are appreciated.

REFERENCES

- ASMUND, G., LUNDGAARD, T. and SØRENSEN, E. (1971). Sulphating roasting, a way to solubilize uranium in refractory minerals. In: The recovery of uranium. Proc. IAEA, Vienna, 185-194.
- BAILEY, J., GWOZDZ, R., ROSE-HANSEN, J. and SØRENSEN, H. (1978). Preliminary geochemical work on the Ilímaussaq alkaline intrusion, South Greenland. Rapp. Grønl. Geol. Unders. 90, 75-79.
- BØGGILD, O.B. (1953). The mineralogy of Greenland. Meddr Grønl. 149(3), 1-444.
- BUCHWALD, V. and SØRENSEN, H. (1961). An autoradiographic examination of rocks and minerals from the Ilímaussaq batholith, Southwest Greenland. Meddr Grønl. 162, 1-35.
- FLEISCHER, R.L., PRICE, P.B. and WALKER, R.M. (1965). Tracks of charged particles in solids. Science 149, 383-393.
- GAMBORG-HANSEN, J.K. (1977). Sulphatising roasting of a Greenlandic uranium ore, reactivity of minerals and recovery. Risø Nat. Lab. Rep. 355, 129 pp.
- LORENZEN, J. (1881). Undersøgelse af nogle mineraler i sodalith-syeniten fra Julianehaabs distrikt. Meddr Grønl. 2, 45-79.
- LØVBORG, L., WOLLENBERG, H., ROSE-HANSEN, J. and NIELSEN, B.L. (1972). Drill-core scanning for radioelements by gamma-ray spectrometry. Geophysics 37, 675-693.
- MAKOVICKY, E. and KARUP-MØLLER, S. (1981). On crystalline steenstrupine from Tunugdliarfik, the Ilímaussaq alkaline intrusion, South Greenland. N. Jahrb. Miner. Abh., in press.
- MASUDA, A., NAKAMURA, N. and TANAKA, T. (1973). Fine structures of mutually normalized rare-earth patterns of chondrites. Geochim. Cosmochim. Acta 37, 239-248.
- MOBERG, J.C. (1898). Zur Kenntniss des Steenstrupins. Z. Krist. 29, 286-398.
- NYEGAARD, P., NIELSEN, B.L., LØVBORG, L. and SØRENSEN, P. (1977). Kvanefjeld uranium project drilling programme 1977. Internal Report Geol. Surv. Greenland. Manuscript, 46 pp + tables and figures.

- SØRENSEN, H. (1962). On the occurrence of steenstrupine in the Ilímaussaq massif, Southwest Greenland. *Meddr Grønl.* 167(1), 1-251.
- SØRENSEN, H., HANSEN, J. and BONDESEN, E. (1969). Preliminary account of the geology of the Kvanefjeld area of the Ilímaussaq intrusion, South Greenland. *Rapp. Grønl. Geol. Unders.* 18, 1-40.
- SØRENSEN, H., ROSE-HANSEN, J., NIELSEN, B.L., LØVBORG, L., SØRENSEN, E. and LUNDGAARD, T. (1974). The uranium deposit at Kvanefjeld, the Ilímaussaq intrusion, South Greenland. *Geology, reserves and beneficiation.* *Rapp. Grønl. Geol. Unders.* 60, 1-54.
- SPRINGER, G. (1967): Die Berechnung von Korrekturen für die quantitative Elektronenstrahl - Mikroanalyse. *Fortschr. Miner.* 45, 103-124.
- SWEATMAN, T.R. and LONG, J.V.P. (1969). Quantitative electron-probe analysis of rock-forming minerals. *J. Petrol.* 10, 332-379.
- STRUNZ, H. (1944). Zur Kristallographie von Steenstrupin. *N. Jahrb. Miner. Mn.* 1944A, 244.
- TAYLOR, S.R. and GORTON, M.P. (1977). Geochemical application of spark source mass spectrography - III. Element sensitivity, precision and accuracy. *Geochim. Cosmochim. Acta* 41, 1375-1380.
- URCH, D.S. and WOOD, P.R. (1978). The determination of the valency of manganese in minerals by X-ray fluorescence spectroscopy. *X-ray Spectrometry* 7, 9-12.
- WOLLENBERG, H. (1971). Fission track radiography of uranium and thorium in radioactive minerals. *Risø Nat. Lab. Rep.* 228, 40 pp.

Table 1. Uranium and thorium contents in rock samples from the drill cores. The analyses represent the contents in 1 metre long core sections. The samples selected for this study may be taken up to 1 metre away from the sections analysed and the results below are thus only indicative for the U, Th contents in the samples.

"Mine area"

B#	Rock type	Depth [m]	U [ppm]	Th [ppm]
1	arfveisonite lujavrite	170,00	410	1 304
	MCG lujavrite	21,45	288	800
2	deformed lava	43,45	287	1 041
3	naufakasite lujavrite	64,05	336	1 305
4	arfveisonite lujavrite	107,00	633	2 739
5	arfveisonite lujavrite	121,30	377	1 482
	arfveisonite lujavrite	128,45	469	1 810
6	deformed lava	44,00	304	1 331
	arfveisonite lujavrite	70,85	641	1 535
7	naufakasite lujavrite	110,00	600	1 800
8	MCG lujavrite	45,40	286	871
9	MCG lujavrite	21,00	384	1 474
	arfveisonite lujavrite	66,65	287	1 070
10	arfveisonite lujavrite	71,75	431	1 329
11	naufakasite lujavrite	134,00	409	1 26
12	arfveisonite lujavrite	134,00	297	755
13	deformed lava	60,10	243	364
14	arfveisonite lujavrite	100,05	616	1 907
16	MCG lujavrite	41,00	319	405
	deformed lava	10,05	226	388
15	arfveisonite lujavrite	11,00	333	1 372
	MCG lujavrite	73,00	468	1 296
17	deformed lava	61,00	328	725
	arfveisonite lujavrite	111,10	615	2 004
18	MCG lujavrite	31,65	279	470
	deformed lava	9,55	370	703
19	naufakasite lujavrite	100,30	250	710
20	MCG lujavrite	20,10	233	810
	arfveisonite lujavrite	63,35	514	1 307
21	MCG lujavrite	59,55	136	300
22	MCG lujavrite	10,20	211	503

Bh	Rock type	Depth (m)	U (ppm)	Th (ppm)
23	MCG lujavrite	37.40	195	519
24	naujakasite lujavrite	74.15	334	603
25	MCG lujavrite	10.05	253	742
	naujakasite lujavrite	78.35	359	484
26	MCG lujavrite	20.00	367	471
27	arfvedsonite lujavrite	29.00	666	1 987
	MCG lujavrite	67.20	284	1 079
28	naujakasite lujavrite	90.70	243	369
29	MCG lujavrite	15.00	253	544
	arfvedsonite lujavrite	29.35	790	2 639
30	MCG lujavrite	47.05	336	937
	arfvedsonite lujavrite	12.50	499	893
31	MCG lujavrite	62.00	241	457
	arfvedsonite lujavrite	90.00	298	749
32	arfvedsonite lujavrite	12.20	440	1 420
33	deformed lava	48.00	208	880
	naujakasite lujavrite	60.25	414	1 365
37	arfvedsonite lujavrite	37.00		
	MCG lujavrite	36.00	515	3 065
39	arfvedsonite lujavrite	140.15	289	739
	naujakasite lujavrite	81.00	348	857
42	deformed lava	30.00	227	675
	naujakasite lujavrite	89.85	432	733
43	arfvedsonite lujavrite	179.50	308	594
	naujakasite lujavrite	105.20	455	677
<u>Extraordinary samples:</u>				
2	arfvedsonite lujavrite	69.15	869	3 389
18	analcime steenstrupine in MCG lujavrite	79.65	1,661	6 242
33	naujaite-naujakasite- lujavrite contact	66.60	1,358	4 530
<u>Northern area</u>				
70	legirine lujavrite	3.85	399	1 920
	naujakasite lujavrite	26.80	332	1 120
	arfvedsonite lujavrite	161.00	341	384
69	arfvedsonite lujavrite	11.05	382	742
	arfvedsonite lujavrite	117.00	189	91
68	arfvedsonite lujavrite	74.00	154	95
67	arfvedsonite lujavrite	83.00	158	94
	arfvedsonite lujavrite	189.70	136	78
66	arfvedsonite lujavrite	87.55	126	185
	arfvedsonite lujavrite	175.40	128	115

Bh	Rock type	Depth (m)	U (ppm)	Th (ppm)
65	arfvedsonite lujavrite	51.10	361	592
	arfvedsonite lujavrite	187.50	180	92
64	comb. arfved. + aegirine lujavrite	29.85	145	161
	arfvedsonite lujavrite	105.65	230	209
63	naujakasite lujavrite	135.30	294	710
62	arfvedsonite lujavrite	67.85	339	165
	arfvedsonite lujavrite	165.90	183	166
61	deformed lava	22.30	333	973
	naujakasite lujavrite	77.00	413	1 320
	arfvedsonite lujavrite	127.85	344	1 490
60	naujakasite lujavrite	109.00	474	1 470
	arfvedsonite lujavrite	147.70	373	1 040
59	arfvedsonite lujavrite	3.20	403	1 140
	arfvedsonite lujavrite	61.85	202	178
	arfvedsonite lujavrite	143.00	148	88
58	arfvedsonite lujavrite	93.10	427	963
57	arfvedsonite lujavrite	109.90	360	577
	arfvedsonite lujavrite	179.30	210	97
56	naujakasite lujavrite	13.00	268	764
	naujakasite lujavrite	157.00	297	504
55	arfvedsonite lujavrite	19.40	103	633
	arfvedsonite lujavrite	155.35	151	82
54	lava	5.75	369	631
	deformed lava	39.85	278	618
	aegirine lujavrite	57.00	232	1 080
50	arfvedsonite lujavrite	31.85	311	711
	arfvedsonite lujavrite	63.00	318	478
49	naujakasite lujavrite	71.30	228	712
	arfvedsonite lujavrite	139.35	284	355
48	naujakasite lujavrite	163.00	450	1 140
46	arfvedsonite lujavrite	59.00	263	666
	naujakasite lujavrite	73.85	153	642
	arfvedsonite lujavrite	157.75	167	259

Table 2

Rock samples with (relatively) homogeneous distribution of fine to medium grained radioactive minerals

No.	concentration	type of rock
27/29.00	medium	arfvedsonite lujavrite
18/79.65	high	NO ₂ lujavrite (analcime steenstrupine vein)
4/107.00	medium to high	arfvedsonite lujavrite
5/128.45	low	naujakasite lujavrite
7/112.20	medium	naujakasite lujavrite
48/163.00	low	naujakasite lujavrite
1/170.00	low	arfvedsonite lujavrite
56/157.00	low to medium	naujakasite lujavrite
39/81.00	low	naujakasite lujavrite
16/52.00	low to medium	arfvedsonite lujavrite
56/13.00	medium	naujakasite lujavrite
59/3.20	medium	arfvedsonite lujavrite
50/31.85	low	arfvedsonite lujavrite
22/120.00	medium	arfvedsonite lujavrite
46/157.75	low	arfvedsonite lujavrite
5/121.30	medium	arfvedsonite lujavrite
60/109.15	medium to high	naujakasite lujavrite
54/39.85	medium	deformed lava
3/68.65	medium	naujakasite lujavrite
49/139.35	low	arfvedsonite lujavrite
14/100.05	medium	arfvedsonite lujavrite
60/147.85	low	arfvedsonite lujavrite
58/93.10	low	arfvedsonite lujavrite
55/19.40	low	arfvedsonite lujavrite
63/135.00	medium	naujakasite lujavrite
3/69.15	medium	naujakasite lujavrite
70/161.00	low	arfvedsonite lujavrite
49/71.30	medium	naujakasite lujavrite
20/63.35	medium	arfvedsonite lujavrite
25/78.35	medium	naujakasite lujavrite

No.	concentration	type of rock
65/51.10	low	arfvedsonite lujavrite
54/5.75	low	"lava"
69/11.05	low	arfvedsonite lujavrite
42/30.00	medium	deformed lava
33/60.35	high	naujakasite lujavrite
17/62.00	medium - low	deformed lava
6/72.85	medium	deformed lava
43/105.20	medium	naujakasite lujavrite
43/179.50	low	arfvedsonite lujavrite
50/63.00	medium	arfvedsonite lujavrite
61/127.00	low to medium	arfvedsonite lujavrite
61/77.00	medium	naujakasite lujavrite
70/3.85	medium	aegirine lujavrite
70/26.80	low to medium	naujakasite lujavrite
32/12.20	low	arfvedsonite lujavrite

Table 3

Rock samples containing veins or layers of medium to fine grained radioactive minerals

No.	concentration	type of rock
18/8.55	medium	deformed lava
61/22.00	medium	deformed lava
13/80.10	medium	deformed lava
30/12.50	low	arfvedsonite lujavrite
6/44.90	low	deformed lava
21/59.55	low	MCG lujavrite
10/71.75	medium	arfvedsonite lujavrite
46/73.85	low	naujakasite lujavrite
15/22.05	low to medium	deformed lava
46/59.00	low	arfvedsonite lujavrite
28/90.70	medium	naujakasite lujavrite
62/67.85	low	arfvedsonite lujavrite
57/179.00	low	arfvedsonite lujavrite
59/61.85	low	arfvedsonite lujavrite
66/87.55	low	arfvedsonite lujavrite
12/134.00	low	arfvedsonite lujavrite

Table 4

Rock samples containing patches or nests of medium to coarse
grained radioactive minerals

No.	concentration	type of rock
9/26.00	medium	MCG lujavrite
9/66.65	low	arfvedsonite lujavrite
54/57.00	medium	aegirin lujavrite
17/111.10	medium to high	arfvedsonite lujavrite
24/74.15	medium	naujakasite lujavrite
23/37.55	low	MCG lujavrite
31/90.60	medium	arfvedsonite lujavrite
42/89.95	medium	naujakasite lujavrite
11/134.90	medium	naujakasite lujavrite
16/73.90	high	MCG lujavrite
33/66.60	high	naujakasite lujavrite-contact

Table 5

Rock samples with large scattered grains of radioactive minerals

No.	concentration	type of rock
33/48.00	very low	deformed lava
26/20.00	medium	MCG lujavrite
18/32.65	medium to high	MCG lujavrite
27/67.20	low	MCG lujavrite
29/15.00	high	MCG lujavrite
1/91.40	low	MCG lujavrite
25/10.05	high	MCG lujavrite
15/42.00	medium	MCG lujavrite
29/29.35	medium	arfvedsonite lujavrite
57/109.00	low	arfvedsonite lujavrite
37/36.00	high	MCG lujavrite
22/10.20	high	MCG lujavrite
30/47.05	medium	MCG lujavrite
8/45.30	medium	MCG lujavrite
37/370.00	low	arfvedsonite lujavrite
2/69.15	high	arfvedsonite lujavrite
20/20.10	medium	MCG lujavrite

Table 6

Rock samples which appear "barren" on autoradiographs

No.	concentration	type of rock
64/29.85		arfvedsonite lujavrite
2/49.80		deformed lava
55/155.25		arfvedsonite lujavrite
59/143.00		arfvedsonite lujavrite
67/83.00		arfvedsonite lujavrite
62/165.85		arfvedsonite lujavrite
31/62.00		MOG lujavrite
64/105.65		arfvedsonite lujavrite
69/117.05		arfvedsonite lujavrite
19/100.30		nanjakasite lujavrite
68/74.00		arfvedsonite lujavrite
65/187.50		arfvedsonite lujavrite

Table 7a

EARLY HYDRATED ROCKS

Sample number	Rock name	Main feldite minerals original	Main mafic hydral. prod. minerals	Main mafic minerals	Type of steensplitine type	Type of steensplitine alteration	Access. min.
61-127.05	Arfvedsonite lujavrite	Nepheline Albite (Microcl.)	Analcime	Arfvedsonite Aegirine	Ae	altered zone	Matrolite
5-128.45	Maujahnite lujavrite	Nepheline Maujahnite Albite	Analcime	Arfvedsonite Aegirine	Ae	altered zone	Matrolite Microcline
5-127.30	Arfvedsonite lujavrite	Nepheline Albite	Analcime (Matrolite)	Arfvedsonite Aegirine- cebite	Ae, s	zone (cebite) altered	Microcline Mica
65-51.10	Arfvedsonite lujavrite	Albite Microcline Nepheline Celsite	Analcime	Arfvedsonite	Ad	extremely altered	Aegirine in Mica Feldspars Vitreous
7-112.20	Maujahnite lujavrite	Maujahnite Nepheline	Analcime	Arfvedsonite cebite	Ae	altered zone	Mica Nephtalite
Sample number	Rock name	Main feldite minerals original	Main mafic hydral. prod. minerals	Main mafic minerals	Type of steensplitine crystal type	Type of steensplitine alteration	Access. min.
37-370	Arfvedsonite lujavrite	Nepheline Albite Microcline	Analcime (Matrolite)	Arfvedsonite			Celsite Aegirine Vitreous
40-161.01	Maujahnite lujavrite	Maujahnite Albite Microcline	Analcime Celsite	Arfvedsonite	Ae, b	cebite partly altered	Lavenderite

Sample number	Rock name	Main felsic minerals original	hydrat. prod.	Main mafic minerals	Type of steenstrupine crystal size & type	Alteration	Access. min.
70-26.85	Naujakasite lujavrite	Naujak. site Nepheline Albite Microcline	(Analcime) (Natrolite)	Arfvedsonite	Ad	extremely altered	
70-3.70	Aegirine lujavrite	Microcline Albite (Nepheline)	Analcime	Aegirine	Ad	extremely altered	Natrolite Neptunite
54-57.00	Aegirine lujavrite	Albite Microcline Nepheline	Analcime	Aegirine	Ad	extremely altered	Vitusite Natrolite Neptunite
54-39.85	Deformed lava	Microcline Albite	(Analcime)	Aegirine	Ad	extremely altered	Mica
19-100.30	Naujakasite lujavrite	Naujakasite Albite	(Analcime) (Ussingite)	Arfvedsonite	Bc	altered	Eudialyte Neptunite
39-14.00	Arfvedsonite lujavrite	Nepheline albite sodalite	Analcime	Arfvedsonite (Aegirine)	Aa, b	metamict few altered	Neptunite Lovoserite Vitusite
9-66.65	Arfvedsonite lujavrite	Nepheline Microcline	Analcime	Arfvedsonite (Aegirine)	Ba Ad	metamict extremely altered	Neptunite Natrolite
33-49.00	Deformed lava	Microcline albite	Natrolite (Analcime)	Arfvedsonite	Ab	altered	Neptunite Aegirine Sodalite
69-11.05	Arfvedsonite lujavrite	Nepheline Albite Eudialyte	Analcime	Arfvedsonite Aegirine- acmite			Natrolite Monazite Neptunite
67-189.70	Arfvedsonite lujavrite	Nepheline Microc. Albite Eudialyte	Analcime	Arfvedsonite (Aegirine)			Sodalite, Vitusite Eriksite, Neptunite

Sample number	Rock name	Main felsic minerals original	Analcime hydrat.prod.	Main mafic minerals	Type of steensandstone crystal size & type	Alteration	Access. min.
21-59.55	MCG lujavrite	Nepheline Microcline	Analcime (natrolite)	Arfvedsonite Aegirine	Bc	altered	Sodalite, Eudialyte Natrolite
22-120.20	Arfvedsonite lujavrite	Nepheline Albite Microcline	Analcime	Arfvedsonite Aegirine	Aa, b, d	metamict partly alter. to extr. alt.	Sodalite, Monasite Natrolite, Erikasite
69-117.05	Arfvedsonite lujavrite	Nepheline Albite	Analcime	Arfvedsonite Aegirine	Ad	highly altered	Monasite
22-120.0	Arfvedsonite lujavrite	Nepheline Albite Sodalite	Analcime	Arfvedsonite	Ac	altered soned	Monasite
1-170.00	Arfvedsonite lujavrite	Nepheline Sodalite Albite	Analcime	Arfvedsonite	Aa, b	metamict altered	Mica
70-161.0	Arfvedsonite lujavrite	Albite Nepheline Microcline	Natrolite	Arfvedsonite			Ussingite Vituite Eudialyte
49-71.30	Naujakasite lujavrite	Naujakasite Nepheline Albite Sodalite	Analcime (Natrolite)		Ac, d	soned extremely altered	Ussingite Li-Mica Monasite
43-65.0	Naujakasite lujavrite	Naujakasite Microcline	Analcime		Ad	extremely altered	
58-93.10	Arfvedsonite lujavrite	Nepheline Naujakasite Albite	A	Arfvedsonite	Aa, b	metamict altered	Ussingite Mica

Table 7b

MEDIUM HYDRATED ROCKS

Sample number	Rock name	Main felsic minerals original	Main felsic minerals hydrat.prod.	Main mafic minerals	Type of steenstrupine crystal size & type	Type of steenstrupine alteration	Access. min.
29-29.35	Arfvedsonite lujavrite	Albite Microcline	Analcime	Arfvedsonite (Aegirine)	Ab, c	altered, zoned + altered	Nefeline Mica, Neptunite
66-175.45	Arfvedsonite lujavrite	Microcline Albite Nepheline	Analcime	Arfvedsonite (Aegirine)	Ad	extremely altered	Eudialyte Monazite
62-165.90	Arfvedsonite lujavrite	Albite Nepheline (Eudialyte)	Analcime (Natrolite)	Arfvedsonite (Aegirine)	none		Neptunite Monazite Vitusite
62-67.85	Arfvedsonite lujavrite	Microcline (Nepheline) Eudialyte	Analcime (Natrolite)	Aegirine	none		Sodalite Arfvedsonite Neptunite
65-187.65	Arfvedsonite lujavrite	Albite Eudialyte Sodalite	Analcime	Arfvedsonite	none		Vitusite
46-73.85	Arfvedsonite lujavrite	Nepheline Albite	Analcime Aegirine	Arfvedsonite Aegirine	Ac	altered zoned	Erikite Natrolite
55-155.35	Arfvedsonite lujavrite	Albite Nepheline Eudialyte	Analcime (Natrolite)	Arfvedsonite	none		Sodalite Aegirine Monazite
11-134.90	Naujakasite lujavrite	Nepheline Naujakasite (Albite)	Analcime	Arfvedsonite Aegirine- acsite	Aa, b	metamict margins altered core	Eudialyte
43-179.50	Arfvedsonite lujavrite	Nepheline Sodalite	Analcime (Natrolite)	Arfvedsonite Aegirine	Ab	altered	Albite, Monazite Neptunite Eudialyte

Sample number	Rock name	Main felsic minerals original	Analcime hydrat.prod.	Main mafic minerals	Type of steenstrupine crystal size & type	Alteration	Access min.
13-80.10	Deformed lava	Microcline Nepheline	Analcime	Arfvedsonite	Ad	extremely altered	Mica, Eudialyte Neptunite Aegirine
12-134.0	Arfvedsonite lujavrite	Nepheline Albite Eudialyte	Analcime	Arfvedsonite Aegirine- acmite	Ab	altered	Sodalite Mica
46-157.75	Arfvedsonite lujavrite	Nepheline Albite	Analcime	Arfvedsonite	Ad	extremely altered	Vitusite Natrolite
39-91.00	Naujakasite lujavrite	Naujakasite Nepheline Albite	Analcime	Aegirine- acmite	none		Neptunite Natrolite Eudialyte
28-90.70	Naujakasite lujavrite	Naujakasite Nepheline Albite	Analcime	Arfvedsonite	Aa, c	zoned metamict + altered parts	Neptunite
16-52.00	Arfvedsonite lujavrite	Albite	Analcime (Natrolite)	(Arfvedsonite) Aegirine- acmite	Aa	metamict	Mica
33-60.25	Naujakasite lujavrite	Naujakasite Microcline Albite	Analcime	Arfvedsonite	Ac	altered zoned	Natrolite
62-47.55	Arfvedsonite lujavrite	Albite Microcline Nepheline	Natrolite	Arfvedsonite	Al	extremely altered	Muscovite
60-147.70	Arfvedsonite lujavrite	Albite Nepheline Microcline	Analcime	Arfvedsonite	Ad	extremely altered	Mica
1-91.45	M.I. lujavrite	Microcline Nepheline Sodalite	Natrolite	Arfvedsonite			Eudialyte Erikite Neptunite

Sample number	Rock name	Main felsic minerals original	Main felsic minerals hydrat. prod.	Main mafic minerals	Type of steenstrupine crystal size & type	Alteration	Access. min.
59-143	Arfvedsonite lujavrite	Albite Microcline	Analcime Natrolite	Arfvedsonite Aegirine	Ad	extremely altered	Monasite
55-19.40	Arfvedsonite lujavrite	Microcline Nepheline	Analcime	Arfvedsonite Aegirite	Ad	extremely altered	Erikite
67-83	Arfvedsonite lujavrite	Microcline Albite Nepheline	Analcime Natrolite	Arfvedsonite Aegirine	Ad	extremely altered	Monasite
16-73.90	M: lujavrite	Nepheline	Analcime Natrolite	Arfvedsonite	Ac	altered (soned)	
61-77.0	Naujakasite lujavrite	Nepheline Albite Naujakasite	Natrolite	Arfvedsonite	Ab,c,d	isotropic altered-soned altered	Mica
2-49.85	Udvalset lava	Microcline sodalite	Analcime Natrolite	Arfvedsonite			Erikite Mica Neptunite
63-135.00	Naujakasite lujavrite	Albite Nepheline	Analcime	Arfvedsonite	Ad	extremely altered	Monasite
27-29.00	Arfvedsonite lujavrite	Albite Microcline	Analcime Natrolite	Arfvedsonite	Aa,c	metamict + altered	Neptunite
46-59.00	Naujakasite lujavrite	Naujakasite Microcline	Analcime	Arfvedsonite	Ac	soned- completely- altered	Erikite
20-63.35	Arfvedsonite lujavrite	Albite Nepheline Microcline	Analcime Natrolite	Arfvedsonite	Ac,d	extremely altered	
60-109.00	Naujakasite lujavrite	Naujakasite Albite Microcline	Analcime Natrolite	Arfvedsonite	Aa,c	metamict altered-soned	Vitunite

Table 7c

VERY INTENSE TO COMPLETE HYDRATION

Sample number	Rock name	Main felsic minerals original	Main felsic minerals hydrat.prod.	Main mafic minerals	Type of steenstrupine crystal size & type	Alteration	Access. min.
31-90.00	Arfvedsonite lujavrite	Albite (Eudialyte)	Analcime Natrolite	Arfvedsonite	Aa, b	metamict + altered	Neptunite Nepheline
15-22.05	Deformed lava	Microcline	Analcime Natrolite	Arfvedsonite Aegirine- acmite	Aa, b	metamict + altered	Micas Nepheline Neptunite
18-79.60	Analcime- steenstrupine vein		Analcime Natrolite	Arfvedsonite	Ba, b	fresh anisot + metamict	Nepheline Microcline Neptunite, Aegirine
15-42.00	MCG lujavrite	Microcline	Natrolite (Analcime)	Arfvedsonite Aegirine- acmite (in felt)	Ba, b	fresh anisotro metamict	Sodalite Nepheline, Neptunite Erikite, Mica
59-3.20	Arfvedsonite lujavrite	Microcline	Analcime Natrolite	Arfvedsonite lujavrite Aegirine	Aa, b	metamict + altered	Eudialyte Vitusite Nepheline
6-72.85	Arfvedsonite lujavrite	Albite (Nepheline) Naujakasite	Analcime Natrolite	Arfvedsonite Aegirine	Ac	altered zoned	Mica Vitusite
3-68.65	Naujakasite lujavrite	Microcline Naujakasite	Analcime Natrolite	Arfvedsonite (Aegirine)	Ab, a	majority alt. + metamict	Mica Erikite
17-111.10	Arfvedsonite lujavrite	(Nepheline)	Analcime Natrolite	Arfvedsonite	Ab	altered	Aegirine
14-100.05	Arfvedsonite lujavrite	Microcline	Analcime Natrolite	Arfvedsonite Aegirine	Ab	altered	Neptunite Vitusite, Nepheline

Sample number	Rock name	Main felsic minerals original	Main felsic minerals hydrat.prod.	Main mafic minerals	Type of steenstrupine crystal size & type	Alteration	Access. min.
32-12.20	Arfvedsonite lujavrite	Albite Microcline	Analcime Natrolite	Aegirine (Arfvedsonite)	Ad	extremely altered	Mica, Neptunite Monazite, Nepheline
4-107.00	Arfvedsonite lujavrite	Microcline	Analcime Natrolite	Arfvedsonite Aegirine	Ac Ba, b	altered zoned metamict + fresh anisot	Mica Eudialyte Nepheline
18-8.55	Deformed lava	Microcline	Analcime Natrolite	Arfvedsonite	Ac	altered zoned	Eudialyte, Vitusite Vertunite, Nepheline
24-74.15	Naujakasite lujavrite	Naujakasite Microcline Albite	Natrolite Analcime	Arfvedsonite	Ad	extremely altered	
42-30.00	Deformed lava	Albite	Analcime Natrolite	Aegirine Arfvedsonite	Ad	extremely altered	Neptunite
64-29.85	Aegirine lujavrite	Microcline	Analcime	Aegirine			Monazite
57-179.80	Arfvedsonite lujavrite	Albite	Analcime	Arfvedsonite Aegirine	Aa, c	metamict + altered zoned	
64-105.65	Arfvedsonite lujavrite	Albite	Analcime Erikite	Arfvedsonite Aegirine			Monazite
6-44.90	Deformed lava	Albite Microcline	Analcime Natrolite	Arfvedsonite	Ac, d	zoned-altered completely altered	Mica Neptunite
2-69.15	Arfvedsonite lujavrite	Albite Nepheline	Analcime	Arfvedsonite	Aa, c	metamict zoned-altered	Mica

Table 7d

STRONGLY HYDRATED ROCKS WITH ABUNDANT MICROCLINE

Sample number	Rock name	Main felsic minerals original	Main felsic minerals hydrat.prod.	Main mafic minerals	Type of steenstrupine crystal size & type	Alteration	Access. min
18-72,65	MCG lujavrite	Microcline	Natrolite (Analcime)	Arfvedsonite	Bb	metasilt	Mica Neptunite
37-36,00	MCG lujavrite	Microcline	Analcime Natrolite	Arfvedsonite	Bb, c	metasilt altered	Neptunite Monazite
30-47,05	MCG lujavrite	Microcline	Analcime (Natrolite)	Arfvedsonite	Ba, b Ab	metasilt + fresh anisot. altered	Neptunite
10-71,75	Arfvedsonite lujavrite	(Microcline)	Analcime	Arfvedsonite	A	some fresh anisot. + altered	Neptunite Monazite
36-20,00	MCG lujavrite	Microcline	Analcime Natrolite	Arfvedsonite	Bb, c	metasilt + altered	Neptunite Monazite
27-67,20	MCG lujavrite	Microcline	Analcime	Arfvedsonite	none		Monazite, Neptunite Natrolite
20-20,10	MCG lujavrite	Microcline	Natrolite (Analcime)	Arfvedsonite	Bb, c	metasilt + altered	Neptunite Monazite, Albite
10-12,5	Arfvedsonite lujavrite	Not possible to recognize	Analcime	Arfvedsonite	Ab, d	altered to extremely altered	Pyrite Neptunite Monazite
29-15,00	MCG lujavrite	Microcline	Analcime	Arfvedsonite	Ab	altered	Mica Neptunite

Sample number	Rock name	Main felsic mineral (optical)	hydrat, prod.	Main mafic mineral	Arfvedsonite Ab	Type of steenstrupine crystal size alteration & type	Accessory, min.
40-43.95	Neufeldite lujavrite	Microcline	Analcime	Arfvedsonite	Ab	altered	Heptunite Erikbite
17-63.00	Deformed lava	Albite (Microcline)	Analcime	Arfvedsonite	Ar	altered somed	Heptunite Microclinalite
64-74.00	Arfvedsonite lujavrite	Albite Microcline	Analcime Natrolite	Arfvedsonite	none		Calcic Microcline
26-10.05	MCG lujavrite	Microcline	Analcime	Arfvedsonite	Ba, b	metamict anisotropic	Natrolite Monasite
31-62.00	MCG lujavrite	Microcline	Analcime Natrolite	Arfvedsonite			Monasite Eudialyte
23-37.40	MCG lujavrite	Microcline Albite	Analcime Natrolite	Arfvedsonite	Ba	extremely altered	Monasite Heptunite Eudialyte
8-45.30	MCG lujavrite	Microcline	Natrolite Analcime	Arfvedsonite	Bb	metamict	conerwinite
9-26.00	MCG lujavrite	Microcline	Natrolite	Arfvedsonite	Bb, c	metamict altered	Heptunite Erikbite
22-10.20	MCG lujavrite Sodalite	Microcline	Natrolite Analcime	Arfvedsonite	Bb	metamict	Heptunite
54-5.75	Lava	Microcline	Analcime	Admite			

Table 7e

HYDRATED ROCKS WITH USSINGITE

Sample number	Rock name	Main felsic minerals original	hydrat. prod.	Main mafic minerals	Type of steenstrupine crystal size & type	Alteration	Access. min.
49-139.35	Arfvedsonite lujavrite	Microcline Nepheline	Ussingite (Analcime)	Arfvedsonite	Ab	altered	Mica Natrolite
25-78.35	Naujakasite lujavrite	Nepheline Microcline Naujakasite	Analcime Ussingite	Arfvedsonite	Ac	altered soned	Neptunite
50-31.95	Arfvedsonite lujavrite	Nepheline Albite Microcline	Analcime Ussingite	Arfvedsonite	Ab, c	altered	Li Mica Natrolite
57-09.95	Arfvedsonite lujavrite	Sodalite Nepheline Albite Microcline	Ussingite	Arfvedsonite	Aa, b	metamict + altered	Vitusite
56-57.0	Naujakasite lujavrite	Nepheline Albite Sodalite	Analcime Ussingite	Arfvedsonite	Aa, b	metamict altered	Vitusite
50-63.0	Arfvedsonite lujavrite	Albite Nepheline Microcline Sodalite	Ussingite Natrolite	Arfvedsonite			Eudialyte Vitusite
33-66.60	Steenstrupine vein in naujaite	Sodalite Eudialyte	Natrolite	Arfvedsonite Aegirine	Aa, c	metamict altered- soned	Mica
18-79.65	Analcime- steenstrupine vein	Analcime Microcline	Natrolite		Ba, b	fresh- anisotropic, metamict	Neptunite

Table ② a-c Correlation between the rock types, degree of hydration and type of steenstrupine in the examined drill core specimens.

Type of steenstrupine:

Type of rock	Aa	Ab	Ac	Ad	Ba,b	Bc	none
Arfvedsonite lujavrite	13	17	13	13	1		11
Naujakasite lujavrite	6	7	9	5		1	1
MCC lujavrite		2	1		10	7	2
Deformed lava	1	2	2	4			2
Aegirine lujavrite				2			1

Degree of hydration	Aa	Ab	Ac	Ad	Ba	Bb	Bc	none
Weakly hydrated	6	9	5	8	1		2	5
Medium hydrated	5	7	7	11				6
Strongly hydrated	6	10	8	5	4	11	5	4
Ussingite	2	3	1					1

Type of rock:

Degree of hydration	Arfvedsonite lujavrite	Naujakasite lujavrite	MCC lujavrite	Deformed lava	Aegirine lujavrite
Weakly	13	7	1	2	2
Medium	18	8	2	3	
Strongly	13	3	14	5	1
Ussingite	4	2			

Table 9 The analytical lines and microprobe standards used for the steenstrupine analyses

Element	Analytical line	Analytical wavelength	Background position	Standard No.	Standard type
Th	Ma	4.138Å	4.05Å	-	Synth.composite
Si	Ka	7.111	7.50	104	Natural quartz
P	Ka	6.142	6.00	205	Natural apatite
La	La	2.660	2.85	-	Synth.composite
Ce	La	2.556	2.70,2.48	Griff.1	- " -
Pr	LB	2.254	2.275	317	- " -
Nd	La	2.365	2.335,2.395	318	- " -
Na	Ka	11.885	12.20	131	Natural albite
Ca	Ka	3.352	3.24	129	Natural CaSiO ₃
Mn	Ka	2.098	2.00	506	Pure metal
Fe	Ka	1.932	2.00	331	Natural Fe ₂ O ₃
Zr	La ₁	6.057	6.06	500	Pure metal
Ti	Ka	2.743	2.71	330	TiO ₂
Al	Ka	8.320	7.80	329	Natural Al ₂ O ₃
Y	La	6.436	6.55	313	Synth. composite
Nb	La	5.712	5.85	504	Pure metal

Table 11 Atomic proportions in steenstrupine 199104 based on (Si+P) = 18

Elt.	Total average comp.		Massive steenstrupine			Total average	Disseminated steenstrupine			
	Average	Range	Zoned port.	Core port.	Rims		Zoned port.	Core port.	Replacem. phase	Total average
No. meas.	36		13	4	1	18	14	1	3	18
Si	13.33(24)	13.93-12.81	13.44(16)	13.31(35)	12.99	13.39(23)	13.28(18)	13.15	13.27(59)	13.27(26)
P	4.67(25)	5.19-4.07	4.56(17)	4.70(35)	5.01	4.61(23)	4.72(18)	4.85	4.73(59)	4.73(26)
Th	0.51(8)	0.71-0.20	0.48(3)	0.56(6)	0.20	0.48(9)	0.51(3)	0.71	0.56(10)	0.53(7)
La	1.94(10)	2.27-1.65	1.94(7)	2.08(14)	2.09	1.98(10)	1.90(9)	2.00	1.86(6)	1.90(8)
Ce	2.82(9)	3.08-2.65	2.87(10)	2.86(5)	2.90	2.88(9)	2.75(5)	2.76	2.79(8)	2.76(6)
Pr	0.40(3)	0.46-0.35	0.40(3)	0.43(3)	0.37	0.40(3)	0.39(2)	0.43	0.38(3)	0.39(2)
Nd	0.69(5)	0.80-0.60	0.72(5)	0.70(8)	0.72	0.71(5)	0.68(3)	0.60	0.66(1)	0.67(3)
Y	0.20(6)	0.36-0.03	0.18(4)	0.27(6)	0.03	0.19(7)	0.20(3)	0.23	0.27(8)	0.22(5)
RE+Y	6.05(19)	6.78-5.74	6.11(15)	6.35(29)	6.11	6.16(16)	5.92(8)	6.05	5.96(3)	5.94(8)
Na	2.35(150)	6.15-0.60	3.44(127)	2.61(122)	6.15	3.40(141)	1.29(46)	0.96	1.44(83)	1.14(49)
Ca	1.03(11)	1.49-0.88	1.05(15)	1.03(13)	1.00	1.04(14)	1.01(14)	1.09	1.00(3)	1.01(7)
Mn	1.79(10)	2.04-1.64	1.78(6)	1.83(12)	2.04	1.80(10)	1.78(9)	1.62	1.80(3)	1.77(9)
Fe	1.70(15)	2.17-1.31	1.71(16)	1.59(24)	1.38	1.69(18)	1.72(8)	1.86	1.71(11)	1.73(9)
Zr	0.38(8)	0.54-0.21	0.42(7)	0.33(7)	0.54	0.41(8)	0.37(6)	0.37	0.29(12)	0.36(8)
Ti	0.09(3)	0.15-0.04	0.11(1)	0.09(4)	0.07	0.10(2)	0.08(4)	0.07	0.09(6)	0.09(3)
Al	0.35	0.45-0.29	0.33(2)	0.31(1)	0.31	0.32(2)	0.38(3)	0.41	0.38(5)	0.38(3)

Table 12 X-ray powder diffraction data for steenstrupine No. 199104 from Tunugdliarfik

d_{obs}	I	hkl _{hexagonal}	d_{calc}	I _{weiss}
15.14 Å	6	003	15.00 Å	m/s
7.56	3	006	7.50	m/s
7.07	3	014	7.05	m/v
6.40	3	015	6.38	m/v
5.89	3 ^x	-	-	-
4.93	1	009	5.00	m
		113	4.94	v
4.42	1	022	4.44	v
4.14	4 ^x	024	4.20	v/v
3.71	2	0.1.11	3.73	v/m
3.27	10	124	3.27	s
3.17	8	0.2.10	3.19	s
3.04	5	1.1.12	3.05	m/v
		(0.2.11	3.04	v/vw)
2.88	5	128	2.924	m
2.74	8	0.2.13	2.749	s
2.60	9	(0.2.14	2.620	w)
		220	2.614	s
		(039	2.584	w)
2.32	1	137	2.339	v
2.11	4	0.3.15	2.127	m
		etc.		
2.01	1 broad	235	2.024	w/m
		0.4.10	2.022	w/m
		0.2.20	2.014	w/m
1.83	4 broad	2.3.11	1.852	m
		1.4.9	1.838	-
		1.3.17	1.822	-
		etc.		
1.73	3	333	1.731	-
		etc.		

Powder diffraction camera Ø 180 mm, CuK α radiation. Peak-to-background ratio is low for all lines. Contributions from the impurities are marked by asterisks.

Table 14 Atomic proportions for the analysed steenstrupine and its alteration products.
Averages for individual aggregate and alteration types in each sample.

Codes: A = Rock types: 1 = MCG lujavrite; 2 = arfvedsonite lujavrite;
 4 = nauyasite lujavrite; 5 = deformed lava; 6 = veins/pegmatites

B = Rock hydration types: 1 = fresh or very weakly hydrated;
 2 = weakly to distinctly hydrated; 3 = strongly hydrated light components

C = Principal genetic categories of steenstrupine: 1 = steenstrupine A;
 2 = steenstrupine B; 3 = steenstrupine in veins, C.

D = Alteration types or genetic subtypes of steenstrupine: 1 = crystalline (anisotropic);
 2 = metamict (isotropic); 3 = slightly altered (primarily still metamict);
 4 = altered (aggregate anisotropy); 5 = strongly altered (brown, black aggregates);
 6 = recrystallized into microscopically heterogeneous mixtures (monazite, U-thorite
 etc.) 7 = amorphous steenstrupine replacing the C-1 type; 8 = red alteration
 (veins, patches) of C-1 and C-2.

Numbers in parentheses represent the estimated standard error in terms of last digit.

Sample no.	No. meas.	Codes				Atomic proportions normalized to Si+P = 18						
		A	B	C	D	Si	P	Th	La	Ce	Pr	Nd
48-163.0	6	4	1	1	2	14.25(27)	3.75(27)	.40(3)	1.84(8)	2.90(6)	.25(4)	.70(4)
	5	4	1	1	4	13.99(38)	4.01(38)	.41(3)	1.85(7)	2.91(11)	.26(2)	.70(17)
	1	4	1	1	5	14.30	3.70	.37	1.70	2.78	.22	.71
29-15.00	8	1	3	2	6	12.01(2.22)	5.99(2.22)	.42(17)	1.74(48)	2.70(71)	.26(7)	.73(19)
39-140.0	10	2	1	1	4	14.08(26)	3.92(26)	.35(4)	1.75(15)	2.65(21)	.23(3)	.64(5)
	6	2	1	1	2	14.05(17)	3.95(17)	.33(4)	1.65(10)	2.50(13)	.24(2)	.68(6)
54-39.85	6	5	1	1	6	12.64	5.36	.22	1.54	2.76	.26	.88
	1	5	1	1	6'	14.69(42)	3.32(42)	.17(12)	.72(18)	1.35(43)	.12(4)	.67(25)
61-127.85	3	2	1	1	1	13.16(1.22)	4.84(1.22)	.29(7)	1.87(29)	3.69(73)	.21(4)	1.06(19)
	1	2	1	1	4	11.92	6.08	.45	2.45	3.24	.17	.80
	9	2	1	1	5	13.21(70)	4.79(70)	.34(6)	1.82(43)	2.99(46)	.18(6)	.72(9)
65-51.10	2	2	1	1	2	13.36(13)	4.65(13)	.21(1)	1.85(17)	2.91(22)	.19(5)	.73(7)
	6	2	1	1	4	13.27(83)	4.73(83)	.33(3)	1.91(9)	2.45(28)	.18(2)	.72(6)

Na	Ca	Mn	Fe	Zr	Ti	Al	Y	RE+Y
11.69(28)	1.06(14)	1.29(10)	2.16(10)	.13(3)	.08(4)	.36(3)	.37(3)	6.07(16)
11.78(25)	1.15(5)	1.48(9)	2.06(33)	.13(7)	.03(3)	.36(1)	.37(11)	6.08(27)
10.37	1.21	1.43	2.19	.11	.09	.34	.34	5.75
3.94(1.13)	1.30(34)	1.44(40)	1.82(1.12)	.26(24)	.10(8)	1.40(93)	.39(17)	5.81(83)
9.13(93)	.99(15)	1.52(25)	2.44(35)	.15(5)	.05(3)	.31(5)	.32(4)	5.60(41)
8.10(47)	.89(14)	1.09(21)	2.16(7)	.18(5)	.05(4)	.29(11)	.32(4)	5.39(30)
1.80	2.97	2.03	1.73	.10	.07	.38	.10	5.55
4.35(60)	4.58(1.25)	1.57(40)	3.14(60)	.08(3)	.09(3)	.80(71)	.38(39)	3.22(1.06)
3.06(22)	.87(15)	2.43(46)	.81(28)	.25(4)	.14(2)	.31(7)	.45(10)	7.22(1.26)
4.53	1.22	2.22	.38	.24	.14	.06	.52	7.18
3.72(67)	.69(36)	.58(36)	1.00(1.07)	.33(16)	.14(2)	.77(1.10)	.41(8)	6.12(75)
9.29(6)	.83(7)	1.62(17)	1.98(53)	.22(6)	.000	.08(11)	.31(3)	5.98(3)
10.44(1.52)	.87(28)	1.39(52)	1.48(60)	.22(4)	.000	.13(18)	.41(4)	6.10(30)

Sample no.	No. meas.	Codes A B C D	Atomic proportions normalized to Si+P = 10						
			Si	P	Ta	La	Ce	Pr	Ba
199115	4	6 - 3 2	14.23(10)	3.77(10)	.56(3)	1.65(12)	2.55(13)	.22(3)	.73(3)
	3	6 - 3 0	15.73(41) [14.73(1.74)]	2.20(41) 3.27(1.75)	.00(3)	2.20(11)	3.79(11)	.37(3)	1.16(11)
	3	6 - 3 0'	14.60(24)	3.32(24)	.61(7)	1.51(9)	2.40(14)	.21(1)	.76(1)
199146	5	6 - 3 2	13.99(35)	4.01(35)	.49(19)	1.50(14)	2.51(16)	.25(5)	.02(0)
	2	6 - 3 3	14.69(12)	3.31(12)	.51(3)	1.62(7)	2.47(2)	.24(1)	.07(3)
	2	6 - 3 0	14.31(14)	3.69(14)	.67(13)	1.50(13)	2.45(16)	.03(5)	.03(7)
230653	4	6 - 3 2	13.92(36)	4.00(36)	.60(9)	1.67(7)	2.54(13)	.21(2)	.72(2)
	4	6 - 3 7	12.02(11)	5.10(11)	.04(1)	1.04(13)	2.70(9)	.29(3)	.05(0)
230749	4	6 - 3 1	14.21(40)	3.79(40)	.22(12)	2.40(15)	3.92(14)	.35(7)	1.23(6)
	3	6 - 3 5	16.23(29)	1.77(29)	.05(6)	2.00(9)	3.92(13)	.30(4)	1.24(14)

Sample no.	NO. MEAS.	Codes A B C D	Atomic proportions normalized to Si+P = 10						
			Si	P	Ta	La	Ce	Pr	Ba
6-72.09	6	2 3 1 2	13.34(31)	4.66(31)	.16(5)	1.51(14)	3.11(16)	.13(2)	1.11(11)
	4	2 3 1 3	13.24(30)	4.76(30)	.20(7)	1.40(30)	2.87(16)	.13(3)	1.01(13)
	3	2 3 1 4	14.00(2.17)	4.00(2.17)	.36(4)	1.52(14)	3.75(15)	.13(2)	1.11(11)
	2	2 3 1 5	15.76(58)	1.03(58)	.41(5)	1.49(11)	2.93(14)	.17(3)	1.11(11)
9-66.65	6	2 1 2 2	14.28(43)	3.72(43)	.44(8)	1.73(12)	3.72(18)	.16(2)	1.11(11)
11-134.3	1	4 2 1 2	13.35	4.67	.29	1.54	3.66	.13	1.01
	3	4 2 1 3	13.97(28)	4.03(28)	.30(23)	1.44(10)	2.59(13)	.13(2)	1.01(11)
	1	4 2 1 3'	9.15	8.85	.40	1.50	2.97	.13	1.01
	1	4 2 1 4	13.49	4.51	.25	1.39	3.83	.14	1.01
	2	4 2 1 5	12.55(6)	5.45(6)	.44(1)	1.69(10)	3.83(11)	.17(4)	1.01(11)
	1	4 2 1 5'	13.73	4.27	.19	1.26	3.89	.19	1.01
18-79.65	12	6 - 3 2	14.07(31)	3.93(31)	.43(7)	1.70(13)	3.48(12)	.13(3)	1.11(11)
	1	6 - 3 3	14.85	3.15	.62	1.44	3.38	.18	1.11

Sm	Tm	Nb	Fe	Co	Ti	Al	Y	RE+Y
7.11(4)	1.23(4)	1.27(7)	1.07(10)	1.38(17)	1.15(3)	1.33	1.34(3)	1.45(17)
1.06(4)	2.15(12)	1.62(37)	1.49(12)	1.67(10)	1.10(3)	1.68(17)	1.48(14)	6.77(14)
							1.4(1)	
1.31(12)	1.34(12)	1.64(6)	1.07(8)	1.43(6)	1.12(4)	1.11(7)	1.24(4)	6.14(11)
3.16(7)	1.37(12)	1.94(10)	1.24(12)	1.25(8)	1.11(4)	1.33	1.36(6)	1.43(11)
1.74(16)	1.23(11)	1.15(17)	1.12(13)	1.18(14)	1.33(1)	1.33	1.33(1)	1.13(3)
1.31(6)	1.13(14)	1.11(13)	1.05(13)	1.16(17)	1.13(1)	1.13(1)	1.13(1)	1.11(12)
1.05(17)	1.13(11)	1.11(13)	1.09(11)	1.11(14)	1.15(3)	1.14(4)	1.15(4)	1.11(14)
1.11(13)	1.05(11)	1.06(14)	1.13(1)	1.13(14)	1.13(1)	1.13	1.13(1)	1.14(1)
1.07(15)	1.13(16)	1.11(17)	1.17(14)	1.11(19)	1.16(3)	1.19(1)	1.21(1)	6.16(13)
1.11	1.09(11)	1.07(14)	1.13(17)	1.11(14)	1.17(1)	1.13(1)	1.13(1)	7.14(18)

La	Ce	Pr	Co	Ti	Al	Y	RE+Y
1.00(1)	1.15(1)	1.13(1)	1.13(1)	1.14(1)	1.14(1)	1.11(1)	6.31(1)
1.07(1)	1.14(1)	1.10(1)	1.11(1)	1.14(1)	1.10(1)	1.11(1)	6.78(1)
1.10(1)	1.16(1)	1.10(1)	1.13(1)	1.16(1)	1.11(1)	1.11(1)	6.49(1)
1.14(1)	1.16(1)	1.09(1)	1.11(1)	1.10(1)	1.11(1)	1.11(1)	6.43(1)
1.10(1)	1.17(1)	1.11(1)	1.11(1)	1.16(1)	1.11(1)	1.11(1)	6.47(1)
1.16	1.17	1.11	1.13	1.13	1.11	1.11	6.18
1.13(1)	1.17(1)	1.11(1)	1.11(1)	1.11(1)	1.11(1)	1.11(1)	6.40(1)
1.13	1.17	1.11	1.13	1.13	1.11	1.11	6.19
1.17	1.16	1.11	1.16	1.11	1.11	1.11	6.17
1.13(1)	1.17(1)	1.11(1)	1.11(1)	1.11(1)	1.11(1)	1.11(1)	1.13(1)
1.17	1.16	1.11	1.13	1.11	1.11	1.11	5.52
1.14(1)	1.16(1)	1.11(1)	1.11(1)	1.11(1)	1.11(1)	1.11(1)	5.46(1)
1.14	1.17	1.11	1.13	1.11	1.11	1.11	4.99

Table 15 Statistical estimates for various partial groups formed from the analysed steenstrupines and their alteration products using the codes from Table 14. The coarse crystallized, mineralogically heterogeneous alteration products were omitted from the averages.

a) All measurements on steenstrupine and its fine-grained alteration products. 162 analyses.

(minus D=6)

Element	Mean	Standard Dev.	Max.	Min.
Si	13,76	0,88	16,55	9,15
P	4,24	0,88	8,85	1,45
Th	0,43	0,17	0,90	0,02
La	1,78	0,25	2,85	1,15
Ce	2,84	0,41	4,20	2,05
Pr	0,27	0,09	0,46	0,0
Nd	0,78	0,16	1,37	0,41
Na	6,13	3,72	12,92	0,0
Ca	1,09	0,39	3,28	0,24
Mn	1,52	0,43	2,92	0,12
Fe	1,76	0,58	3,44	0,18
Zr	0,29	0,14	0,77	0,05
Ti	0,09	0,07	0,34	0,0
Al	0,29	0,46	3,77	0,0
Y	0,31	0,10	0,57	0,03
RE+Y	5,98	0,72	8,61	4,60

b) Genetic types of steenstrupine. Steenstrupine A and its finegrained alteration products. 63 analyses

C=1

Element	Mean	Standard Dev.	Max.	Min.
Si	13,63	0,98	16,21	9,15
P	4,37	0,98	8,85	1,79
Th	0,33	0,09	0,53	0,11
La	1,71	0,26	2,85	1,15
Ce	2,89	0,38	4,19	2,05
Pr	0,21	0,04	0,30	0,12
Nd	0,76	0,15	1,15	0,41
Na	7,96	2,71	12,92	2,73
Ca	0,95	0,25	1,48	0,24
Mn	1,34	0,52	2,92	0,12
Fe	1,72	0,74	3,44	0,18
Zr	0,19	0,09	0,64	0,05
Ti	0,08	0,06	0,18	0,0
Al	0,38	0,64	3,77	0,0
Y	0,37	0,07	0,55	0,19
RE+Y	5,95	0,61	7,97	4,60

Steenstrupine B and its fine-grained alteration products.
9 analyses.

C=2				
Element	Mean	Standard Dev.	Max.	Min.
Si	14,28	0,43	15,00	13,73
P	3,72	0,43	4,27	3,00
Th	0,44	0,06	0,54	0,35
La	1,73	0,12	1,91	1,61
Ce	2,72	0,08	2,82	2,60
Pr	0,26	0,02	0,29	0,23
Nd	0,69	0,06	0,75	0,60
Na	9,65	0,78	10,54	8,61
Ca	1,01	0,13	1,19	0,84
Mn	1,37	0,12	1,57	1,26
Fe	2,21	0,10	2,34	2,05
Zr	0,27	0,11	0,41	0,16
Ti	0,06	0,04	0,12	0,0
Al	0,32	0,04	0,37	0,26
Y	0,27	0,07	0,36	0,17
RE+Y	5,67	0,18	5,87	5,36

Steenstrupine C and its alteration products. 15 analyses.

C=3				
Element	Mean	Standard Dev.	Max.	Min.
Si	13,84	0,79	16,55	12,67
P	4,16	0,79	5,33	1,45
Th	0,51	0,18	0,90	0,02
La	1,85	0,24	2,52	1,38
Ce	2,81	0,44	4,20	2,23
Pr	0,32	0,10	0,46	0,0
Nd	0,79	0,18	1,37	0,60
Na	4,26	3,64	10,74	0,0
Ce	1,22	0,46	3,28	0,75
Mn	1,69	0,27	2,31	0,84
Fe	1,76	0,39	3,02	0,80
Zr	0,37	0,12	0,77	0,09
Ti	0,11	0,06	0,34	0,02
Al	0,21	0,20	1,21	0,0
Y	0,26	0,09	0,57	0,03
RE+Y	6,03	0,83	8,61	4,91

c) Rock hydration types. Steenstrupine and its fine-grained alteration products from fresh to weakly hydrated rocks. 62 analyses.

B=1				
Element	Mean	Standard Dev.	Max.	Min.
Si	13,77	0,71	15,00	11,81
P	4,23	0,71	6,19	3,00
Th	0,36	0,07	0,54	0,20
La	1,81	0,23	2,85	1,40
Ce	2,85	0,37	4,19	2,25
Pr	0,22	0,05	0,30	0,12
Nd	0,71	0,11	1,12	0,41
Na	8,51	2,97	12,92	2,73
Ca	0,94	0,24	1,28	0,24
Mn	1,31	0,48	2,92	0,12
Fe	1,83	0,77	3,44	0,18
Zr	0,21	0,11	0,64	0,05
Ti	0,07	0,05	0,17	0,0
Al	0,50	0,69	3,77	0,0
Y	0,36	0,08	0,55	0,17
RE+Y	5,95	0,63	7,97	4,80

Steenstrupine and its fine-grained alteration products from medium hydrated rocks. 9 analyses.

B=2				
Element	Mean	Standard Dev.	Max.	Min.
Si	12,97	1,54	14,22	9,15
P	5,03	1,54	8,85	3,78
Th	0,35	0,15	0,53	0,11
La	1,49	0,17	1,77	1,26
Ce	2,87	0,39	3,66	2,27
Pr	0,19	0,02	0,23	0,15
Nd	0,87	0,14	1,15	0,69
Na	7,27	1,38	8,94	4,64
Ca	1,01	0,34	1,48	0,69
Mn	1,48	0,71	2,40	0,66
Fe	1,38	0,62	2,34	0,46
Zr	0,13	0,04	0,16	0,05
Ti	0,00	0,01	0,01	0,0
Al	0,16	0,18	0,46	0,0
Y	0,38	0,06	0,48	0,31
RE+Y	5,80	0,52	6,81	4,99

Steenstrupine and its fine-grained alteration products from strongly hydrated rocks. 15 analyses.

B=3				
Element	Mean	Standard Dev.	Max.	Min.
Si	13.77	1.22	16.21	11.07
P	4.23	1.22	6.13	1.79
Th	0.27	0.11	0.45	0.12
La	1.50	0.15	1.87	1.15
Ce	2.97	0.34	3.44	2.05
Pr	0.21	0.04	0.27	0.15
Nd	0.87	0.17	1.08	0.65
Na	7.05	1.33	9.38	3.81
Ca	0.97	0.19	1.30	0.65
Mn	1.36	0.40	1.93	0.55
Fe	1.70	0.58	3.33	1.21
Zr	0.18	0.05	0.24	0.07
Ti	0.15	0.02	0.18	0.11
Al	0.06	0.03	0.12	0.0
Y	0.36	0.09	0.50	0.22
RE+Y	5.91	0.51	6.51	4.60

d) Petrological rock types. Steenstrupine in arfvedsonite lujavrites. 58 analyses.

A=2				
Element	Mean	Standard Dev.	Max.	Min.
Si	13.69	0.89	16.21	11.81
P	4.31	0.89	6.19	1.79
Th	0.33	0.09	0.54	0.12
La	1.72	0.27	2.85	1.15
Ce	2.87	0.40	4.19	2.05
Pr	0.21	0.04	0.30	0.12
Nd	0.75	0.14	1.12	0.56
Na	7.49	2.49	12.92	2.73
Ca	0.91	0.23	1.30	0.24
Mn	1.31	0.51	2.91	0.12
Fe	1.74	0.78	3.44	0.18
Zr	0.22	0.10	0.64	0.07
Ti	0.09	0.06	0.18	0.0
Al	0.42	0.70	3.77	0.0
Y	0.36	0.08	0.55	0.17
RE+Y	5.92	0.65	7.97	4.60

Steenstrupine in nauyasite leucrites. 27 analyses.

A=4				
Element	Mean	Standard Dev.	Max.	Min.
Si	13.64	1.17	14.56	9.15
P	4.36	1.17	8.05	3.44
Th	0.38	0.10	0.53	0.11
La	1.68	0.23	1.93	1.26
Ce	2.88	0.25	3.66	2.27
Pr	0.23	0.01	0.30	0.15
Nd	0.77	0.15	1.15	0.41
Sm	9.75	2.40	12.19	4.64
Eu	1.07	0.24	1.48	0.69
Gd	1.42	0.46	2.40	0.66
Fe	1.80	0.57	2.40	0.46
Zr	0.13	0.04	0.24	0.05
Ti	0.04	0.04	0.17	0.0
Al	0.27	0.15	0.46	0.0
Y	0.37	0.06	0.48	0.19
RE+Y	5.94	0.39	6.81	4.99

Steenstrupine in veins and pegmatites. 83 analyses.

A = 6				
Element	Mean	Standard Dev.	Max.	Min.
Si	13.84	0.79	16.55	12.67
P	4.16	0.79	5.33	1.45
Th	0.51	0.18	0.90	0.02
La	1.85	0.24	2.52	1.38
Ce	2.81	0.44	4.20	2.23
Pr	0.32	0.10	0.46	0.0
Nd	0.79	0.18	1.37	0.60
Sm	4.26	3.64	10.74	0.0
Eu	1.22	0.46	3.28	0.75
Gd	1.69	0.27	2.31	0.84
Fe	1.76	0.39	3.02	0.80
Zr	0.37	0.12	0.77	0.09
Ti	0.11	0.06	0.34	0.02
Al	0.21	0.20	1.21	0.0
Y	0.26	0.09	0.57	0.03
RE+Y	6.03	0.83	8.61	4.91

e) Alteration and replacement groups. Crystalline steenstrupine.
40 analyses.

D = 1				
Element	Mean	Standard Dev.	Max.	Min.
Si	13,41	0,46	14,68	11,81
P	4,59	0,46	6,19	3,32
Th	0,46	0,13	0,71	0,11
La	1,98	0,19	2,52	1,55
Ce	3,00	0,43	4,19	2,65
Pr	0,38	0,06	0,46	0,16
Nd	0,77	0,18	0,31	0,60
Na	2,32	1,48	6,14	0,64
Ca	1,19	0,56	3,28	0,72
Mn	1,86	0,24	2,92	1,62
Fe	1,62	0,28	2,17	0,57
Zr	0,41	0,12	0,77	0,21
Ti	0,09	0,03	0,16	0,03
Al	0,32	0,09	0,45	0,01
Y	0,22	0,09	0,55	0,03
RE+Y	6,35	0,77	8,61	5,74

Metamict steenstrupine. 53 analyses

D = 2				
Element	Mean	Standard Dev.	Max.	Min.
Si	13,96	0,44	15,00	12,94
P	4,04	0,44	4,06	3,00
Th	0,42	0,16	0,75	0,03
La	1,68	0,14	2,04	1,38
Ce	2,69	0,29	3,66	2,27
Pr	0,24	0,04	0,31	0,15
Nd	0,77	0,12	1,08	0,60
Na	8,46	2,47	11,98	1,49
Ca	1,04	0,16	1,31	0,65
Mn	1,47	0,26	2,31	0,69
Fe	1,88	0,34	2,35	0,80
Zr	0,25	0,09	0,51	0,09
Ti	0,09	0,06	0,22	0,0
Al	0,13	0,15	0,51	0,0
Y	0,33	0,06	0,44	0,09
RE+Y	5,70	0,39	6,81	5,04

Slightly altered steenstrupine. 11 analyses.

D = 3				
Element	Mean	Standard Dev.	Max.	Min.
Si	13,48	1,58	14,85	9,15
P	4,52	1,58	8,85	3,15
Th	0,39	0,15	0,60	0,11
La	1,49	0,19	1,87	1,15
Ce	2,68	0,30	3,22	2,27
Pr	0,20	0,03	0,25	0,15
Nd	0,85	0,12	1,03	0,69
Na	7,78	1,18	9,87	6,36
Ca	1,06	0,29	1,48	0,69
Mn	1,69	0,53	2,40	0,65
Fe	1,46	0,55	2,34	0,46
Zr	0,19	0,09	0,39	0,05
Ti	0,13	0,12	0,34	0,0
Al	0,09	0,13	0,46	0,0
Y	0,37	0,09	0,50	0,25
RE+Y	5,59	0,39	6,11	4,98

Altered steenstrupine. 26 analyses.

D = 4				
Element	Mean	Standard Dev.	Max.	Min.
Si	13,76	0,90	16,21	11,87
P	4,24	0,90	6,13	1,79
Th	0,36	0,05	0,45	0,25
La	1,79	0,22	2,45	1,39
Ce	2,79	0,31	3,44	2,05
Pr	0,22	0,04	0,30	0,16
Nd	0,71	0,13	1,15	0,41
Na	9,59	1,89	12,92	4,53
Ca	1,02	0,21	1,30	0,46
Mn	1,48	0,31	2,36	0,97
Fe	1,93	0,67	2,85	0,38
Zr	0,16	0,06	0,27	0,05
Ti	0,05	0,05	0,17	0,0
Al	0,24	0,15	0,49	0,02
Y	0,36	0,08	0,52	0,19
RE+Y	5,87	0,54	7,18	4,60

Extremely altered steenstrupine. 18 analyses.

D = 5				
Element	Mean	Standard Dev.	Max.	Min.
Si	14,01	1,44	16,55	12,51
P	3,99	1,44	5,49	1,45
Th	0,44	0,21	0,90	0,19
La	1,76	0,35	2,85	1,26
Ce	3,11	0,51	4,20	2,35
Pr	0,21	0,09	0,42	0,12
Nd	0,81	0,22	1,37	0,56
Na	4,49	2,98	10,37	0,0
Ca	0,98	0,52	2,04	0,24
Mn	0,75	0,34	1,43	0,12
Fe	1,55	1,11	3,44	0,18
Zr	0,28	0,17	0,64	0,07
Ti	0,13	0,07	0,26	0,0
Al	0,91	1,11	3,77	0,0
Y	0,35	0,09	0,52	0,20
RE+Y	6,25	0,91	8,11	5,05

Heterogeneous alteration products of steenstrupine A and B.
15 analyses.

D = 6				
Element	Mean	Standard Dev.	Max.	Min.
Si	13,12	2,07	15,30	8,96
P	4,88	2,07	9,04	2,70
Th	0,31	0,19	0,74	0,07
La	1,32	0,62	2,10	0,34
Ce	2,16	0,88	3,93	0,87
Pr	0,19	0,10	0,32	0,02
Nd	0,71	0,21	1,05	0,37
Na	3,96	1,08	5,24	1,80
Ca	2,72	1,81	6,18	0,63
Mn	1,53	0,40	2,23	0,70
Fe	2,34	1,10	4,11	0,76
Zr	0,18	0,19	0,65	0,0
Ti	0,10	0,06	0,25	0,01
Al	1,09	0,86	2,81	0,26
Y	0,36	0,27	1,02	0,04
RE+Y	4,76	1,56	7,22	1,96

Anisotropic steenstrupine replacing steenstrupine C-1. 6 analyses.

D = 7				
Element	Mean	Standard Dev.	Max.	Min.
Si	13,03	0,46	13,93	12,67
P	4,97	0,46	5,33	4,07
Th	0,30	0,30	0,68	0,02
La	1,87	0,07	1,97	1,78
Ce	2,77	0,08	2,86	2,67
Pr	0,33	0,06	0,41	0,24
Nd	0,73	0,08	0,83	0,65
Na	4,80	3,81	9,28	0,60
Ca	0,93	0,12	1,12	0,75
Mn	1,72	0,14	1,82	1,45
Fe	1,72	0,07	1,82	1,60
Zr	0,41	0,16	0,58	0,21
Ti	0,06	0,05	0,15	0,03
Al	0,19	0,21	0,43	0,0
Y	0,22	0,08	0,36	0,12
RE+Y	5,94	0,03	5,99	5,90

The red replacement product of steenstrupine C. 8 analyses.

D = 8				
Element	Mean	Standard Dev.	Max.	Min.
Si	14,61	0,96	16,01	12,75
P	3,39	0,96	5,25	1,99
Th	0,70	0,11	0,84	0,54
La	0,80	0,41	0,39	1,41
Ce	2,93	0,72	3,89	2,23
Pr	0,22	0,14	0,40	0,0
Nd	0,93	0,21	1,29	0,75
Na	0,86	0,73	1,93	0,02
Ca	1,52	0,51	2,29	1,05
Mn	1,69	0,29	2,09	1,24
Fe	2,00	0,86	2,98	0,83
Zr	0,38	0,15	0,59	0,11
Ti	0,18	0,06	0,27	0,09
Al	0,30	0,41	1,21	0,02
f	0,35	0,14	0,57	0,21
RE+Y	6,23	1,54	8,20	4,91

Table 16 Correlation matrix for the atomic proportions in steenstrupine (all compositional data)

Elem.	Si	P	Th	La	Ce	Pr	Nd	Na	Ca	Mn	Fe	Zr	Ti	Al	Y	REE	Square multip. correl.
Si	1.00																.69
P	-.10	1.00															.10
Th	.31	-.31	1.00														.76
La	-.26	.26	-.08	1.00													.69
Ce	-.54	.54	-.39	.24	1.00												.87
Pr	-.30	.30	-.20	.59	.23	1.00											.74
Nd	-.18	.18	-.36	.49	.27	.23	1.00										.74
Na	.22	-.22	.41	-.17	-.01	-.53	-.08	1.00									.63
Ca	.28	-.28	.82	-.06	-.22	-.03	-.02	-.08	1.00								.57
Mn	-.29	.29	.17	.09	.13	.33	.30	.42	.10	1.00							.83
Fe	.45	-.45	-.07	.10	-.16	.02	.45	.22	-.04	-.49	1.00						.81
Zr	-.12	.12	.22	.31	-.05	.52	-.07	-.48	-.12	.28	-.09	1.00					.87
Ti	.27	-.27	.34	-.24	-.17	-.02	.21	-.20	.20	.21	.32	.12	1.00				.48
Al	-.02	.02	.09	.48	.22	.57	-.38	-.04	-.05	.04	.10	.05	.27	1.00			.60
Y	.01	-.01	.15	.40	.10	.17	.41	.47	.04	-.13	.19	.66	.17	.32	1.00		.88
REE	-.57	.57	-.09	.53	.89	.41	.24	-.10	-.17	.24	-.19	.08	-.19	.31	.07	1.00	1.00

Table 17 Factor loadings for principal components (all compositional data)

Elmt.	Commu- nality	Unrotated					Rotated				
		Factor 1	Factor 2	Factor 3	Factor 4	Factor 5	Factor 1	Factor 2	Factor 3	Factor 4	Factor 5
Si	.95	-.79	-.39	-.02	.20	.37	-.12	-.31	.90	-.02	.17
P	.95	.79	.39	.02	-.20	-.37	.12	.31	-.90	-.02	-.17
Th	.79	-.14	-.65	.43	.32	-.26	.36	-.35	.15	-.09	.72
La	.77	.60	-.40	-.34	.34	-.13	.38	.42	-.16	-.61	.21
Ce	.84	.67	.45	-.15	.26	.32	-.07	.86	-.28	.07	-.11
Pr	.82	.70	-.54	-.07	-.03	.16	.77	.39	-.08	-.26	.04
Nd	.84	.07	.64	.50	-.11	.41	-.21	.28	-.12	.83	-.12
Na	.67	-.44	.51	-.36	.28	.02	-.78	.07	.19	-.09	-.10
Ca	.57	-.24	-.24	.38	.54	-.13	-.05	-.12	.19	.04	.72
Mn	.60	.47	-.08	.60	-.02	.10	.46	.20	-.28	.44	.27
Fe	.76	-.34	-.31	-.70	.10	.21	-.11	.00	.60	-.57	-.24
Zr	.59	.41	-.53	.24	-.29	.08	.76	-.02	-.08	.04	.01
Ti	.64	-.19	-.18	.66	-.05	.36	.27	-.14	.30	.63	.25
Al	.65	.38	-.44	-.47	.19	.23	.38	.43	.22	-.52	-.06
Y	.75	-.34	.71	.02	.34	-.13	-.83	.07	-.10	.19	.13
(REE+Y)	.97	.81	.31	-.13	.37	.26	.06	.92	-.33	-.04	.04

Table 18 Correlation matrix for the atomic proportions in metamict steenstrupine A

Elements	Si	P	Th	La	Ce	Pr	Nd	Na	Ca	Mn	Fe	Zr	Ti	Al	Y	REE
Si	1.00															
P	-.100	1.00														
Th	.86	-.86	1.00													
La	.47	-.47	.63	1.00												
Ce	-.53	.53	-.38	-.25	1.00											
Pr	.18	-.18	.23	-.23	-.26	1.00										
Nd	-.79	.79	-.77	-.59	.75	-.02	1.00									
Na	.63	-.63	.79	.81	-.15	.21	-.60	1.00								
Ca	.16	-.16	.44	.39	.22	.43	.00	.44	1.00							
Mn	-.52	.52	-.55	-.09	.58	-.18	-.56	-.31	-.12	1.00						
Fe	.68	-.68	.71	.69	-.67	.41	-.78	.63	.28	-.59	1.00					
Zr	-.29	.29	-.45	-.36	.06	-.43	.24	-.42	-.22	.23	-.27	1.00				
Ti	-.07	.07	-.32	-.35	.28	-.13	.51	-.29	-.03	.39	-.42	-.19	1.00			
Al	.81	-.81	.82	.46	-.18	.26	-.71	.67	.28	-.59	.66	-.44	-.25	1.00		
Y	-.31	.31	-.19	-.29	.68	.14	.63	-.13	.18	.38	-.41	-.09	.33	-.38	1.00	
REE	-.51	.51	-.33	-.05	.95	-.02	.75	-.04	.35	.61	-.52	-.04	.31	-.45	-.73	1.00

Table 19 Factor loadings for principal components - metamict steenstrupine A

Element	Communality	Unrotated				Rotated			
		Factor 1	Factor 2	Factor 3	Factor 4	Factor 1	Factor 2	Factor 3	Factor 4
Si	.96	.88	.03	.15	-.40	.93	-.28	.11	-.06
P	.96	-.88	-.08	-.15	.40	-.93	.28	-.11	.06
Th	.91	.89	.32	-.15	-.13	.87	-.09	.29	-.01
La	.79	.63	.40	-.48	.10	.58	.17	.17	-.63
Ce	.89	-.71	.58	-.18	-.14	-.33	.87	-.10	.13
Pr	.87	.31	.37	.59	.64	.05	-.10	.92	.08
Nd	.91	-.91	.24	.23	.10	-.72	.51	.25	.40
Na	.90	.71	.51	-.34	-.09	.77	.23	.21	-.45
Ca	.60	.23	.69	-.02	.27	.24	.42	.16	-.25
Mn	.61	-.68	.29	-.13	-.23	-.33	.62	-.26	.20
Fe	.82	.87	.02	-.06	.22	.59	-.40	.36	-.13
Zr	.46	-.47	-.41	-.09	-.35	-.25	-.07	-.17	.04
Ti	.74	-.39	.21	.17	-.47	-.02	.28	-.03	.81
Al	.80	.87	.15	.09	-.12	.80	-.26	.28	-.13
Y	.70	-.50	.60	.29	-.03	-.22	.64	.30	.39
REE	.96	-.64	.73	-.14	.01	-.31	.92	.11	.16

Table 20 Correlation matrix for steenstrupine A from the sample 6-72.88

Elements	Si	P	Th	La	Ce	Pr	Nd	Na	Ca	Mn	Fe	Zr	Ti	Al	Y	REE
Si	1.00															
P	-.00	1.00														
Th	.64	-.64	1.00													
La	-.15	.15	.19	1.00												
Ce	-.59	.59	-.46	.10	1.00											
Pr	-.45	.45	-.64	-.20	.19	1.00										
Nd	-.40	.40	-.89	-.42	.29	.68	1.00									
Na	-.25	.25	.30	.23	-.14	-.07	-.46	1.00								
Ca	.49	-.49	.51	.01	-.24	-.00	-.37	.09	1.00							
Mn	-.31	.31	-.67	-.31	.10	.33	.73	-.34	-.51	1.00						
Fe	.86	-.86	.56	-.14	-.24	-.26	-.30	-.27	.58	-.49	1.00					
Zr	-.34	.34	-.55	-.15	.01	.14	.49	.03	-.63	.40	-.46	1.00				
Ti	.44	-.44	.53	.35	-.23	-.53	-.44	-.04	.36	-.13	.34	-.54	1.00			
Al	.34	-.34	.40	.08	-.35	-.18	-.23	.02	.08	-.24	.37	-.03	.14	1.00		
Y	-.60	.60	-.73	-.28	.47	.30	-.73	-.09	.67	.74	-.55	.56	-.34	-.19	1.00	
REE	-.72	.72	-.73	.16	.90	.42	.59	-.20	-.40	.38	-.42	.24	-.29	-.36	.67	1.00

Tab. 21 Correlation matrix for steenstrupine A from the sample 11-134.9

Elements	Si	P	Th	La	Ce	Pr	Nd	Na	Ca	Mn	Fe	Zr	Ti	Al	Y	REE
Si	1.00															
P	-.00	1.00														
Th	-.14	.14	1.00													
La	-.27	.27	.60	1.00												
Ce	-.22	.22	.58	.03	1.00											
Pr	-.12	.12	.59	-.62	.22	1.00										
Nd	-.04	.04	-.61	-.51	.46	.85	1.00									
Na	-.48	.48	.38	.70	.35	-.26	-.11	1.00								
Ca	.58	-.58	.04	-.16	-.29	-.05	-.09	-.37	1.00							
Mn	-.30	.30	-.26	-.30	.05	.76	.73	-.03	.20	1.00						
Fe	.53	-.53	.08	.22	-.14	-.34	-.24	.14	.72	.01	1.00					
Zr	-.41	.41	-.56	-.41	.43	.52	.68	.10	-.40	.54	-.24	1.00				
Ti	.38	-.38	.11	-.50	-.50	-.13	-.07	-.53	-.10	-.30	-.24	.04	1.00			
Al	.26	-.26	-.53	-.15	.15	.43	.52	.02	.11	.47	.45	.48	-.19	1.00		
Y	-.57	.57	-.04	-.23	.39	.51	.54	.38	-.25	.54	-.39	.53	-.20	-.14	1.00	
REE	-.34	.34	-.45	.16	.95	.30	.56	.50	-.33	.24	-.16	.46	-.59	.22	.50	1.00

Table 22. Correlation matrix for the atomic proportions in steenstrupine 199704

Elements	Si	P	Th	La	Ce	Pr	Nd	Na	Ca	Mn	Fe	Zr	Ti	Al	Y	REE+Y
Si	1.00															
P	-0.00	1.00														
Th	0.29	-0.29	1.00													
La	-0.07	0.07	-0.15	1.00												
Ce	-0.00	0.00	-0.21	0.23	1.00											
Pr	0.20	-0.20	0.34	0.21	0.05	1.00										
Nd	-0.03	0.03	-0.30	0.09	0.24	0.08	1.00									
Na	0.07	-0.07	-0.57	0.35	0.39	-0.02	0.40	1.00								
Ca	0.06	-0.06	-0.03	0.20	0.19	0.31	0.33	0.11	1.00							
Mn	-0.30	0.30	-0.46	0.18	0.26	0.01	0.31	0.29	0.09	1.00						
Fe	0.17	-0.17	0.31	-0.27	-0.16	0.20	-0.04	-0.24	-0.02	-0.49	1.00					
Zr	0.21	-0.21	-0.29	-0.08	0.19	0.15	0.33	0.53	-0.15	0.13	0.20	1.00				
Ti	0.75	-0.75	0.16	-0.17	0.08	-0.01	-0.08	0.10	-0.13	-0.30	0.15	0.11	1.00			
Al	-0.04	0.04	0.11	-0.22	-0.30	-0.04	-0.37	-0.56	-0.09	-0.33	0.32	-0.33	0.02	1.00		
Y	0.04	-0.04	0.66	0.17	-0.05	0.27	-0.17	-0.50	0.05	-0.12	0.05	-0.40	-0.07	0.11	1.00	
REE+Y	-0.00	0.00	-0.02	0.75	0.67	0.30	0.37	0.34	0.29	0.27	-0.19	-0.01	-0.09	-0.37	0.18	1.00

Table 23 Statistical estimates of the uranium recovery for different types of overall rock hydration

Hydration	Mean recovery x) %	St.dev. x) %	Range	No. of samples
Weak	88.0	6.28	98-75	16
Medium	82.05	9.39	97-65	20
Strong	69.34	12.81	97-50	35
Ussingite bearing xx)	80.33	15.18	97-61	6

x) the statistical estimates represent robust estimates, i.e. the thinly dispersed outlying values were omitted

xx) a very heterogeneous group with different hydration and yield values

Table 24 Statistical estimates of the recovery of uranium for different types of steenstrupine

Type of steenstrupine	Mean recovery (%)	Standard dev. (%)	Range (%)	No of samples
Weakly and medium hydrated rocks ^{x1}				
Aa	91.3	3.9	90-86	11
Ab	87.2	6.9	90-75	15
Ac	88.7	4.1	97-83	15
Ad	81.6	10.6	95-65	11
none	42.1	17.9	67-20	11
Strongly hydrated rocks				
Aa	67.2	11.2	92-50	5
Ab	63.5	10.3	78-50	10
Ac	80.3	12.8	94-57	8
Ad	69.0	12.0	82-53	5
Ba,b	73.3	13.3	94-53	12
Bc	68.4	10.3	85-60	5
none	49.0	13.3	61-30	4
All hydration types with monazite and mostly no steenstrupine				
	42.4	14.9	61-27	10

^{x1} All the statistical values for the weakly and medium hydrated rocks (Aa-Ad) represent robust estimates, i.e. only the densely populated core region of the data array has been taken into account (the outliers were omitted).

Table 25 Statistical estimates of uranium recovery for different rock types

Rock type	Mean recovery (%)	Standard dev. (%)	Range (%)	No of samples
Arfvedsonite lujavrite ^{x1}	74.37	15.44	97-43	37
Naujakasite lujavrite	83.69	12.85	98-53	19
Medium-coarse gr. lujavrite	70.94	13.07	92-51	16
Deformed lava	77.32	10.84	91-57	11

^{x1} The values do not include the recovery percentages for the monazite-bearing rocks.

Table 26. The uranium content and the uranium yield under standard conditions for the samples described in Tables 2-7.

Sh	Depth (m)	U (ppm)	Recovery	Sh	Depth (m)	U (ppm)	Recovery	
1	170.00	377	94	21	59.55	225	85	
	97.45	337	92		22	10.20	326	85
2	49.05	264	97	23		37.40	245	70
	60.65	300	75		24	74.15	117	60
4	107.00	813	94	25		10.05	250	79
	121.30	470	90		26	70.35	307	84
5	120.45	385	89	27		20.00	365	60
	44.90	387	76		28	29.00	530	86
6	72.05	470	90	29		67.20	90	67
	112.20	679	90		30	90.70	277	97
8	45.30	148	89	31		15.00	487	58
	26.00	587	60		32	29.35	766	76
9	66.65	356	58	33		47.05	230	60
	77.75	325	87		34	12.50	394	57
11	134.90	334	82	35		60.00	181	57
	134.00	274	78		36	90.00	307	70
13	80.10	260	72	37		12.20	494	74
	100.05	473	73		38	48.00	220	84
15	42.00	359	67	39		60.25	360	83
	22.05	227	63		40	370.00	180	29
16	52.00	444	79	41		36.00	477	85
	73.90	375	68		42	140.15	269	97
17	62.00	269	73	43		87.00	294	67
	117.10	246	72		44	30.00	183	80
18	32.65	305	73	45		89.95	326	57
	8.55	306	67		46	179.50	285	57
19	100.30	344	98	47		104.20	320	92
	20.10	147	67		48	60.15	367	92
20	67.35	389	50	49		79.65	193	76
	33	66.60	976		85	50	103.00	470
70	3.05	597	87	51	147.70		439	74
	26.90	357	79		52	3.20	424	60
	161.00	267	43			53	67.05	147
69	11.05	319	60	54	143.00		137	50
	117.00	200	0		55	93.70	363	75
68	74.00	172	30	56		109.90	370	62
	83.00	155	29		57	179.90	320	70
67	189.70	126	20	58		13.00	470	86
	87.55	106	48		59	157.00	372	90
66	175.40	138	17	60		19.40	324	91
	51.10	290	92		61	155.35	155	22
65	107.50	133	25	62		5.75	317	90
	29.95	136	54		63	39.95	366	86
64	105.65	212	60	64		57.00	307	86
	135.30	304	69		65	37.05	366	89
62	67.95	295	48	66		43.00	293	67
	165.90	203	28		67	77.30	376	89
61	22.30	104	82	68		139.35	380	97
	77.00	567	88		69	163.00	343	98
	127.95	372	65			70	59.00	225
				71	73.85		273	90
					72	157.75	277	65

**Sales distributors:
Jul. Gjellerup, Sølvgade 87,
DK-1307 Copenhagen K, Denmark**

**Available on exchange from:
Risø Library, Risø National Laboratory,
P. O. Box 49, DK-4000 Roskilde, Denmark**

**ISBN 87-550-0681-7
ISSN 0106-2840**